Studies on the Cellular Behaviour on Gelatin-Based Hydrogels Obtained through Hydrogen Peroxide-Mediated Cross-Linking and Degradation

WILDAN MUBAROK

SEPTEMBER 2022

Studies on the Cellular Behaviour on Gelatin-Based Hydrogels Obtained through Hydrogen Peroxide-Mediated Cross-Linking and Degradation

A dissertation submitted to

THE GRADUATE SCHOOL OF ENGINEERING SCIENCE

OSAKA UNIVERSITY

in partial fulfillment of the requirements for the degree of

DOCTOR OF PHILOSOPHY IN ENGINEERING

BY

WILDAN MUBAROK

SEPTEMBER 2022

Preface

This dissertation was conducted under the supervision of Professor Shinji Sakai at the Division of Chemical Engineering, Graduate School of Engineering Science, Osaka University, from 2019 to 2022.

The objective of this dissertation is to investigate the contradictory effect of hydrogen peroxide that simultaneously induces cross-linking and degrades polymer in horseradish peroxidase-catalysed cross-linking and its subsequent effect on modulating cell behaviour. The influence of the contradictory effect of hydrogen peroxide on the mechanical property of gelatin-based hydrogels is investigated. Furthermore, the effect of the mechanical property changes on modulating cell adhesion, myogenesis, and cell-cycle progression are reported.

The author hopes this research will contribute to the development of *in vitro* artificial tissue by incorporating the effect of the mechanical property on modulating cell behaviour.

Wildan Mubarok

Division of Chemical Engineering
Graduate School of Engineering Science
Osaka University
Toyonaka, Osaka, 560-8531, Japan

Abstract

Hydrogel fabrication through horseradish peroxidase (HRP)-catalysed cross-linking has garnered great interest due to its safety for cells. In HRP cross-linking, hydrogen peroxide (H_2O_2) is used as an electron donor to induce the cross-linking of polymer possessing phenol groups (Polymer-Ph). However, H_2O_2 can also degrade the Polymer-Ph through oxidation. This contradictory effect of H_2O_2 can affect the properties of the hydrogel. Subsequently, the changes in the properties of the hydrogel play a key role in regulating cell behaviours. The objective of this thesis is to investigate the contradictory effect of H_2O_2 on the hydrogel properties and its role in controlling cell behaviour.

Chapter I describes the general explanation regarding the interaction between cells and their extracellular matrix (ECM). The role of the physicochemical properties of the ECM, *e.g.*, stiffness, viscoelasticity, molecular weight and cell adhesive ligands, in regulating cell behaviour was discussed. Attempts to study the cell-ECM interaction *in vitro* using hydrogels were discussed. The application and cross-linking of gelatin-based hydrogels and studies on H_2O_2 role in HRP-catalysed cross-linking were presented.

Chapter II describes the contradictory effect of H_2O_2 on Gelatin-Ph hydrogel. The mechanical property of the Gelatin-Ph hydrogel could be controlled by adjusting the HRP concentration and the exposure time to air containing H_2O_2. Increasing the exposure time to air containing H_2O_2 resulted in a non-linear trend of the Gelatin-Ph hydrogels Young's modulus, with initial stiffening followed by a gradual decrease in hydrogel stiffness. This phenomenon is mediated by the contradictory effect of H_2O_2 which degrades the polymer in extended exposure time. The changes in the properties of the Gelatin-Ph hydrogels could alter the adhesion of human adipose-derived stem cells and rat fibroblasts. Overall, this system allows hydrogel fabrication with tunable properties for controlling cell behaviour.

Chapter III describes the application of air containing H_2O_2 exposure–mediated control of the physicochemical properties of Gelatin-Ph on modulating myogenesis. To address this, the behaviour of mouse myoblasts (C2C12) cells on Gelatin-Ph hydrogels fabricated through different exposure times to air containing H_2O_2 was studied. The cytocompatibility of the hydrogelation system was demonstrated. The myoblasts showed stiffness-dependent adhesion and differentiation, with higher cell elongation and myotube formation observed on stiffer hydrogels. The findings of this study can be applied in skeletal muscle tissue engineering to control the cell fate to form new muscle cells.

Chapter IV describes the possibility of controlling the cell-cycle progression of the cells cultured on Gelatin-Ph/hyaluronic acid (HA)-Ph composite hydrogels obtained through H_2O_2-mediated cross-linking and degradation of the polymers. Human cervical cancer cells (HeLa) and mouse mammary gland epithelial cells (NMuMG) expressing cell-cycle reporter Fucci2 showed the exposure time-dependent cell-cycle progression on the hydrogels. Cells cultured on softer hydrogel showed arrested cell-cycle progression. Additionally, the cell-cycle progression of NMuMG/Fucci2 cells was not only governed by the hydrogel stiffness but also by the low-molecular-weight HA-Ph resulting from H_2O_2-mediated degradation. These findings could be useful in cancer studies and tissue engineering purposes.

This thesis describes the potential of H_2O_2-mediated control of hydrogel properties to modulate cell behaviour. The findings of this study are expected to contribute to the application of HRP-catalysed cross-linking in cell studies and the development of functional tissues in the biomedical engineering field.

Table of Contents

Chapter I

General Introduction

The extracellular matrix (ECM) is a network of macromolecules surrounding the cells that provide an anchoring point for the cells. In addition to its function as a cell scaffold, ECM is important to provide biochemical and biomechanical cues that regulate the cell behaviours for morphogenesis or tissue regeneration (Frantz et al. 2010). ECM is mainly comprised of fibrous proteins (collagen, elastin, fibronectin, and laminin) and proteoglycans, including hyaluronic acid, that fill the interstitial space of the matrix, which provides structural integrity against compressive forces (Järveläinen et al. 2009; Frantz et al. 2010). ECM is a dynamic structure in which cells can synthesise, modify, or degrade the ECM depending on the physiological condition. Subsequently, the changes in the ECM composition that alter the physicochemical properties of the ECM, in turn, can impact the cell behaviour (Calvo et al. 2013; Rainer et al. 2019).

Clinically, genetic abnormalities in ECM proteins can lead to several diseases, including brittle bone disease (osteogenesis imperfecta) and Ehlers-Danlos syndromes (EDS) characterised by the hyperelasticity of the skin and vascular fragility caused by a mutation in genes encoding collagen (Nuytinck et al. 2000; Glorieux 2008), or Marfan's syndrome caused by deficiency of fibrillin (Milewicz et al. 1992; Judge and Dietz 2005). Furthermore, changes in ECM also can induce the development of many critical diseases, such as hypertension in cardiovascular disease caused by increased stiffness in blood vessels (Bertero et al. 2016; Schäfer et al. 2016), asthma and chronic pulmonary diseases caused by loss of tissue elasticity (Sicard et al. 2017; Zemła et al. 2018), and liver cirrhosis caused by protein accumulation in response to inflammation (Wallace et al. 2008).

1. Physical Properties of ECM

From the clinical cases above, the ECM's physicochemical properties are important regulators of cell behaviour that can have wider consequences to the tissue or organs. Previous studies have recognised several physical properties, *e.g.*, stiffness, viscoelasticity, pore size, and architecture, that regulate the cell behaviour **(Table 1)** (Lim et al. 2010; Iskratsch et al. 2014; Janmey et al. 2020).

Table 1. Physical properties of ECM that affect cell behaviour.

Physical properties	Cell behaviour	References
Stiffness	• Breast cancer cells adhesion	(Sun et al. 2019)
	• Breast adenocarcinoma cells migration and metastasis	(Vasudevan et al. 2020)
	• Stem cells migration and differentiation	(Hadden et al. 2017)
	• Hepatocytes apoptotic cell death	(Ganesan et al. 2018)
Viscoelasticity	• Cancer cells migration	(Wisdom et al. 2018)
	• Cancer cells division	(Nam and Chaudhuri 2018)
Pore size	• Neural stem / progenitor cells differentiation	(Li et al. 2012)
	• Mesenchymal stem cells chondrogenic differentiation	(Matsiko et al. 2015)
	• Osteoblasts adhesion, proliferation, and calcium deposition	(Thangprasert et al. 2019)
	• Cancer cells migration	(Wolf et al. 2013)
Degradability	• Cancer metastasis	(Peláez et al. 2017)
	• Stemness regulation of neural progenitor cell	(Madl et al. 2017)
	• Skeletal stem cell differentiation	(Tang et al. 2013)

Table 1. Continued

Architecture	• Myotubes alignment • Sarcoma cell-cycle progression and division	(Du et al. 2019) (Moriarty and Stroka 2018)

1.1 Stiffness

Stiffness is an important cue for the cells, considering that different tissues/organs have different stiffness (Engler et al. 2006). Previous studies have reported that substrate stiffness can affect the cell adhesion, migration, differentiation, and even cell death (Hadden et al. 2017; Ganesan et al. 2018; Vasudevan et al. 2020). Cells can actively sense the stiffness of their substrate, which then converts the mechanical forces into biochemical cues to determine the cell fate.

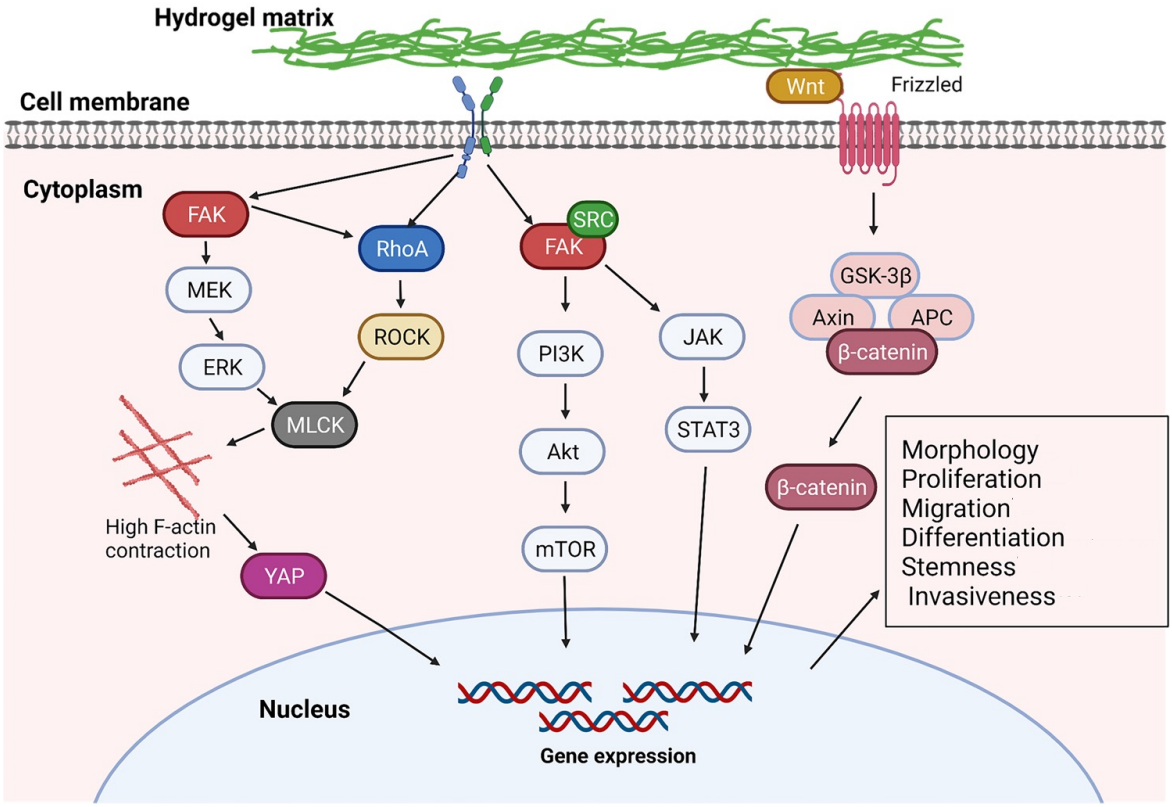

Fig. 1-1 Mechanism of cell behaviour regulation by the stiffness of the extracellular matrix (ECM). Reprinted from (Cao et al. 2021). Copyright Springer Nature.

Integrins, as transmembrane adhesion molecules, can interact with the ECM ligand and sense the stiffness of the substrate (Sun et al. 2016). Integrins then activate the mechanosensing pathways, including focal adhesion kinase (FAK) signalling (Zhao and Guan 2011), Rho-A/Rho-associated protein kinase (ROCK) pathway (Chen et al. 2002), Yes-associated protein (YAP) / transcriptional co-activator with PDZ-binding motif (TAZ) signalling (Piccolo et al. 2014), or Wnt signalling pathway (Du et al. 2016). These pathways can lead to the cytoskeleton (*e.g.*, F-actin, myosin) re-organization, which leads to cell elongation and migration or activates differentiation and apoptosis pathway **(Fig. 1-1)**.

In a stiff substrate, cells generally have better adhesion and exhibit elongated morphology since the substrate allows the cells to maintain their tension (Martino et al. 2018). Subsequently, cells also have better migration and proliferation on a stiffer substrate. In contrast, a soft substrate can be deformed or even broken by the contraction force of the cells (Romanazzo et al. 2012), thus, inhibiting the cells from maintaining their tension. Consequently, cells cultured on soft substrate have low adhesion, no elongation, arrested cell-cycle, and eventually undergo apoptosis (Paszek et al. 2005; Chiu et al. 2007; Wall et al. 2007).

However, it is also important to note that cells have an optimum range of stiffness. Engler et al. reported that mesenchymal stem cells (MSCs) commit to specific lineage depending on the matrix's stiffness. MSCs show neurogenic commitment on 0.1 – 1 kPa, myogenic on 8 – 17 kPa, and osteogenic at 25 – 40 kPa (Engler et al. 2006). Additionally, while a stiffer substrate is better for the fibroblasts adhesion (Yeung et al. 2005), the opposite effect is observed in neurons, in which less neurite branching is observed on a stiff substrate (Flanagan et al. 2002). Previous studies have also reported that stem cells exhibit “durotaxis” behaviour, in which the stem cells have the tendency to migrate to the highest stiffness point on the gradient (Tse and Engler 2011; Vincent et al. 2013).

Cells also actively respond to the temporal changes of the substrate stiffness. In the progression of cancer, injury, or ageing process, re-organisation of the ECM results in gradual stiffening or softening of the substrate (Lacraz et al. 2015; Ondeck et al. 2019; Silver et al. 2021). Studies by the Engler group showed that gradual stiffening of the substrate results in cytoskeleton re-organisation in the fibroblast (Ondeck and Engler 2016) and promotion of malignant transformation of breast cancer cells (Ondeck et al. 2019). Stiffening of the substrate post-injury also activates the resident muscle stem cells to proliferate and regenerate the muscle tissue (Silver et al. 2021). A recent study by Hayashi et al. also reported that myoblasts readily change their morphology upon switching the substrate stiffness (Hayashi et al. 2022). In stem cells, the gradual stiffening of the substrate is also an important cue for differentiation. Early stiffening (1 day) will induce osteogenic differentiation, while later stiffening (7 days) increases the adipogenic differentiation of human mesenchymal stem cells (Guvendiren and Burdick 2012).

1.2 Viscoelasticity

In addition to stiffness, the viscoelasticity of the ECM is also an important regulator for cell behaviour. Natural tissues and ECM-derived materials are known to possess viscoelastic properties (Maccabi et al. 2018; Huang et al. 2019). Physiologically, viscoelasticity is widely correlated with cancer progression. Cancer cells are tightly packed by their surrounding tissues. Therefore, their ability to divide and migrate (metastasis) depends on the viscoelasticity of the ECM. Wisdom et al. reported that breast cancer cells' migration in physical confinement depends on the viscoelasticity of the microenvironment. In an elastic matrix, the cancer cells can protrude and break the confinement, which allows them to migrate **(Fig. 1-2 (a))** (Wisdom et al. 2018).

Viscoelasticity of the substrate also regulates the cancer cell division. Confining the cancer cells in an elastic matrix increase the percentage of division failure due to abnormal mitotic spindle **(Fig. 1-2 (b-c))**. Meanwhile, cancer cells confined in a viscoelastic matrix can exert forces to deform their surrounding environment, allowing cells to undergo a normal mitosis process (Nam and Chaudhuri 2018). While these studies demonstrate the importance of viscoelasticity, the effect of viscoelasticity is considered negligible, particularly in 2D culture with high stiffness substrate, and considered of importance in soft 3D confinement.

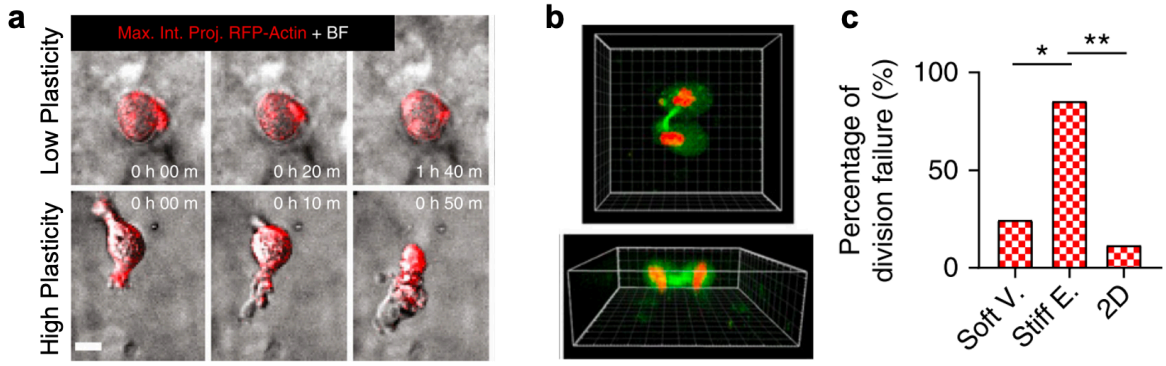

Fig. 1-2 Effect of viscoelasticity to (a) breast cancer cell migration and (b-c) cell division. (a) Protruding of cancer cells to migrate in 3D confinement. Reprinted from (Wisdom et al. 2018). Copyright Springer Nature. (b) Buckling of mitotic spindle of cancer cells in elastic substrate. (c) Failure of cell division in elastic substrate. Reprinted from (Nam and Chaudhuri 2018). Copyright Springer Nature.

1.3 Pore Size

Similar to viscoelasticity, the substrate's pore size is also important in regulating confined cells. Several studies have reported that pore size controls stem cells differentiation. Li et al. reported that neural stem/progenitor cells show higher differentiation to neurons, astrocytes, and oligodendrocytes, in the matrix with a larger pore size (4060 – 7600 μm^2) (Li et al. 2012). Another study reported that pore size of 300 μm is effective in inducing chondrogenic differentiation in MSCs (Matsiko et al. 2015). Pore size is also important in bone regeneration. Thangprasert et al. reported that pore size can control the osteoblasts' adhesion, proliferation,

and calcium deposition, with pore size of 67.38 μm being the most effective in inducing bone formation (Thangprasert et al. 2019).

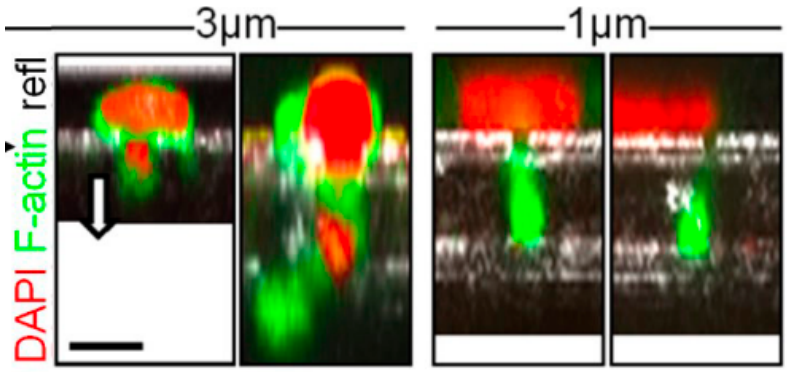

Fig. 1-3 Migration of neutrophil through different pore size. ©2013 Wolf et al. Originally published in Journal of Cell Biology. https://doi.org/10.1083/jcb.201210152

In addition to regulation of stem cell differentiation and bone regeneration, pore size is also important in controlling the 3D migration of the confined cells. Stem cells homing require the cells to migrate through the tight confinement of the tissue or blood vessel (Doolin et al. 2020). Similarly, cancer cell invasion also depends on their ability to overcome the confinement (Alexander et al. 2008). Harada et al. reported that MSCs and cancer cells could migrate through 3D confinement when the pore size is > 3 μm, as cells cannot deform their nucleus through pore size < 3 μm (Harada et al. 2014).

Furthermore, Wolf et al. reported cell type-dependent physical limits of the cell migration. The physical limits of cancer cells, T-cells, and neutrophils, to migrate are 7 μm^2, 4 μm^2, and 2 μm^2, respectively (Wolf et al. 2013). To squeeze through > 3 μm pore size, cells can deform their shape into amoeboid or mesenchymal **(Fig. 1-3)** (Friedl and Alexander 2011; Wisdom et al. 2018). In the case of tighter confinement < 3 μm, the cells have to re-model the matrix by physically "ripping" the matrix using invadopodium or degrading the matrix by proteases **(Fig. 1-4)** (Wisdom et al. 2018).

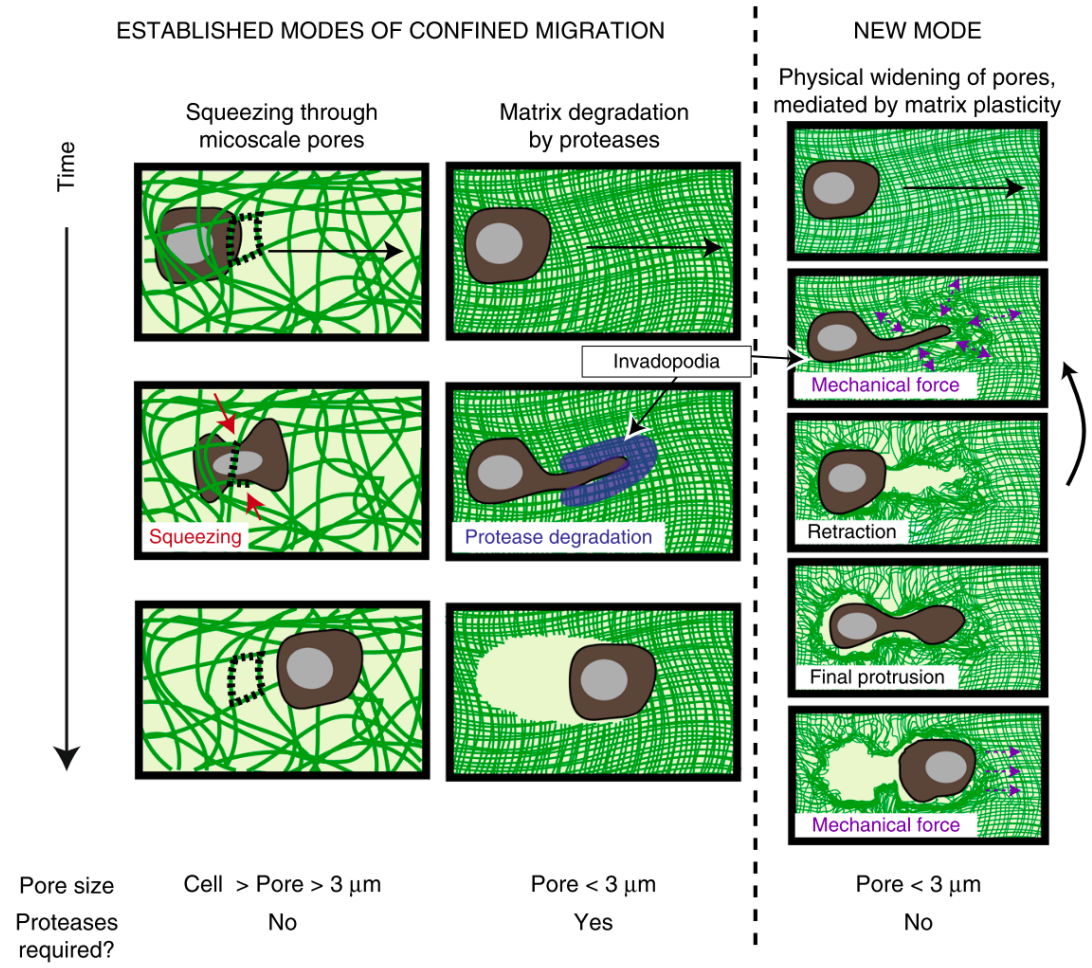

Fig. 1-4 Cell migration modes in 3D physical confinement. Cells can change its shape to squeeze through pore, release protease to degrade the ECM, or physically widening the pore by protrusion. Reprinted from (Wisdom et al. 2018). Copyright Springer Nature.

1.4 Degradability

The cancer cell is known to produce matrix metalloproteinases (MMPs) that can degrade the ECM, allowing them to migrate and metastasise into distant tissues (Kessenbrock et al. 2010). A wide variety of MMPs that degrade the ECM components have been reported, such as collagen (MMP-1, MMP-8), gelatin (MMP-2, MMP-9), laminin (MMP-3), and elastin (MMP-12) (Jabłońska-Trypuć et al. 2016). Cells can protrude, forming pseudopodium or invadopodium, which then produce the MMP, releasing the cells from the confining matrix **(Fig. 1-4)** (Sabeh et al. 2004; Wolf et al. 2007). In gastric cancer, increasing the collagen cross-

linking induces the MMP-2 and MMP-9 expression to degrade the ECM, further promoting the cancer invasion (Zhao et al. 2019).

Degradability of the matrix is also crucial for controlling stem cell behaviour. Madl et al. reported that matrix degradation is important to maintain the stemness of neural progenitor cells. Neural progenitor cells require cell-cell contact to maintain stemness. Low degradability of the matrix limits the cadherin-mediated cell-cell contact, which results in the loss of stemness (Madl et al. 2017). The ability of stem cells to degrade their matrix by MMP is also important to control the differentiation lineage. Deletion of membrane-anchored metalloproteinase MT1-MMP (Mmp14) alters the differentiation lineage of skeletal stem cells from osteogenic to adipogenic and chondrogenic (Tang et al. 2013). Matrix degradation is also important to allow the transmigration of leukocytes and MSCs through the blood-brain barrier (Liu et al. 2013). MMP-2 and MT1-MMP are reported to be the regulators in MSCs transmigration through the endothelial layer, which is important for successful stem cell therapy (De Becker et al. 2007; Steingen et al. 2008). These results show that matrix remodelling, which depends on the viscoelasticity, pore size, and degradability of the matrix, can alter various cells' behaviour with high clinical relevance.

1.5 Architecture

As a consequence of matrix remodelling, the architecture of the ECM can be altered. Naturally, ECM consists of aligned collagen fibres. However, in cases like wound healing, disturbed alignment of collagen fibres can result in scar formation (Xue and Jackson 2015). In Osteogenic Imperfecta, in which collagen I synthesis and organisation are disrupted due to mutation, bone architecture is altered, resulting in a reduced bone mass (Morello 2018).

The architecture of the ECM also acts as a topological cue for the cells. Multiple studies have reported that myotubes alignment is important in skeletal muscle tissue regeneration **(Fig.**

1-5) (Hosseini et al. 2012; Bettadapur et al. 2016; Denes et al. 2019). In addition, the architecture of the cell environment can also regulate the cell-cycle progression of sarcoma cells (Moriarty and Stroka 2018).

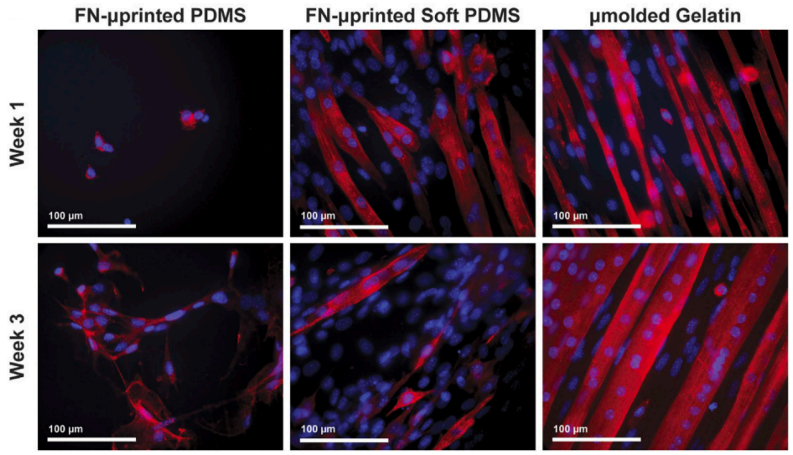

Fig. 1-5 Effect of matrix architecture on the myotubes formation and orientation. Reprinted from (Bettadapur et al. 2016). Copyright Springer Nature.

2. Chemical Properties of ECM

2.1 Molecular Weight

In addition to the physical properties, the chemical properties of the ECM, including molecular weight and cell attachment sites, can also affect the cell biology by the interaction with cell receptors **(Table 2)** (Dupont 2016; Tavianatou et al. 2019). While molecular weight is known to affect to physical properties of the substrate, the component of ECM, such as hyaluronic acid (HA), has a direct modulatory effect based on their molecular weight. In cancer, growth inhibition and increased apoptosis are observed in human colon carcinoma and murine mammary carcinoma cultured in the presence of high-molecular-weight HA (HMW-HA) (2.5×10^6 Da) (Ghatak et al. 2002). Meanwhile, low-molecular-weight HA (LMW-HA) ($1.5 – 4.0 \times 10^5$ Da) promotes the tumour growth. This process is reported to be mediated by the Hippo signalling. The presence of LMW-HA inhibits the CD44 (HA receptor) clustering, which

inactivate the Hippo pathway, resulting in the increase in breast cancer aggressiveness **(Fig. 1-6 (a))** (Ooki et al. 2019).

Table 2. Chemical properties of ECM that affect cell behaviour.

Chemical properties	**Cell behaviour**	**References**
Molecular weight	HA:	
	Cancer aggressiveness	(Ooki et al. 2019)
	Immune response	(Mascarenhas et al. 2004)
	Collagen:	
	Osteoblasts differentiation	(Liu et al. 2015)
	Gelatin:	
	Human corneal endothelial cells pro-inflammatory response	(Lai et al. 2006)
	Fibrinogen:	
	Angiogenesis	(Kaijzel et al. 2006)
Cell-attachment sites	RHAMM:	
	Fibrosarcoma cell adhesion	(Kouvidi et al. 2011)
	Collagen I:	
	Stem cells osteogenic differentiation	(Rowlands et al. 2008)
	CD44:	
	Stem cells migration	(Avigdor et al. 2004)

The molecular weight of HA also plays a key role in regulating the immune response. LMW-HA ($< 5 \times 10^5$ Da) is accumulated following tissue injury. The presence of this LMW-HA then induces the immune response. Ohkawara et al. reported that LMW-HA (2×10^5 Da) activates the transforming growth factor-β (TGF-β) production by eosinophil, but not HMW-HA (5.8×10^6 Da) (Ohkawara et al. 2000). LMW-HA (3.7×10^5 Da) is also reported to induce interleukin-8 (IL-8) production, while increasing the HA molecular weight to $6 – 23 \times 10^5$ Da reduces the IL-8 production up to 5 times (Mascarenhas et al. 2004). Small HA fragments (sHA: 6 – 20 ×

10^3 Da) also act as an activator of dendritic cells and macrophages during inflammation (Termeer et al. 2000; Termeer et al. 2002).

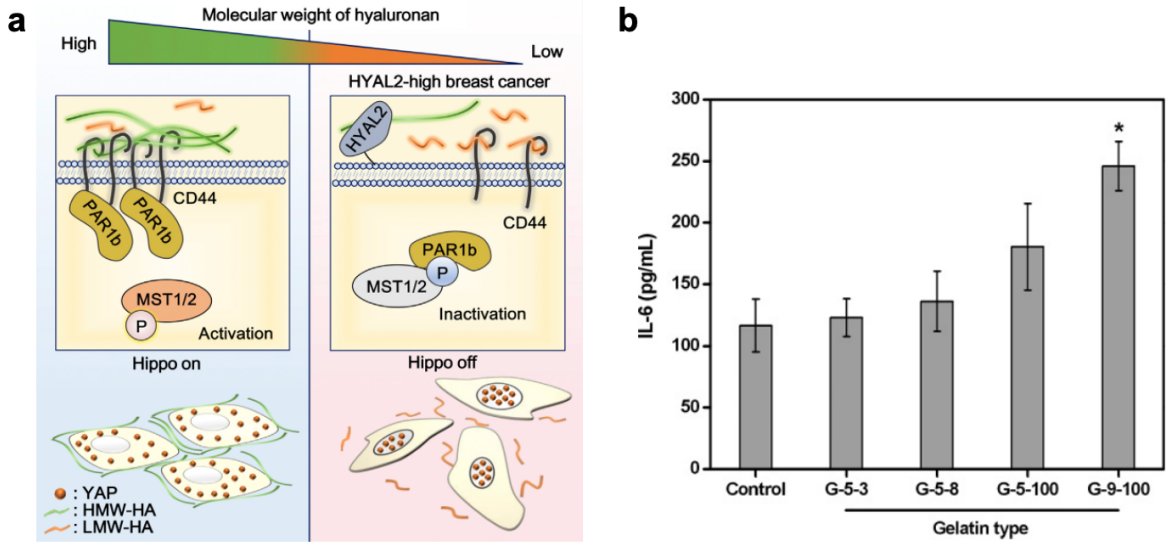

Fig. 1-6 Effect of substrate molecular weight on cell behaviour. (a) Molecular weight of HA regulates the cancer aggressiveness by CD44 clustering. Reprinted from (Ooki et al. 2019). Copyright Elsevier. (b) Effect of gelatin molecular weight to IL-6 release by human corneal endothelial cell. Reprinted (adapted) with permission from (Lai et al. 2006). Copyright 2006 American Chemical Society.

In addition to HA, the molecular weight of other ECM components, including collagen, gelatin, and fibrinogen, also affect cell behaviour. Liu et al. reported that the molecular weight of collagen can control the osteoblasts differentiation, in which higher differentiation and mineral production are observed in the presence of HMW-collagen (2.9 – 7.7 × 10^3 Da) (Liu et al. 2015). Lai et al. compared the human corneal endothelial cells (HCEC) response to gelatin with an average molecular weight of 3 – 100 × 10^3 Da. While a minimum effect is observed on the proliferation and viability of the cells, gelatin with a molecular weight of 1.0 × 10^5 Da stimulates the IL-6 release **(Fig. 1-6 (b))** (Lai et al. 2006), indicating the inflammatory regulation by gelatin molecular weight. Fibrinogen molecular weight is also reported to play a

role in the formation of capillary tubes (angiogenesis). Higher angiogenesis is observed in the HMW-fibrinogen (3.4×10^5 Da) than in the LMW-fibrinogen ($2.7 – 3.0 \times 10^5$ Da) (Kaijzel et al. 2006). This is probably mediated by the presence of RGD-sequence in the HMW-fibrinogen that is removed in the LMW-fibrinogen (Brooks et al. 1994; Clark et al. 1996).

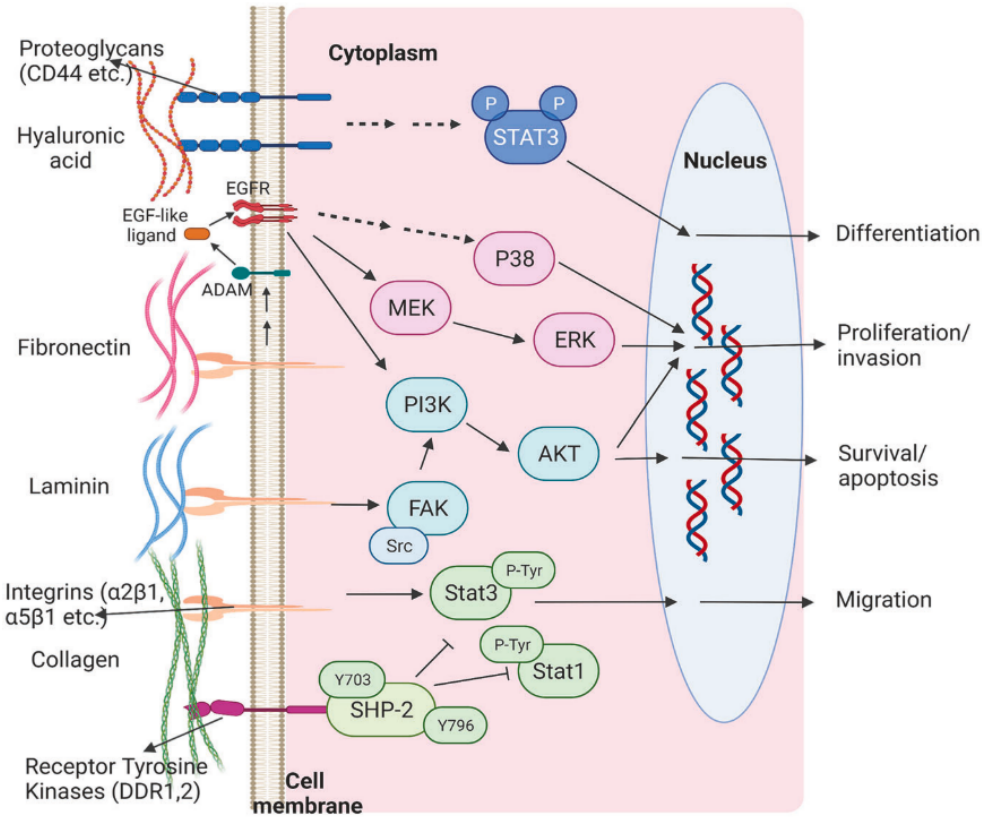

Fig. 1-7 Interaction of cell adhesive ligands with cell receptors and their signalling pathways to regulate cell behaviour. Reprinted from (Cao et al. 2021). Copyright Springer Nature.

2.2 Cell Adhesive Ligands

Apart from perceiving the physical properties of the substrate, the cell receptors can directly interact with the cell adhesive ligands of the ECM **(Fig. 1-7)**. Several adhesive ligands have been identified, *i.e.*, collagen or gelatin that interact with integrins and receptor tyrosine kinase; HA that interact with CD44 and receptor for HA-mediated motility (RHAMM) (Kouvidi et al.

2011); cytokines, growth factors, or receptors, such as epidermal growth factor receptor (EGFR) can interact with a disintegrin and metalloprotease (ADAM) (Blobel 2005). Fibronectin can interact with several cell receptors, including integrins, CD44, and toll-like receptor 4 (TLR4) (Wirth et al. 2020). Integrins can also act as a receptor for the laminin (Arimori et al. 2021).

Interaction between the cell adhesive ligands and the cell receptors then activates several signalling pathways that can affect cell behaviour **(Fig. 1-7)**. Kouvidi et al. reported that HA regulates the adhesion of fibrosarcoma cells via RHAMM that activates the focal adhesion kinase (FAK) and extracellular signal-regulated kinases (ERK1/2) (Kouvidi et al. 2011). HA interaction with CD44 also mediates the trans-endothelial migration of $CD34^+$ stem/progenitor cells in bone marrow via interaction with CXCR4 (Avigdor et al. 2004).

3. Hydrogels as ECM Model

Due to the importance of the ECM in regulating cell behaviours, understanding the cell-ECM interaction is crucial. The tissue engineering approach employing hydrogels is a valuable technique to model the native ECM and study the cell behaviour concerning cell-ECM interaction *in vitro*. Hydrogel is a network of cross-linked polymers that can contain a large amount of water (Ahmed 2015). The advantage of hydrogel is that its physicochemical properties can be tuned to mimic the physiological condition by changing the materials and cross-linking technique.

Hydrogels can be fabricated from natural materials and synthetic materials. Synthetic material allows fabrication of hydrogels with tailored molecular weight, high mechanical property and possessing stimulus-responsive properties (Madduma-Bandarage and Madihally 2021). Recent studies have utilised polyvinyl alcohol (PVA) / graphene oxide (GO)–hydroxyapatite (HA) nano-composite hydrogels for artificial cartilage replacement (Meng et

al. 2020), polyacrylic acid (PAA)-impregnated PVA (PVA/PAA) hydrogel for vascular access application (Mannarino et al. 2020), and polyacrylamide (PA) hydrogels to study collective cell migration (Vazquez et al. 2022). In addition, polyethylene glycol (PEG), polyurethane (PU), poly(2-methoxyethyl acrylate) (PMEA), and poly(lactide-co-glycolic) acid (PLGA) are also used (Hoshiba et al. 2017; Abreu-Rejón et al. 2022; Ghandforoushan et al. 2022).

Most of these synthetic polymers, however, suffer from low cell adhesion. Additionally, these polymers can also induce protein adsorption and denaturation (Felgueiras et al. 2017; Abreu-Rejón et al. 2022). Consequently, these materials have low biocompatibility, even inducing thrombogenic reactions (Zheng et al. 2010). Additionally, while improving cell adhesion is attempted by incorporating cationic polymers such as poly-L-Lysine (Zheng et al. 2021), these materials lack interaction with cell receptors such as integrins.

Based on these limitations, natural materials are preferable for hydrogel fabrication to study cell-ECM interaction and biomedical applications. While the mechanical property of the hydrogel obtained from natural materials is lower than those obtained from synthetic materials (Abalymov et al. 2020), the natural materials exhibit low or no cytotoxicity. In particular, gelatin, a product of hydrolysed collagen, is extensively used due to its biological property in supporting cell adhesion (Gomez-Guillen et al. 2011; Bae et al. 2015; Agheb et al. 2017). More importantly, gelatin-based hydrogels also have good biocompatibility, biodegradability, and non-immunogenic (Farris et al. 2010).

4. Gelatin-Based Hydrogels

Previous studies have utilised various methods to fabricate gelatin hydrogel **(Table 3)**. Most commonly, gelatin hydrogel is fabricated by cooling gelatin solution to temperature < 30 °C that induces sol-gel transition. However, this temperature-induced gelation method cannot be used in *in vitro* or *in vivo* conditions since the hydrogel is readily dissolved in a physiological

temperature (Gillmor et al. 1999). Various physical, chemical, and enzymatic cross-linking methods are developed to solve this problem.

Table 3. Examples of cross-linking methods to fabricate gelatin-based hydrogels.

Cross-linking categories	Cross-linking methods	References
Physical cross-linking	High energy electron irradiation	(Wisotzki et al. 2014)
	γ-ray irradiation	(Kojima et al. 2004; Cataldo et al. 2008)
	Plasma treatment	(Prasertsung et al. 2013)
Chemical cross-linking	Formaldehyde	(Ninan et al. 2013)
	Glutaraldehyde	(Poursamar et al. 2016; Yang et al. 2018)
	Genipin	(Nickerson et al. 2006; Kirchmajer et al. 2013)
	Photocross-linking	(Zhao et al. 2016; Lim et al. 2019)
Enzymatic cross-linking	Transglutaminase	(Chen et al. 2003; Ito et al. 2003; Gupta et al. 2021)
	Horseradish peroxidase	(Hu et al. 2009; Sakai et al. 2009a; Wang et al. 2010b)

4.1 Physical Cross-Linking

Physical cross-linking is mainly conducted via irradiation. Using high-energy electron or γ-ray irradiation, scission in the gelatin chain can occur, resulting in the formation of free radicals that consequently induce cross-linking between the gelatin chains (Bessho et al. 2007; Wisotzki et al. 2014). Similarly, plasma treatment of gelatin solution will induce the formation of free radicals, which then activate the cross-linking (Prasertsung et al. 2013). The advantage of this system is that in addition to cross-linking, irradiation with γ-ray or electron beam can simultaneously sterilise the materials, making it suitable for cell study or biomedical

applications. In addition, physical cross-linking also does not require the use of toxic chemicals to induce the cross-linking. However, this system suffers from a low cross-linking degree, resulting in hydrogels with a low mechanical property (Ratanavaraporn et al. 2010; Rose et al. 2014).

4.2 Chemical Cross-Linking

In chemical cross-linking, several studies have utilised aldehydes, *i.e.*, formaldehyde and glutaraldehyde, to induce gelatin cross-linking (Ninan et al. 2013; Poursamar et al. 2016; Yang et al. 2018). In glutaraldehyde cross-linking, the reaction between the carbonyl groups of the glutaraldehyde and the amine groups of the gelatin induces the formation of cross-linking networks. However, the use of formaldehyde and glutaraldehyde can have a toxic effect on cells (Lee and Mooney 2001; Yang et al. 2018).

As an alternative to the glutaraldehyde cross-linking, genipin is also used. While genipin has lower toxicity than glutaraldehyde, genipin is limited by the high cost, limited source, and difficulty in the extraction process (Zhao and Sun 2018). Moreover, genipin also spontaneously forms dark blue colour when reacted with gelatin (Makita et al. 2018), which limits the cells' observation.

Alternatively, a photocross-linking technique is developed in which gelatin methacrylate (GelMA) can be cross-linked by UV light irradiation to the solution containing GelMA and photocross-linker, *e.g.*, 2-Hydroxy-4'-(2-hydroxyethoxy)-2-methylpropiophenone (Irgacure 1929), Lithium phenyl(2,4,6-trimethylbenzoyl)phosphinate (LAP), or Eosin Y (Jaipan et al. 2017). However, UV light irradiation can cause DNA damage, limiting cell-laden hydrogel fabrication. In addition, the photocross-linker is also reported to have a cytotoxic effect on mammalian cells (Nguyen et al. 2020).

4.3 Enzymatic Cross-Linking

4.3.1 Transglutaminase

In addition to the physical and chemical cross-linking, gelatin hydrogel can be fabricated through enzymatic cross-linking. Transglutaminase is an ubiquitous enzyme found in plants, animals, or microbes (Yung et al. 2007). Particularly, microbial transglutaminase (mTG) is widely used to fabricate gelatin hydrogel (Chen et al. 2003; Ito et al. 2003; Gupta et al. 2021). mTG catalyses the gelatin cross-linking by inducing the formation of covalent lysine amide bonds of the gelatin strands (Yokoyama et al. 2004; Yung et al. 2007). While the safety of mTG is widely reported, this method requires a long gelation time (> 4 h) (Yung et al. 2007; Bettadapur et al. 2016; Gupta et al. 2021).

4.3.2 Horseradish Peroxidase

As an alternative, horseradish peroxidase (HRP)-catalysed cross-linking of gelatin derivatives possessing phenolic hydroxyl moieties (Gelatin-Ph) is a promising method, since gelation occurs in rapid time and within physiological conditions (Sakai et al. 2009a; Sakai and Nakahata 2017). Additionally, the biocompatibility of HRP-catalysed cross-linking of Gelatin-Ph is already well-established, which allows it to be applied in cell transplantation (Park et al. 2019), as drug carrier (Kondo et al. 2013), wound dressing (Yao et al. 2019), as well as bioprinting (Sakai et al. 2018).

In the HRP-catalysed cross-linking system, HRP reacts with hydrogen peroxide (H_2O_2), forming an intermediate complex (Compound I) that reduces the phenol to phenoxy radical, converting it to Compound II. The reaction of Compound II with another phenol reduced Compound II back to its native state. The phenoxy radicals can form C–C or C–O coupling, forming cross-linking between the phenol groups in the polymer chains (Hou et al. 2015; Khanmohammadi et al. 2018) **(Fig. 1-8)**.

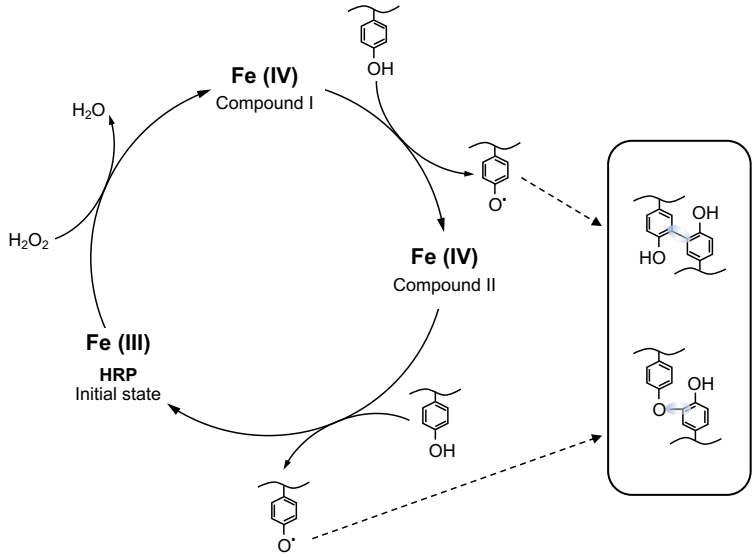

Fig. 1-8 Schematic illustration of the HRP-catalysed cross-linking of the polymers possessing phenol group.

Using this system, the hydrogel can be fabricated by using a wide range of materials possessing Ph moieties. In addition to natural polymers, including gelatin, hyaluronic acid, chitosan, and carboxymethylcellulose, HRP-catalysed cross-linking also can be applied to synthetic polymers such as PVA, PEG, and poly(propylene oxide)-poly(ethylene oxide) **(Table 4)**.

Table 4. Examples of natural and synthetic polymers used in HRP-catalysed cross-linking.

Natural polymer	**Reference**
Gelatin	(Hu et al. 2009; Sakai et al. 2009a)
Hyaluronic acid	(Lee et al. 2008; Sakai et al. 2015)
Chitosan	(Sakai et al. 2009b)
Alginate	(Sakai et al. 2010)
Carboxymethylcellulose	(Ogushi et al. 2009)
Synthetic polymer	**Reference**
Poly(vinyl alcohol)	(Sakai et al. 2013)
Poly(ethylene glycol)	(Ren et al. 2017)
poly(propylene oxide)-poly(ethylene oxide)	(Kim et al. 2012)

4.4 H_2O_2 in HRP Cross-Linking

H_2O_2 has been a subject of interest in the HRP-catalysed cross-linking. Previously, multiple studies have developed several approaches to supply the H_2O_2 in the cross-linking system. While direct mixing of solution containing Polymer-Ph and HRP with aqueous H_2O_2 is the most common method, this method suffers from inhomogeneity of the hydrogelation and cytotoxic effect of the remaining H_2O_2. Furthermore, direct supply method can also inactivate the HRP (Sakai and Nakahata 2017).

As an alternative, a variety of indirect H_2O_2 supply methods have been developed. Sakai et al. reported the HRP-catalysed cross-linking utilising the glucose oxidase (GOX) (Sakai et al. 2012). GOX can produce H_2O_2 as a by-product of D-glucose conversion to D-gluconic acid (Dinda et al. 2018). The produced H_2O_2, thus, can be used to induce the HRP cross-linking. Using this approach, *in situ* cross-linking exploiting the presence of glucose in the body fluid is reported for wound healing application using PVA-Ph (Sakai et al. 2013).

In addition, Liu et al. reported an interesting approach to achieving HRP cross-linking on the cell membrane by utilising the H_2O_2 as reactive oxygen species (ROS) produced by the cells. Using this technique, cross-linking can be achieved by simply immersing the cells in a solution containing Polymer-Ph and HRP without the need to immerse them in solution containing H_2O_2 (Liu et al. 2014b). Another novel approach is reported in which H_2O_2 is supplied as a ppm-level gas-phase (Sakai et al. 2018). Using this method, homogenous cross-linking can be achieved. More importantly, the cross-linking period can be easily controlled by a simple switch of the air containing H_2O_2 exposure to the solution containing Polymer-Ph + HRP.

While the supply method has been extensively studied, less attention has been given to the function of H_2O_2 as an oxidant that can degrade the polymers. H_2O_2 can produce free radicals that can lead to cleavage of the polymer chain (Chang et al. 2001). Indeed, it is widely used for

degrading various polymers, including gelatin, alginate, chitosan, and HA (Takahashi et al. 1998; Chang et al. 2001; Li et al. 2010).

In particular to gelatin, a previous study has reported that degradation by H_2O_2 reduces the high molecular weight fractions ($> 2 \times 10^5$ Da) and increases the low molecular weight fractions ($< 1 \times 10^5$ Da). H_2O_2 treatment also induces the decomposition of various amino acids in the gelatin molecules, including methionine, tyrosine, and lysinoalanine residues. In general, H_2O_2 degrades gelatin molecules by oxidative cleavage of peptide bonds (Takahashi et al. 1998).

Based on this, H_2O_2 can have a contradicting effect in the HRP-mediated cross-linking: inducing the cross-linking while degrading the Polymer-Ph. Consequently, the contradictory effect of H_2O_2 can affect the mechanical property of the hydrogels. Understanding the dynamics of the mechanical property of the Gelatin-Ph-based hydrogel by H_2O_2, therefore, would be crucial, as it would impact the behaviour of cells cultured on the Gelatin-Ph hydrogel.

5. Overview

The objective of this study is to investigate the influence of H_2O_2-mediated cross-linking and degradation of gelatin-based hydrogels on the cell behaviour. Chapter II focuses on investigating the contradictory effect of H_2O_2 on mechanical property and molecular weight of the Gelatin-Ph and its effect on cell adhesion. Chapter III describes the application of the H_2O_2-mediated cross-linking and degradation of the Gelatin-Ph hydrogel to control myogenesis. Chapter IV describes the modulation of the cell-cycle progression by the stiffness and molecular weight of the Gelatin-Ph/HA-Ph composite hydrogel controlled by H_2O_2 **(Fig. 1-9)**.

In Chapter II, the contradictory effect of H_2O_2 on Gelatin-Ph hydrogel was investigated. H_2O_2 was supplied by exposing air containing 16 ppm H_2O_2 to aqueous Gelatin-Ph and HRP, allowing control of Gelatin-Ph cross-linking by adjusting the exposure time. First, hydrogelation of the Gelatin-Ph was investigated in different HRP concentrations. Next, the

mechanical property of the Gelatin-Ph hydrogel fabricated through different HRP concentrations and the exposure time to air containing H_2O_2 was measured. To demonstrate the role of H_2O_2 in degrading Gelatin-Ph, the molecular weight of Gelatin-Ph was analysed following H_2O_2 exposure. Finally, the effect of these changes on modulating the cell adhesion was studied using human adipose-derived stem cells (hASCs) and rat fibroblast (3Y1) cells.

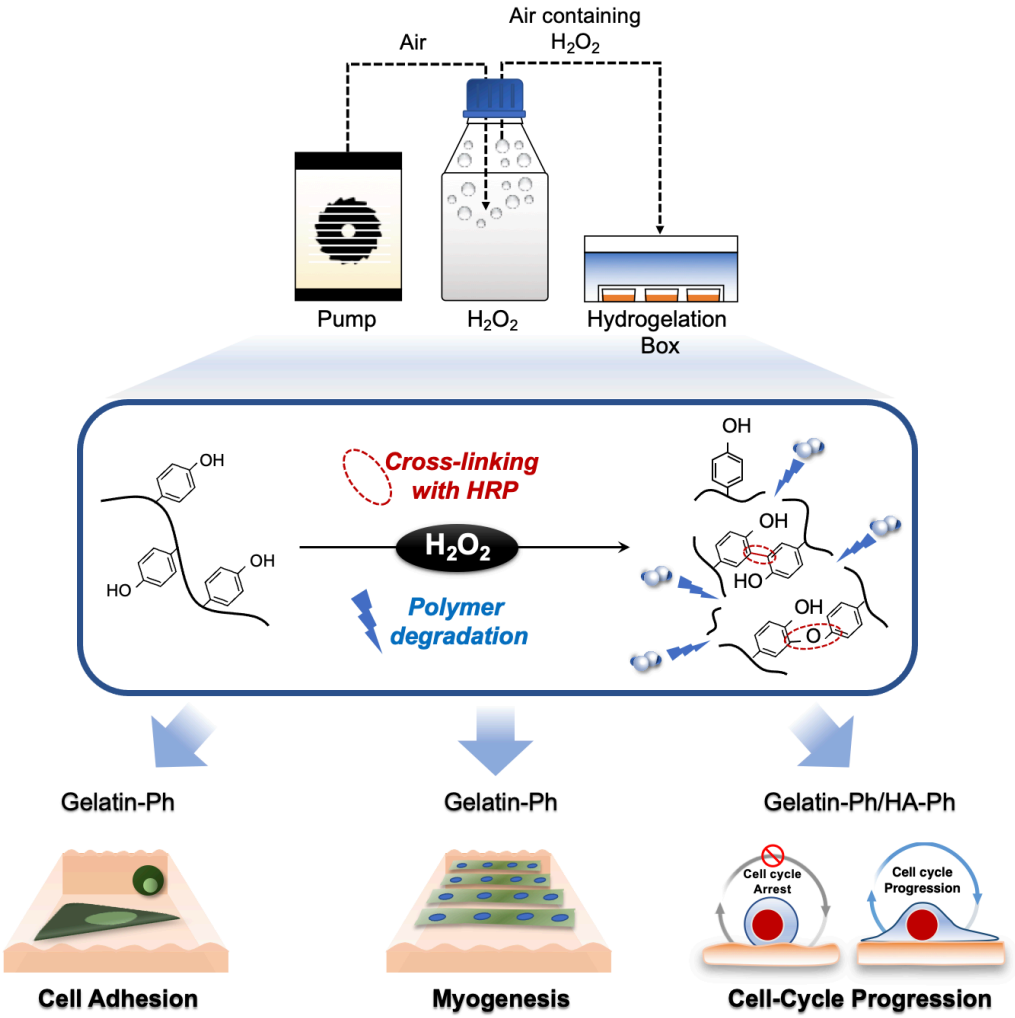

Fig. 1-9 Overview of this study. The contradictory effect of H_2O_2 that simultaneously induce HRP-catalysed cross-linking while also degrade the polymer as oxidant is studied by controlling the exposure time to air containing H_2O_2. The effect of the mechanical property changes of the gelatin-based hydrogels controlled by the air containing H_2O_2 exposure on regulating cell behaviour is studied on cell adhesion, myogenesis, and cell-cycle progression.

In Chapter III, the role of mechanical property of Gelatin-Ph hydrogels mediated by H_2O_2 to control the myoblasts' behaviour was investigated. Mouse myoblast (C2C12) cells were seeded on Gelatin-Ph hydrogel, obtained through different exposure time to air containing H_2O_2. To confirm the cytocompatibility of this method, myoblasts viability was investigated. The adhesion of myoblasts was investigated based on the morphological analysis. Furthermore, the effect of mechanical property changes of Gelatin-Ph on regulating myogenesis was studied by investigating the myoblasts' differentiation to multinucleated myotubes on the resultant hydrogels.

In Chapter IV, this system was applied to control the mechanical property of composite hydrogel composed of Gelatin-Ph and HA-Ph. The composite hydrogel mimics the composition of native ECM. In addition, HA-Ph provides chemical cues in the form of molecular weight and cell-adhesive ligands. This system was utilised to investigate the effect mechanical property of ECM on regulating the cell-cycle progression. Cell-cycle was studied using fluorescent ubiquitylation-based cell-cycle indicator (Fucci2)-expressing human cervical cancer cell line HeLa cells as a widely used cancer cell model and non-transformed mouse mammary gland epithelial cell line NMuMG cells. Initially, the viability of the cells was investigated. Next, the adhesion of the cells was investigated based on their morphological characteristics. The cell-cycle progression on the hydrogels was observed based on the fluorescent changes of the nuclei expressing Fucci2 that changes depending on the cell-cycle phase. To study the mechanism of the cell-cycle regulation, cytoskeleton re-organisation was analysed by F-actin staining.

The results of this study are summarised in General Conclusions. Suggestion for the application of this system is presented in Future Works.

Chapter II

Influence of Hydrogen Peroxide-Mediated Cross-Linking and Degradation on Cell-Adhesive Gelatin Hydrogels

1. Introduction

Gelatin is an important material for various applications in the food, pharmaceutical, and medical fields because of its biodegradability and biocompatibility. Gelatin hydrogel is particularly useful in the tissue engineering due to its ability to promote cell adhesion in/on substrates (Gomez-Guillen et al. 2011; Bae et al. 2015; Agheb et al. 2017). It is well-known that gelatin hydrogels can be obtained by cooling a hot aqueous solution of gelatin to less than 30 °C. However, the gelatin hydrogels obtained through the thermally induced gelation readily dissolve at around 37 °C. It means that the gelatin hydrogels show a gel-to-sol transition in the body and the environment conventionally used for cell culture. Therefore, various methods have been developed to induce the gelatin-based hydrogels to be stable at around 37 °C (Lee and Mooney 2001).

Horseradish peroxidase (HRP)-catalysed gelation of aqueous solutions containing a gelatin derivative with phenolic hydroxyl (Ph) moieties (Gelatin-Ph) is one of the methods which has been used for obtaining gelatin-based hydrogels stable at around 37 °C (Sakai et al. 2009a; Sakai and Nakahata 2017). Due to the good cytocompatibility and biocompatibility (Kondo et al. 2013; Le Thi et al. 2017; Nakahata et al. 2018; Gantumur et al. 2020), the hydrogels have been studied for varieties of biomedical applications, such as vehicles for retinal progenitor cell transplantation (Park et al. 2019), carriers of drugs for bone regeneration (Kondo et al. 2013), cell-laden wound dressing (Yao et al. 2019), and inks for bioprinting (Sakai et al. 2018).

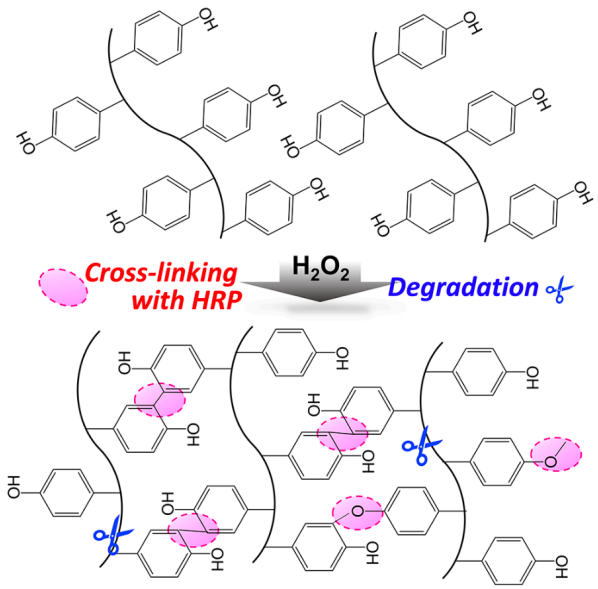

Fig. 2-1 Schematic illustration of contradictory effect of hydrogen peroxide to induce HRP-mediated enzymatic hydrogelation and degradation of the Gelatin-Ph. Reprinted (adapted) with permission from (Mubarok et al. 2021). Copyright 2021 American Chemical Society.

To fabricate the Gelatin-Ph hydrogel via the HRP-catalysed enzymatic gelation, H_2O_2 is consumed for inducing the cross-linking of Ph moieties (**Fig. 2-1**). Apart from the function of inducing the gelation, H_2O_2 is known to induce degradation/depolymerisation of various polymers through oxidation (Takahashi et al. 1998; Li et al. 2010; Liu et al. 2014a). Takahashi *et al*. reported that treatment of gelatin with H_2O_2 reduced the viscosity of its aqueous solution and the melting point of the resultant hydrogels (Takahashi et al. 1998). They demonstrated that these results were caused by the degradation of gelatin molecules through oxidative cleavage of peptide bonds and cross-links (Takahashi et al. 1998).

Although the degradation of polymers by H_2O_2 is widely accepted, its effect on the properties of hydrogels obtained through HRP-catalysed reaction has not been fully studied. In addition, the changes in the properties of hydrogels may affect the surrounding cells. It has been reported that cell behaviours, such as cell morphology (Ni and Chiang 2007; Sun et al. 2018), proliferation (Hadjipanayi et al. 2009; Kalli and Stylianopoulos 2018), differentiation

(Engler et al. 2006; Zhan 2020), and cell death (Ma et al. 2008; Marastoni et al. 2008), were influenced by the properties of adhering substrates.

In this chapter, the contradictory functions of H_2O_2 in increasing hydrogel strength by inducing HRP-catalysed cross-linking; while also reducing hydrogel strength as an oxidant that induces the degradation of gelatin molecules were demonstrated. Moreover, the behaviours of human adipose-derived stem cells and rat fibroblast cells on the hydrogels obtained through the H_2O_2-mediated crosslinking and degradation were reported.

2. Materials and Methods

2.1 Materials

Gelatin from bovine skin (Gelatin Type B) was purchased from Sigma-Aldrich (St. Louis, MO, USA). HRP (200 U mg^{-1}), H_2O_2 aqueous solution (31% w/w), *N*-hydroxysuccinimide (NHS), *N,N*-Dimethylformamide (DMF), catalase from bovine liver, and mitomycin C were purchased from Wako Pure Chemical Industries (Osaka, Japan). Water-soluble carbodiimide hydrochloride (WSCD·HCl) was obtained from Peptide Institute (Osaka, Japan). Gelatin-Ph (1.1×10^{-4} mol-Ph g-Gelatin-Ph^{-1}) was synthesised by conjugating 3-(4-hydroxyphenyl) propionic acid (HPPA) with gelatin in DMF buffered solution (pH 4.7) using WSCD / NHS as previously reported (Hu et al. 2009; Sakai et al. 2017; Gantumur et al. 2019). Human adipose-derived stem cells (hASCs) were obtained from Lonza (Walkersville, MD, USA) and cultured in human Adipose-Derived Stem Cell Growth BulletKit™ Medium (PT-4505, Lonza, Walkersville, MD, USA) containing 10% (v/v) fetal bovine serum (FBS). Rat fibroblast 3Y1 cells were obtained from the Riken BioResource Center (BRC) (Ibaraki, Japan) and grown in Dulbecco's Modified Eagle's Medium (DMEM, Nissui Pharmaceutical, Tokyo, Japan) supplemented with 10% v/v FBS (Bio-fill, Victoria, Australia) in a humidified CO_2 incubator at 37 °C. For cellular morphology analysis, cells were stained with Acti-stain™ 488 Phalloidin

(PHDG1-A, Cytoskeleton Inc., Denver, USA) and DAPI (D9542-5MG, Sigma Life Sciences, St. Louis, MO, USA).

2.2 Gelation Time Measurement

Gelation time was measured according to the method in the literature (Murakami et al. 2007; Sakai and Kawakami 2007; Peng et al. 2009). Briefly, 200 µL of a solution containing 5% w/v Gelatin-Ph and 1, 5, or 15 U mL^{-1} HRP was added to a well of a 48-well plate and stirred using a magnetic bar. The solution was then exposed to air containing H_2O_2 (16 ppm) obtained by blowing air into 1 M H_2O_2 aqueous solution at room temperature (Gantumur et al. 2019). The formation of a gel state was signalled when the magnetic stirring was hindered, and the surface of the solution swelled.

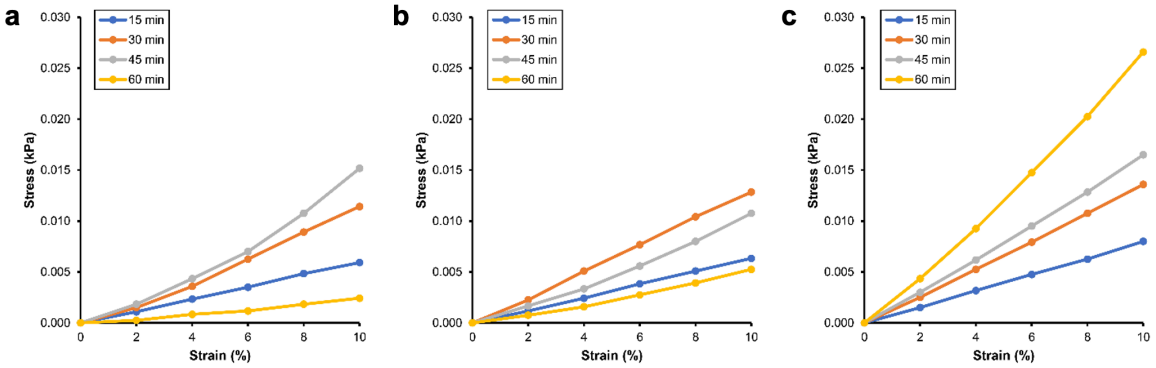

Fig. 2-2 Stress-strain curve of Gelatin-Ph hydrogels containing (a) 1 U mL^{-1}, (b) 5 U mL^{-1}, and (c) 15 U mL^{-1} HRP. Reprinted (adapted) with permission from (Mubarok et al. 2021). Copyright 2021 American Chemical Society.

2.3 Mechanical Property Measurement

The aqueous solution containing Gelatin-Ph and HRP was poured into a 12-well plate at 500 µL $well^{-1}$ and put into a plastic box (13.5 cm × 9.5 cm × 7 cm). The air containing 16 ppm H_2O_2 was continuously supplied into the plastic box for 15, 30, 45, and 60 min. The mechanical

property of the resultant Gelatin-Ph hydrogels was measured using a material tester (EZ-Test, Shimadzu, Kyoto, Japan). The hydrogels were compressed with a probe (diameter, 8 mm) at a compression rate of 1.0 mm min^{-1}. The Young's modulus was calculated from the data obtained in the range of 1 – 10% compression **(Fig. 2-2).**

2.4 Molecular Weight Measurement

Aqueous solutions containing 5% w/v Gelatin-Ph and 0 – 0.15% w/v H_2O_2 were stirred overnight at 60 °C. The molecular weights of Gelatin-Ph contained in the resultant solutions were measured using HPLC equipped with a UV detector (GL-7480, GL Sciences, Tokyo, Japan) and RI detector (RID-20A, SHIMADZU, Kyoto, Japan).

2.5 Cell Adhesion Analysis

Gelatin-Ph hydrogels obtained from a solution containing 5% w/v Gelatin-Ph and 5 U mL^{-1} HRP with different exposure times to air containing H_2O_2 were immersed in PBS for 3 h. Then, the hydrogels were immersed in a culture medium containing 0.1% w/v catalase for 21 h to remove the remaining H_2O_2. Before seeding, hASCs and 3Y1 cells were exposed to 10 μg mL^{-1} mitomycin C for 2 h to terminate cell proliferation and prevent the effect of proliferation influencing the cell morphology evaluation (Bryja et al. 2006). Cells were then seeded on the hydrogels at 5.0×10^3 cells $well^{-1}$ in a fresh cell culture medium. After 24 h of seeding, F-actin and the cell nuclei were stained with Acti-stain™ 488 phalloidin and DAPI, respectively, to observe the cell adhesion. Briefly, cells were fixed with 4% paraformaldehyde for 10 min and permeabilised in 4-(2-hydroxyethyl)-1-piperazineethanesulfonic acid (HEPES) buffer for 5 min. Acti-stain™ 488 Phalloidin (100 nM in PBS) was added for F-actin staining, and the cells were incubated for 30 min, followed by nuclei staining via the addition of 100 nM DAPI in PBS for 10 min. Cell morphology was evaluated by measuring the cell length and width of

more than 50 cells for each set of conditions using ImageJ 15.2k (NIH, Bethesda, MD, USA). The cell aspect ratio was calculated as the ratio between cell length and cell width.

2.6 Statistical Analysis

Data were analysed using SPSS software (IBM SPPS Statistics, Chicago, IL, USA). Statistical analysis was performed by one-way analysis of variance (ANOVA) followed by a post-hoc *t*-test using Tukey HSD for multiple comparisons. Data are presented as means ± standard error (S.E.). Values of $p < 0.05$ were considered to indicate significance.

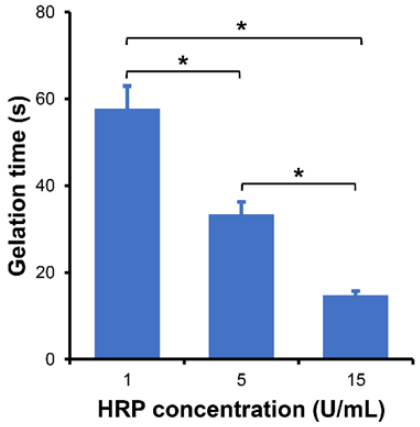

Fig. 2-3 Effect of horseradish peroxidase (HRP) concentration on gelation time of 5% w/v Gelatin-Ph solutions exposed to air containing 16 ppm H_2O_2. Values: means ± S.E. ($n = 5$). *$p < 0.05$, Tukey HSD. Reprinted (adapted) with permission from (Mubarok et al. 2021). Copyright 2021 American Chemical Society.

3. Results and Discussion

3.1 Gelation Time

First, the effect of HRP concentration on the gelation behaviour of Gelatin-Ph solutions exposed to air containing 16 ppm H_2O_2 was investigated. The gelation time was 57 s at 1 U mL^{-1} HRP and decreased with increasing HRP concentration ($p < 0.05$) (**Fig. 2-3**). The shortest gelation time was observed at 15 U mL^{-1} HRP, which had a gelation time of 15 s. This trend is

consistent with those reported in previous publications (Sakai and Kawakami 2007; Sakai et al. 2010; Ren et al. 2015; Sakai et al. 2018). The shorter gelation times at higher HRP concentrations could be caused by the accelerated formation of the phenolic radicals (Ren et al. 2015). The important information obtained from this experiment was that the hydrogels could be obtained within 1 min for all the conditions tested.

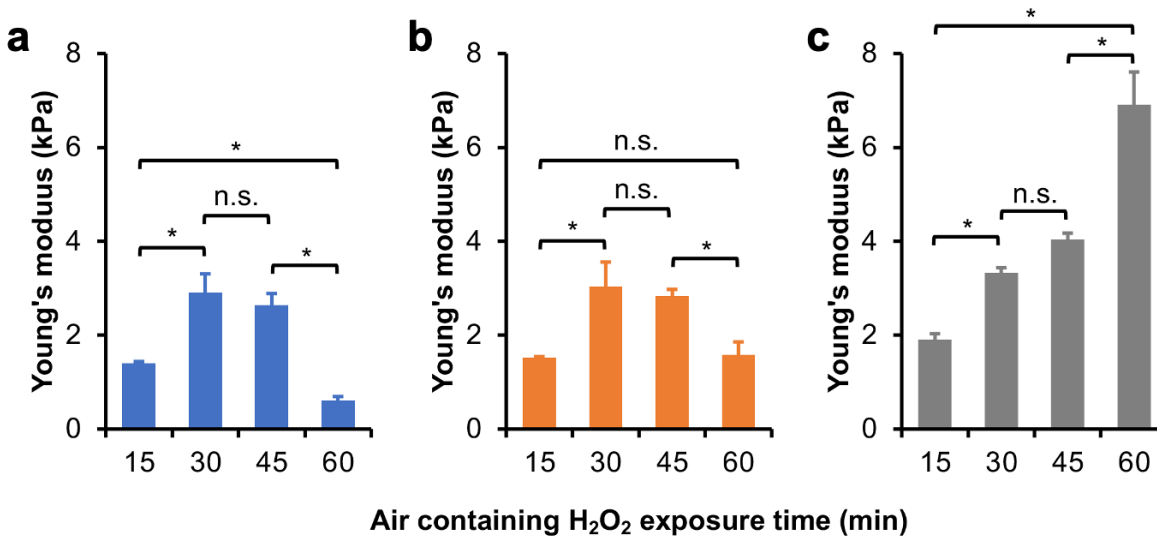

Fig. 2-4 Effect of HRP concentration on Young's modulus of hydrogels obtained from 5% w/v Gelatin-Ph solutions through exposure to air containing 16 ppm H_2O_2 for 15, 30, 45, and 60 min. HRP concentration: (a) 1 U mL^{-1}, (b) 5 U mL^{-1}, and (c) 15 U mL^{-1}. Values: means ± S.E. (n = 3). n.s : $p > 0.05$, *$p < 0.05$, Tukey HSD. Reprinted (adapted) with permission from (Mubarok et al. 2021). Copyright 2021 American Chemical Society.

3.2 Mechanical Property

Next, the effect of the duration of the exposure to air containing H_2O_2 on the stiffness of Gelatin-Ph hydrogels obtained at different HRP concentrations was investigated by measuring the Young's modulus. HRP concentration and the exposure time governed the Young's modulus of Gelatin-Ph hydrogels ($p < 0.05$) (**Fig. 2-4**). The Young's modulus of Gelatin-Ph hydrogels obtained from 5% w/v Gelatin-Ph solution containing 1 U mL^{-1} HRP, increased as

the exposure time was extended to 30 min (**Fig. 2-4 (a)**). The Young's moduli after 15 and 30 min of exposure were 1.4 and 2.9 kPa, respectively. A further increase of the exposure time to 60 min reduced the Young's modulus to 0.6 kPa. The Young's modulus of the hydrogel obtained from the solution containing 5 U mL^{-1} HRP also decreased when the exposure time was increased to 60 min, with the values at 15 min and 60 min of exposure being similar at 1.5 kPa ($p > 0.05$) (**Fig. 2-4 (b)**). In contrast, the Young's modulus of the hydrogels obtained from the solution containing 15 U mL^{-1} HRP did not decrease after 60 min of exposure (**Fig. 2-4 (c)**).

The mechanism of the exposure time-dependent transition of the stiffness of the hydrogels can be explained by the correlation between the degrees of the progress of cross-linking formation catalysed by HRP, HRP inactivation, and Gelatin-Ph degradation, which all involving H_2O_2. The inactivation of HRP (Arnao et al. 1990; Baynton et al. 1994; Carvalho et al. 2006) and degradation of organic molecules including gelatin (Li et al. 2010; Liu et al. 2014a; Mad-Ali et al. 2016) by H_2O_2 has been reported. In this study, H_2O_2 was supplied continuously to the system containing Gelatin-Ph and HRP. It means that the content of the cross-linked Ph moieties should increase with increasing the exposure time to the air containing H_2O_2, unless there are occurrences of HRP inactivation and Gelatin-Ph degradation. Therefore, the results shown in **Fig. 2-4 (a-b)**, showing the decrease of Young's modulus with increasing the exposure time from 45 to 60 min, indicate the occurrences of Gelatin-Ph degradation.

The non-decrease of Young's modulus of the specimens obtained at 15 U mL^{-1} HRP even after increasing the exposure time to 60 min (**Fig. 2-4 (c)**) can be explained by the fact(s) that the extent of the effect of Gelatin-Ph degradation did not outweigh the extent of the effect of crosslink formation due to the high content of HRP, and/or the result of the larger amount of H_2O_2 consumption in HRP-mediated reaction. The higher amount of H_2O_2 consumed for cross-linking means that the amount of H_2O_2 involved in the degradation of Gelatin-Ph was less.

Fig. 2-5 shows the degradation of Gelatin-Ph by H_2O_2: The molecular weight of Gelatin-Ph exposed to H_2O_2 overnight decreased with increasing H_2O_2 concentration. In the Gelatin-Ph gelation system of this study, it is difficult to estimate the amount of H_2O_2 involved in the Gelatin-Ph degradation due to the supply of H_2O_2 from the gas phase and the continuous consumption of the supplied H_2O_2 in HRP-mediated reaction. In addition, it is also difficult to estimate the degree of degradation due to the formation of cross-links between Gelatin-Ph molecules. However, the result shown in **Fig. 2-5** would be sufficient to demonstrate the degradation of Gelatin-Ph in the gelation system.

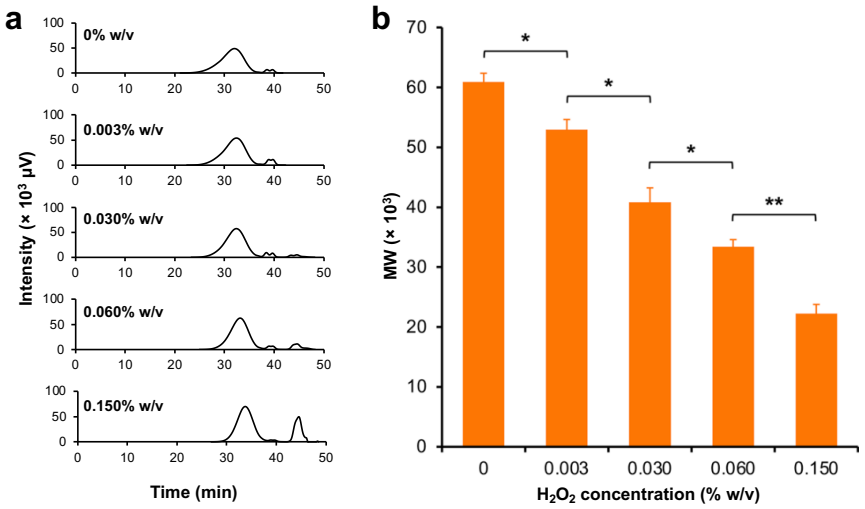

Fig. 2-5 (a) Intensity-time curve and (b) molecular weight of Gelatin-Ph after overnight incubation of 5% w/v Gelatin-Ph solution in the presence of 0, 0.003, 0.030, 0.060, and 0.150% w/v H_2O_2 at 60 °C. Values: means ± S.E. (n = 3). *p < 0.05, **p < 0.005, Tukey HSD. Reprinted (adapted) with permission from (Mubarok et al. 2021). Copyright 2021 American Chemical Society.

Apart from them, it might be thought the effect of drying of the Gelatin-Ph hydrogels during the exposure to air containing H_2O_2 on the Young's modulus of the resultant hydrogels. However, the thought was denied by the result for the change in the weight of hydrogels during 60 min of exposure to air containing H_2O_2 (**Fig. 2-6**). The changes in weight of hydrogels were

less than 0.5% for all the hydrogels obtained from the solutions containing 5% w/v Gelatin-Ph and 1, 5, 15 U mL^{-1} HRP. The very small degree of drying would attribute to the air rich in moisture obtained by blowing air into H_2O_2 aqueous solution.

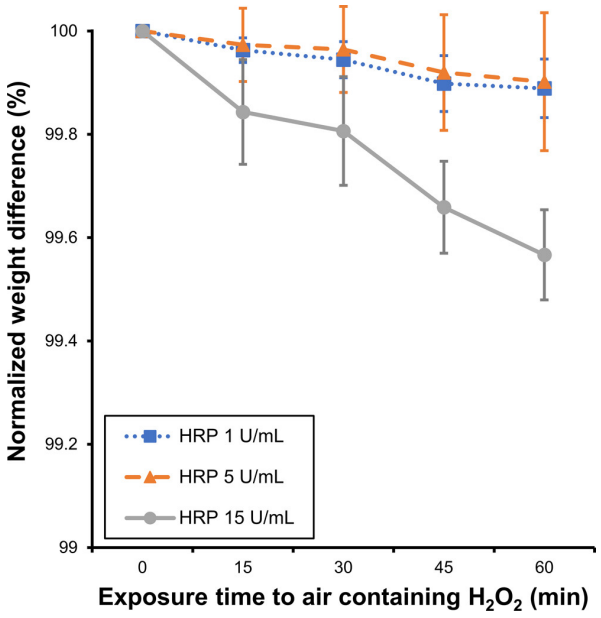

Fig. 2-6 Effect of exposure time to air containing 16 ppm H_2O_2 on the weight of Gelatin-Ph hydrogels obtained from 5% w/v Gelatin-Ph solutions containing 1, 5, and 15 U mL^{-1} HRP. Data normalised against weight measured before exposure to air containing H_2O_2. Values: means ± S.E. (n = 3). Reprinted (adapted) with permission from (Mubarok et al. 2021).

3.3 Cell Adhesion

As described above, the hydrogels obtained from the solution containing 5 U mL^{-1} HRP as a result of 15 and 60 min exposures to air containing 16 ppm H_2O_2, showed similar Young's moduli, despite having different cross-linking densities and different degrees of Gelatin-Ph degradation (**Fig. 2-4 (b)**). It has been reported that substrate mechanical property governs various cell behaviours including proliferation, differentiation, and morphology (Cao et al. 2021). Therefore, next, the effect of these hydrogels on cell morphologies was investigated.

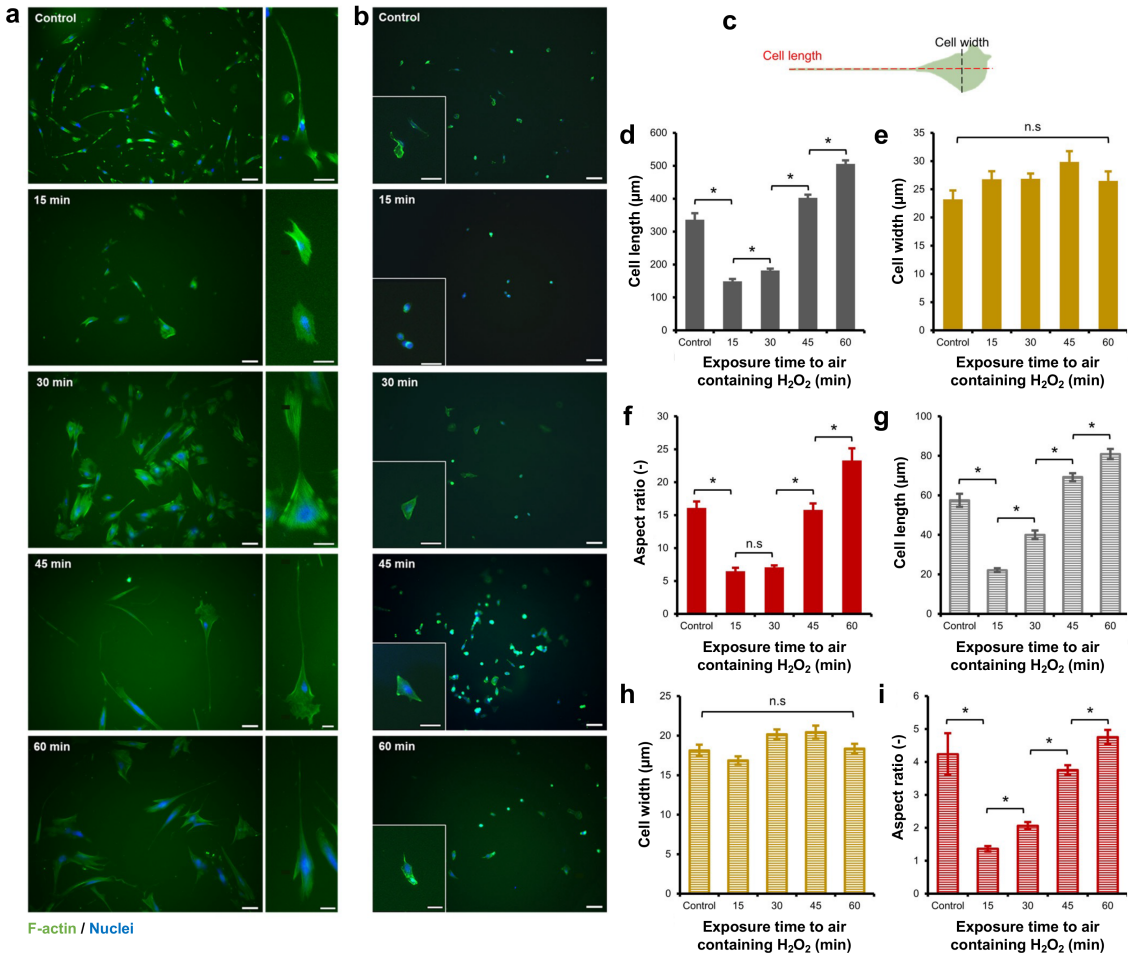

Fig. 2-7 Effect of exposure time to air containing 16 ppm H_2O_2. (a) Morphologies of human adipose-derived stem cells (hASCs) and (b) rat fibroblast 3Y1 cell on Gelatin-Ph hydrogels. Bars: 50 μm. (c) Definitions of cell length and width. (d) Cell length, (e) cell width, and (f) cell aspect ratio of hASCs; (g) cell length, (h) cell width, and (i) cell aspect ratio of 3Y1 cells on Gelatin-Ph hydrogels. Values: means ± S.E. ($n \geq 50$). *$p < 0.05$, Tukey HSD. Gelatin-Ph hydrogels were obtained from 5% w/v Gelatin-Ph solution containing 5 U mL^{-1} HRP. Reprinted (adapted) with permission from (Mubarok et al. 2021). Copyright 2021 American Chemical Society.

The morphologies of hASCs cells and rat fibroblast 3Y1 cells were different, respectively, on each Gelatin-Ph hydrogel obtained following different exposure times to air containing H_2O_2 (**Fig. 2-7**). To visualize the morphological differences, F-actin and the cell nuclei were stained with fluorescent dyes (**Fig. 2-7 (a-b)**), and the aspect ratio of the cells was calculated

as the ratio of cell length and cell width (**Fig. 2-7 (c)**). The aspect ratio of hASCs was the lowest for the hydrogels obtained after 15 min of exposure to air containing H_2O_2 (**Fig. 2-7 (f)**). The value was approximately 40% of that for the cells on the cell culture dish (Control). This marked contrast in the aspect ratio is attributed to the difference in the cell length (**Fig. 2-7 (d)**). The width of the hASCs did not change significantly, regardless of the exposure time or substrate (**Fig. 2-7 (e)**). The length of hASCs on the hydrogels increased with increasing exposure time to air containing H_2O_2, and the length of cells on the hydrogel obtained through 60 min of exposure was about 3.6 times longer than those on the hydrogel obtained through 15 min of exposure. In addition, the longest cells (60 min exposure) were approximately 1.4 times longer than those cultured on the cell culture dish (Control) (**Fig. 2-7 (d)**).

This trend was not specific for hASCs. Similar results were also obtained for rat fibroblast (3Y1) cells (**Fig. 2-7 (g-i)**). The general trend between hASCs and 3Y1 cells is similar. Short exposure time to air containing H_2O_2 resulted in small and circular cells. Meanwhile, increasing the exposure time to air containing H_2O_2 increased the cell elongation, similar to control cells.

The lowest cell size, circularity, and aspect ratio of hASCs and 3Y1 cells found on the hydrogels obtained through 15 min of exposure were consistent with previous reports. It has been reported that hASCs and fibroblasts show circular morphologies on softer substrates and elongated morphologies on stiffer substrates (Yeung et al. 2005; Hadjipanayi et al. 2009; Johnson et al. 2013; Asano et al. 2017).

A notable result inconsistent with these previous reports was that both hASCs and 3Y1 cells showed completely different morphologies (**Fig. 2-7**) on the hydrogels with similar stiffness obtained through 15 and 60 min of exposure (**Fig. 2-4 (b)**). Scott et al. reported a similar result for human aortic adventitial fibroblasts cultured on poly(ethylene glycol)-based hydrogel: the degree of cell elongation was enhanced despite a decrease in Young's modulus (Scott et al. 2020). They explained that the result could be attributed to a smaller hydrogel mesh size (Scott

et al. 2020). In addition, it has been reported that cell adhesion increased for hydrogels obtained from low-molecular-weight polymers (Alsberg et al. 2003; Suga et al. 2015).

In this study, the decrease in Young's modulus when the exposure time of the Gelatin-Ph hydrogels with 5 U mL^{-1} HRP was extended from 45 to 60 min, is thought to be due to the degradation of Gelatin-Ph molecules by H_2O_2. Therefore, the different cell morphologies observed on hydrogels that had similar Young's modulus but different degrees of Gelatin-Ph degradation can be explained by the differences in the molecular weight of Gelatin-Ph in the hydrogels (**Fig. 2-5**).

4. Conclusion

The results presented in this chapter demonstrated the contradictory effect of H_2O_2 on Gelatin-Ph hydrogels obtained through horseradish peroxidase (HRP)-catalysed cross-linking. The exposure of aqueous solutions containing 5% w/v Gelatin-Ph and 1 and 5 U mL^{-1} HRP to the air containing 16 ppm H_2O_2 resulted in gelation within 60 sec. The Young's modulus of the hydrogels increased for 30 min of the exposure. However, extending the exposure time to 60 min reduced the stiffness of the hydrogels. The reduction of the hydrogel stiffness was demonstrated as a result of the degradation of Gelatin-Ph by H_2O_2 from the change in molecular weight of Gelatin-Ph exposed to H_2O_2. Interestingly, in contrast to the observations for Young's modulus, prolonging the exposure time to air containing H_2O_2 resulted in a continued increase of the cell length and aspect ratio of human adipose-derived stem cells and rat fibroblast cells that adhered to the resulting hydrogels. From these results, it is concluded that the effects of H_2O_2-induced changes in the mechanical property of the Gelatin-Ph can be used to control the behaviour of the adhering cells.

Chapter III

Tuning Myogenesis by Controlling Gelatin Hydrogel Properties through Hydrogen Peroxide-Mediated Cross-Linking and Degradation

1. Introduction

In previous chapter, the air containing H_2O_2-mediated changes in stiffness and molecular weight of Gelatin-Ph are demonstrated to affect the adhesion of stem cells and fibroblast cells. Following this demonstration, the possibility of using this system in skeletal muscle tissue engineering is investigated. This chapter focuses on the application of the contradictory function of H_2O_2 to control the properties of the Gelatin-Ph hydrogel on modulating the myogenesis.

Skeletal muscle is the largest component of the human body, accounting for 30% – 40% of body mass (Kim et al. 2002; Csapo et al. 2020). In the occurrence of traumatic injuries or degenerative diseases, skeletal muscle can be damaged, which causes a physiological impairment. To rescue the physiological function, the formation of new muscle cells (myogenesis) is needed. While native cells could regenerate the muscle tissue, controlling the fate of these cells to differentiate into muscle cells is difficult due to the complex interaction between the intrinsic factors of the cells and external factors, including their microenvironment. The tissue engineering approach has garnered great interest since it provides an *in vitro* model to study the physiological phenomenon regulating myogenesis that could improve the efficiency of cell therapy (Rossi et al. 2010; Alarcin et al. 2021).

Among the important factors that govern myogenesis are the materials comprising the extracellular matrix (ECM) and the mechanical property of the ECM. To study the mechanical property effect of the substrate on myoblasts, most studies utilised synthetic materials such as

poly(ethylene glycol) diacrylate (PEGDA), poly(vinyl alcohol) (PVA), and poly(acrylamide) (Maleiner et al. 2018; Narasimhan et al. 2021). Zahari et al. utilised laminin-coated poly(methyl methacrylate) nanofiber scaffold (Zahari et al. 2017), while Shin et al. reported the use of poly(lactic-co-glycolic acid) (Shin et al. 2015a). Additionally, graphene oxide-based matrix is also widely used to control myoblast differentiation (Shin et al. 2015b; Kumar and Parekh 2020). However, these materials are not components of natural ECM and suffer from the toxicity of the uncross-linked monomers and photo-crosslinkers (Maleiner et al. 2018; Narasimhan et al. 2021).

To model the native ECM environment, gelatin is widely used due to its excellent biocompatibility and biodegradability (Jaipan et al. 2017). In recent years, several studies have reported the application of gelatin-based hydrogel to control myoblasts behaviour. Hayashi et al. reported gelatin-conjugated supramolecular hydrogels with switchable stiffness (Hayashi et al. 2022). While C2C12 adhesion showed dynamic changes according to the stiffness, this study does not report the myoblasts differentiation. Denes et al. fabricated micropatterned gelatin hydrogels to study the myotube orientation (Denes et al. 2019). Du et al. also successfully achieved directed cell migration and myotube formation using 3D-printed gelatin methacrolyl (GelMA) micropatterns on surface coated with thermo-responsive material poly(*N*-isopropylacrylamide) (Du et al. 2019). However, these studies do not consider the effect of mechanical property of the gelatin hydrogel which also plays a key role in myogenesis.

In Chapter II, the contradictory effect of H_2O_2 in Gelatin-Ph hydrogel is demonstrated, which impacted the mechanical property and molecular weight of the hydrogel (Mubarok et al. 2021). This system exploits the contradictory effect of H_2O_2 that simultaneously induces the HRP-catalysed cross-linking while also degrading the polymer as oxidant **(Fig. 3-1 (a))**. Using this system, the adhesion of stem cells and fibroblast can be controlled (Mubarok et al. 2021).

However, there are no reports that study the effect of the dynamics of the mechanical property of the Gelatin-Ph hydrogel by H_2O_2 to control the myogenesis.

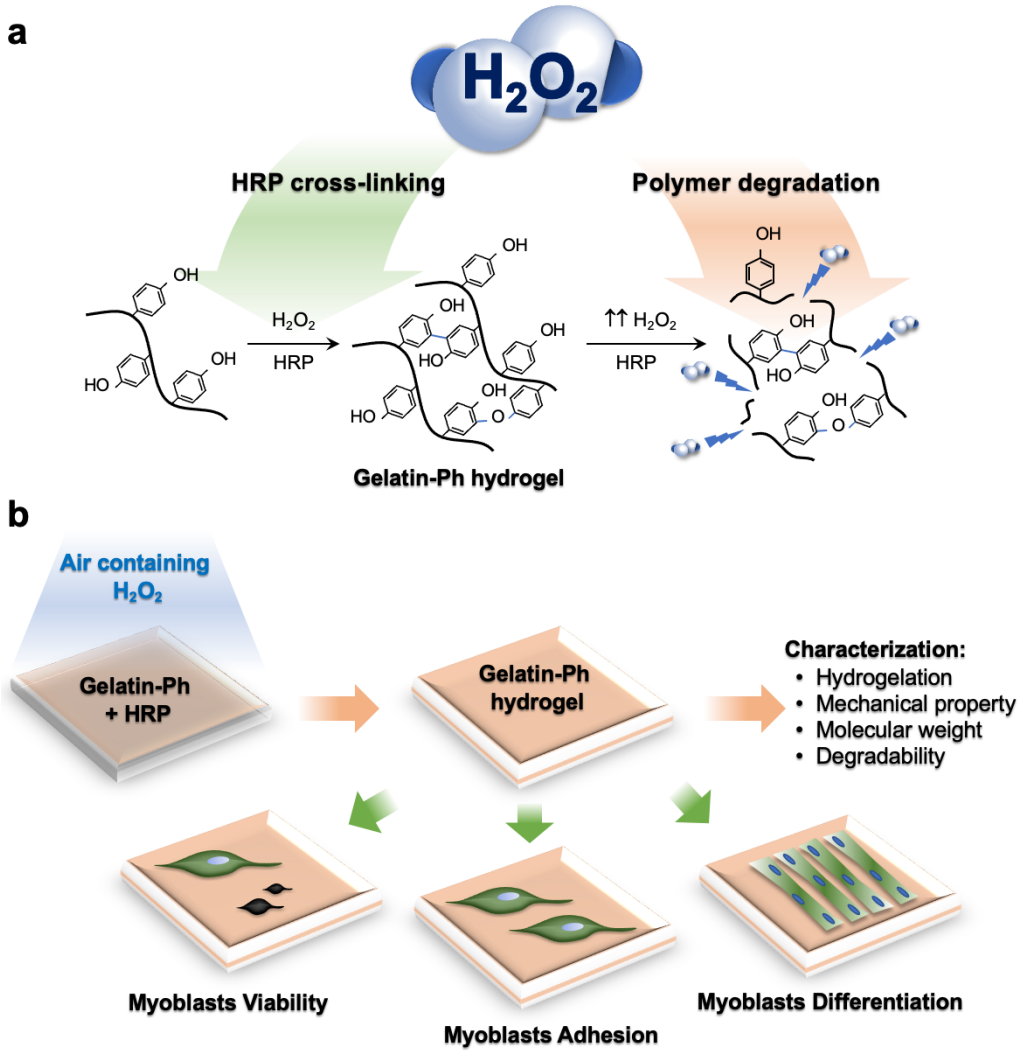

Fig. 3-1 (a) The conceptual scheme of the contradictory function of hydrogen peroxide (H_2O_2) to induce horseradish peroxidase (HRP)-catalysed cross-linking and polymer degradation of the Gelatin-Ph. (b) Experimental scheme of this study. Gelatin-Ph hydrogels fabricated by tuning air containing H_2O_2 exposure time were characterized, and the effect on myoblasts viability, adhesion, and differentiation was studied. Reprinted from (Mubarok et al. 2022a) with permission from MDPI.

In this chapter, the effect of H_2O_2–mediated control of the mechanical property of Gelatin-Ph on modulating myogenesis was reported. To address this, the Gelatin-Ph hydrogel by

exposing air containing H_2O_2 at different exposure time and the hydrogel properties were characterised. The modulatory effect of these mechanical property changes of Gelatin-Ph on myoblasts behaviour is studied to the myoblasts' adhesion and viability. In addition, the influence of the H_2O_2 contradicting effect on the formation of myotubes on the Gelatin-Ph hydrogel was investigated **(Fig. 3-1 (b))**.

2. Materials and Methods

2.1 Materials

Gelatin from bovine (type B, ~226 g Bloom) was purchased from Sigma-Aldrich (St. Louis, MO, USA). NHS, DMF, HPPA, H_2O_2 aqueous solution (31% w/w), HRP (190 U mg^{-1}), catalase from bovine liver, collagenase, and 4% w/v paraformaldehyde in PBS were purchased from FUJIFILM Wako Pure Chemical (Osaka, Japan). WSCD·HCl was purchased from Peptide Institute (Osaka, Japan). DMEM was purchased from Nissui (Tokyo, Japan). Calcein-AM was purchased from Nacalai Tesque Inc. (Kyoto, Japan). Propidium iodide (PI) and -Cellstain®- DAPI solution were purchased from Dojindo, (Kumamoto, Japan). Phalloidin-iFluor 647 Reagent (ab176759) was purchased from Abcam (Cambridge, UK).

2.2 Gelatin-Ph Preparation

Gelatin-Ph was prepared based on the previously reported methods (Hu et al. 2009; Wang et al. 2010b). Briefly, gelatin was conjugated with HPPA in DMF buffer (pH 4.7) via WSCD / NHS chemistry. After 20 h, the solution was dialysed in H_2O to remove the remaining HPPA, followed by freeze-drying. The presence of the Ph group introduced to the Gelatin-Ph was observed based on the peak at 275 nm **(Fig. 3-2)** using a UV-Vis spectrometer (UV-2600, Shimadzu, Kyoto, Japan). The Ph-content was measured at 2.3×10^{-4} mol-Ph g-Gelatin-Ph^{-1} based on the tyramine standard**.**

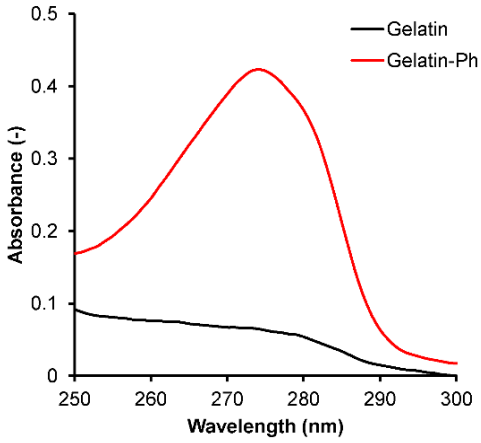

Fig. 3-2 UV-Vis absorbance of unmodified gelatin and Gelatin-Ph. Reprinted from (Mubarok et al. 2022a) with permission from MDPI.

2.3 Gelation Time Measurement

Gelation time was measured based on previous reports (Peng et al. 2009; Mubarok et al. 2021). PBS (pH 7.4) containing 3.0% w/v Gelatin-Ph and 0.1, 0.5, and 1 U mL^{-1} HRP was added to a well of a 48-well plate at 200 µL $well^{-1}$. Air containing H_2O_2 (16 ppm) prepared by blowing air into 1 M H_2O_2 solution was then exposed to the polymer solution that was continuously stirred with a magnetic stirrer. Gel formation was indicated by the swelling of the surface and the hindrance of the magnetic stirrer.

2.4 Mechanical Property Measurement

Air containing H_2O_2 was exposed for 15 – 60 min to 600 µL PBS containing 3.0% w/v Gelatin-Ph and 1 U mL^{-1} HRP in a 12-well plate. Young's modulus of the fabricated Gelatin-Ph hydrogel was measured using a material tester (EZ-SX, Shimadzu, Kyoto, Japan). Hydrogels were compressed with a probe (⌀: 8 mm) at a compression rate of 6.0 mm min^{-1}. The Young's modulus was calculated based on the stress-strain curve with compression strain of 1 – 3% **(Fig. 3-3)**.

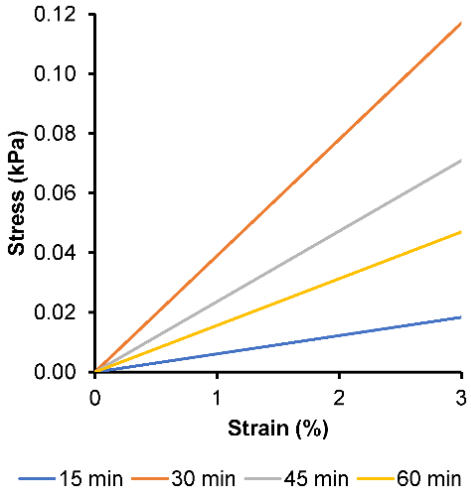

Fig. 3-3 Stress-strain curve of Gelatin-Ph hydrogel fabricated by exposing solution containing 3.0% w/v Gelatin-Ph and 1 U mL^{-1} HRP with air containing H_2O_2 for 15, 30, 45 and 60 min. Reprinted from (Mubarok et al. 2022a) with permission from MDPI.

2.5 Enzymatic Degradation

Gelatin-Ph hydrogels were immersed in PBS for 24 h to reach an equilibrium state. PBS was then changed to PBS containing 120 µg mL^{-1} collagenase. Time for complete degradation of the hydrogel was observed using OLYMPUS Provi CM20 (Olympus, Tokyo, Japan).

2.6 Molecular Weight Measurement

PBS containing 3.0% w/v Gelatin-Ph was exposed with air containing H_2O_2 for 0, 15, 30, 45, and 60 min. The molecular weights of Gelatin-Ph were then measured based on the intensity-time curve **(Fig. 3-4)** using HPLC (LC-20AD, Shimadzu, Kyoto, Japan) and RI detector (RID-20A, Shimadzu, Kyoto, Japan).

2.7 Cell Culture

Mouse muscle myoblasts C2C12 cell line was obtained from RIKEN Cell Bank (Ibaraki, Japan). C2C12 was cultured in growth medium consisting of low glucose DMEM supplied

with 10% v/v fetal bovine serum (FBS). Cells were cultured at 37 °C incubator supplied with 5% CO_2.

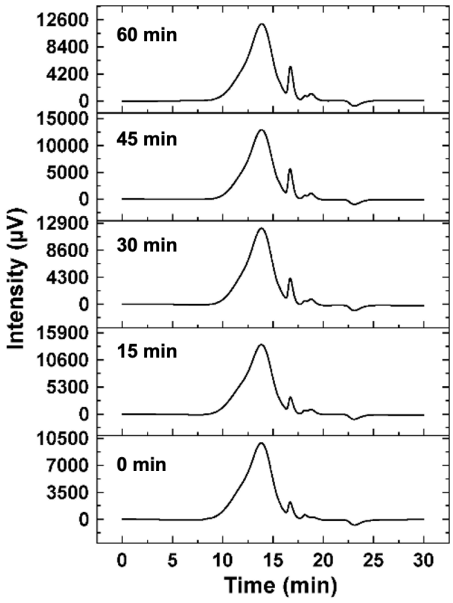

Fig. 3-4 Intensity-time curve of the Gelatin-Ph exposed with air containing H_2O_2 for 0 – 60 min. Reprinted from (Mubarok et al. 2022a) with permission from MDPI.

2.8 Cell Viability and Adhesion Analysis

The hydrogel was fabricated by exposing 600 μL well^{-1} PBS containing 3.0% w/v Gelatin-Ph and 1 U mL^{-1} HRP to air containing H_2O_2 for 15 – 60 min. One millilitre of growth medium containing 1 mg mL^{-1} catalase was added to the hydrogel to remove the remaining H_2O_2. After overnight incubation in medium containing catalase, the hydrogels were washed with PBS and growth medium. C2C12 cells were then seeded on the hydrogel or culture well plate as control at 3.6×10^3 cells cm^{-2}. The viability of the cells was observed after 2 days of culture by staining the cells with 3.3 μg mL^{-1} Calcein-AM / 3.3 μg mL^{-1} propidium iodide (PI) in PBS for 10 min, which stained the viable and dead cells, respectively. Calcein-AM/PI-stained cells were observed using a fluorescence microscope (BZ-9000, Keyence, Osaka, Japan). The viability of the cells was calculated as the percentage of the number of viable cells / total number of cells.

To confirm the adhesion of the cells on the hydrogels, cells stained with Calcein-AM were observed using confocal laser-scanning microscope (C2; Nikon, Tokyo, Japan). Cell adhesion was analysed based on the morphological characteristics of the Calcein-AM-stained cells observed on day 2 of culture using fluorescence microscope. Cell morphological parameters, including cell area and circularity, were measured using ImageJ. Circularity was calculated as $4\pi \times (\text{area} / \text{perimeter}^2)$.

2.9 Cell Differentiation Analysis

C2C12 were seeded onto the culture well plate (control) and Gelatin-Ph hydrogels at a density of 2.6×10^4 cells cm^{-2}. After one day, growth medium was changed to a differentiation medium consisting of DMEM containing 2% v/v horse serum. The differentiation medium was replenished every two days and the multinucleated myotubes were observed on day 6 post-induction (Asano et al. 2012; Asano et al. 2015). Myotubes were observed by staining the cells with Phalloidin-iFluor 647 Reagent and -Cellstain®- DAPI solution. Briefly, cells were fixed with 4% paraformaldehyde in PBS for 30 min, permeabilised in HEPES (pH 5.5) for 10 min, followed by staining with Phalloidin (1×) in PBS for 60 min and DAPI (100 nM) in PBS for 30 min. The numbers of myotubes and nuclei, as well as myotubes length, were analysed using ImageJ. The fusion index was calculated as the percentage of the number of nuclei in myotubes/total number of nuclei.

2.10 Statistical Analysis

Data were analysed using Microsoft® Excel® 2019 version 1808 (Microsoft Corp., Redmond, WA, USA). Statistical analysis was conducted using a one-way analysis of variance (ANOVA). Post hoc *t*-test was conducted using Tukey HSD, with p-value of < 0.05 was considered significantly different.

3. Results and Discussion

3.1 Preparation and Characterisation of Gelatin-Ph Hydrogel

Gelatin-Ph was prepared by conjugating the gelatin with HPPA via WSCD / NHS chemistry in DMF buffer pH 4.7 **(Fig. 3-5 (a))**. Next, the hydrogelation of Gelatin-Ph was investigated. In this study, hydrogelation is induced by HRP-catalysed cross-linking in the presence of air containing H_2O_2 **(Fig. 3-5 (b))**. Exposing air containing 16 ppm H_2O_2 to a PBS containing 3.0% w/v Gelatin-Ph and 0.1, 0.5, and 1.0 U mL^{-1} HRP resulted in hydrogel formation within 35 s. Additionally, the increase in the HRP concentration resulted in a shorter gelation time **(Fig. 3-5 (c))**. The shorter gelation time could be mediated by the higher phenolic radical generation in the higher HRP concentration (Ren et al. 2015).

The effect of the exposure time to air containing H_2O_2 on the properties of the Gelatin-Ph hydrogel was then investigated. The hydrogel was fabricated by exposing PBS containing 3.0% w/v Gelatin-Ph and 1 U mL^{-1} HRP with air containing H_2O_2 for 15, 30, 45, and 60 min. These parameters were selected considering the ease of handling in room temperature. At 5.0% w/v, Gelatin-Ph solution quickly form hydrogel at room temperature, while at 1.0% w/v, the resultant hydrogels are too weak to handle for experiments. In addition, 1 U mL^{-1} HRP is used since previous studies have reported an H_2O_2-mediated dynamic of stiffening and softening of the hydrogels using a similar setup (Mubarok et al. 2021). The mechanical property of the hydrogel was investigated by measuring the Young's modulus. The Young's modulus of Gelatin-Ph hydrogels increased as the exposure time was extended, from 0.77 ± 0.07 kPa at 15 min and peaked at 30 min at 3.53 ± 0.55 kPa. Further extending the exposure time to 45 and 60 min led to gradual decreases in the Young's modulus of the hydrogel to 2.79 ± 0.10 kPa and 1.97 ± 0.21 kPa, respectively **(Fig. 3-5 (d))**. Additionally, enzymatic degradation by collagenase showed a shorter time for complete degradation on softer hydrogel obtained from 15 and 60 min of the exposure **(Fig. 3-5 (e))**.

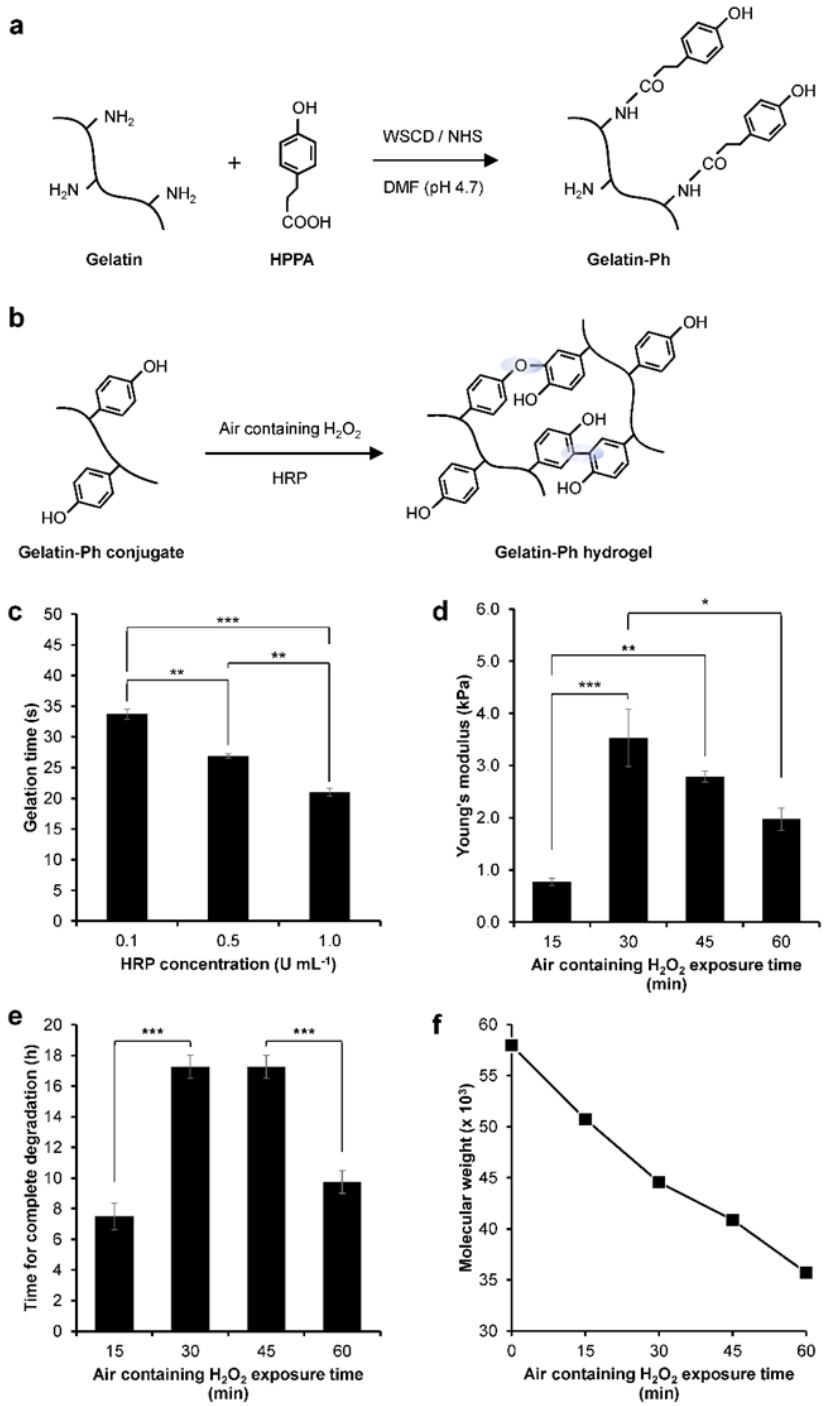

Fig. 3-5 (a) Schematic of Gelatin-Ph preparation by conjugating gelatin with 3-(4-hydroxyphenyl) propionic acid (HPPA) using WSCD / NHS reaction. (b) Schematic of HRP-catalysed cross-linking. (c) Gelation time of Gelatin-Ph hydrogel. Bar: S.E. (n = 3). (d) Young's modulus of Gelatin-Ph hydrogel obtained through exposing 16 ppm air containing H_2O_2 for 15 – 60 min. Bar: S.E. (n = 5). (e) Degradability of Gelatin-Ph hydrogel by collagenase. Bar: S.E. (n = 4). (f) Molecular weight of Gelatin-Ph exposed with air containing H_2O_2 for 0 – 60 min. *p < 0.05, **p < 0.005, ***p < 0.0005, Tukey HSD. Reprinted from (Mubarok et al. 2022a) with permission from MDPI.

The trend in the mechanical property of the hydrogel that shows an initial increase, peaked at 30 min, followed by a reduction in the Young's modulus in prolonged exposure time **(Fig. 3-5 (d))** is consistent with the results demonstrated in the previous chapter. Decreased Young's Moduli of Gelatin-Ph hydrogel in prolonged exposure to air containing 16 ppm H_2O_2 could be a consequence of cross-linking inhibition due to HRP inactivation. Prolonged exposure increased the concentration of H_2O_2 that generated excess phenoxy radicals. The attack of these excess radicals induces side reactions in the peroxidase catalytic cycle that inhibit the cross-linking (Huang et al. 2005; Carvalho et al. 2006; Reihmann and Ritter 2006; Ogushi et al. 2009). Further inactivation in higher H_2O_2 could also have occurred due to HRP denaturation (Carvalho et al. 2006).

Additionally, the decreasing Young's modulus at 45 – 60 min exposure time could also be caused by the degradation of Gelatin-Ph by H_2O_2. Molecular weight measurements showed a decreasing molecular weight of Gelatin-Ph following exposure with air containing H_2O_2 for 15 – 60 min **(Fig. 3-5 (f))**, demonstrating the Gelatin-Ph degradation in extended H_2O_2 exposure. H_2O_2 produced free radicals such as $H\cdot$, $O\cdot$, and $OH\cdot$ that could induce cleavage to degrade the polymer (Chen et al. 2019). Indeed, previous studies have reported that H_2O_2 could degrade a variety of materials, including gelatin, via oxidation (Takahashi et al. 1998; Chang et al. 2001; Li et al. 2010).

3.2 Myoblasts Viability

Cell-substrate interaction is important in forming muscle cells (myogenesis) during embryonic development and post-injury. In addition, understanding the effect of the mechanical property of the microenvironment is also important for studying muscle regeneration *in vitro*, which provides a crucial foundation for developing functional artificial tissues and *in vivo* or translational study (Rossi et al. 2010; Alarcin et al. 2021). Therefore, the

effect of Young's moduli and molecular weight changes of the Gelatin-Ph hydrogel by air containing H_2O_2 to regulate myoblasts' behaviour is investigated.

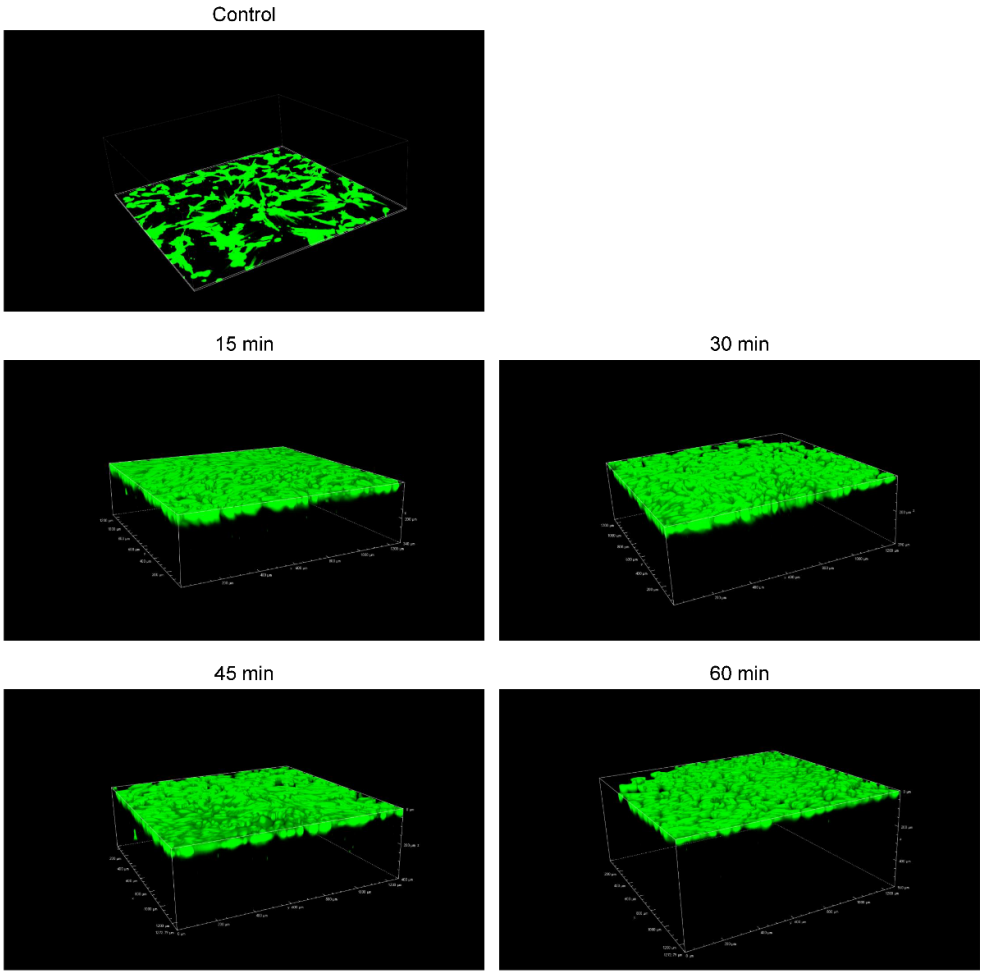

Fig. 3-6 Confocal laser-scanning microscope observation of the C2C12 myoblasts on culture well plate (control) and Gelatin-Ph hydrogel obtained through exposure to air containing H_2O_2 for 15, 30, 45 and 60 min. Reprinted from (Mubarok et al. 2022a) with permission from MDPI.

In this study, C2C12 cells were used as the well-established myoblast cell line widely used as skeletal muscle model (McMahon et al. 1994; Burattini et al. 2004; Ikeda et al. 2017; Denes et al. 2019). Initially, the cell attachment on the hydrogel was confirmed using confocal laser scanning microscopy **(Fig. 3-6)**. The viability of C2C12 myoblasts on the Gelatin-Ph hydrogels

was then investigated. Viability was analysed based on Calcein-AM / propidium iodide (PI) staining, which stained live and dead cells, respectively **(Fig. 3-7 (a))**. C2C12 cells showed high viability (> 94%) of the cells, independent of the exposure time to air containing H_2O_2 **(Fig. 3-7 (b))**. This result showed that while air containing H_2O_2 used in this study might intuitively be thought to induce cell death, removal by catalase is sufficient to minimise or remove the toxic effect on cells. Additionally, the high viability of the cells could also be mediated by the well-known biocompatibility of Gelatin-Ph (Kondo et al. 2013; Le Thi et al. 2017).

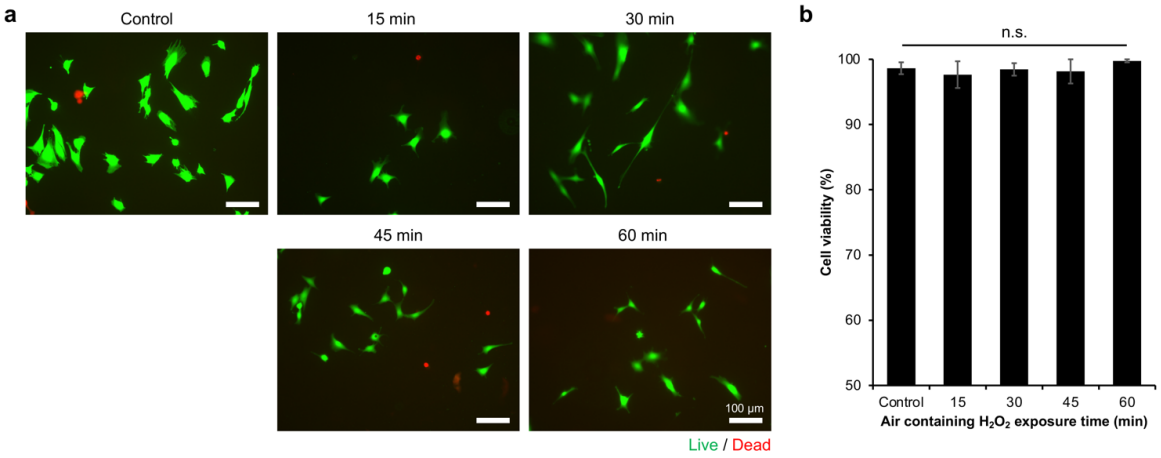

Fig. 3-7 The viability of C2C12 myoblasts on Gelatin-Ph hydrogels obtained through varying air containing H_2O_2 exposure time. (a) Fluorescence micrograph of C2C12 myoblasts on day 2 of culture stained with Calcein-AM and propidium iodide (PI), which stained live and dead cells, respectively. (b) Viability of C2C12 myoblasts on the Gelatin-Ph hydrogels. Cells cultured on the culture well plate were used as control. Data presented as means ± S.E. (n = 6). n.s.: p > 0.05, Tukey HSD. Reprinted from (Mubarok et al. 2022a) with permission from MDPI.

3.3 Myoblasts Adhesion

Based on the Calcein-AM staining during viability analysis, it was observed that cells had different morphology on the hydrogels (**Fig. 3-7 (a)**). Previous studies have also reported that the Calcein-AM, which stained the cytoplasm, allows observation of the cell morphology

(Catelas et al. 2006; Agarwal et al. 2014). The difference in cell morphology could reflect the cell adhesion on the hydrogel. Therefore, the adhesion of myoblasts was investigated by analysing the morphology of the Calcein-AM-stained cells on the resultant Gelatin-Ph hydrogel.

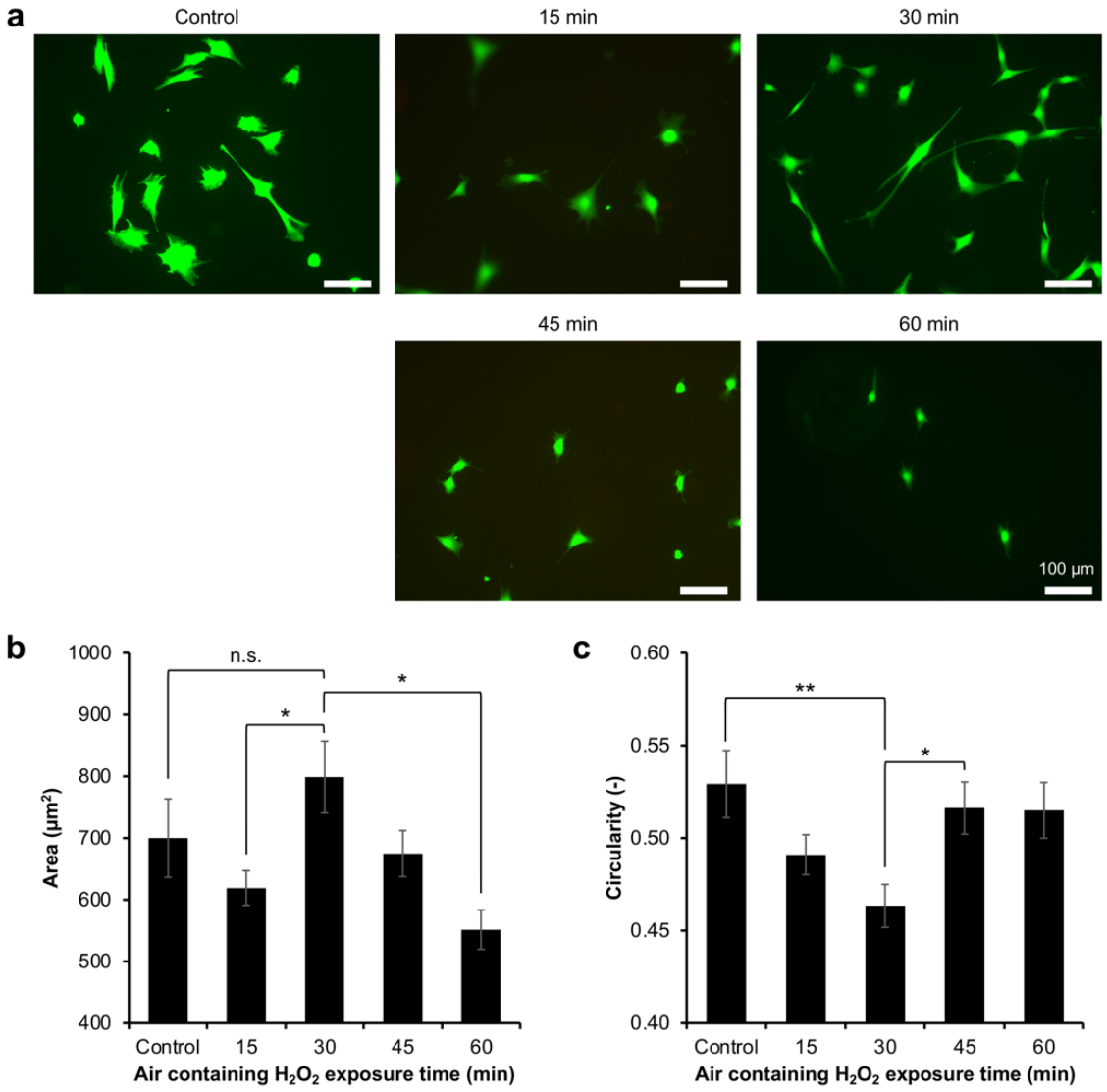

Fig. 3-8 Adhesion of C2C12 myoblasts on Gelatin-Ph hydrogels obtained through exposure to air containing 16 ppm H_2O_2 for 15 to 60 min. (a) Fluorescence observation of C2C12 myoblasts stained with Calcein-AM cultured on the hydrogel for 2 days. As a control, cells were cultured on the culture well plate. (b) Cell area and (c) circularity of C2C12 cells cultured on the resultant hydrogel. Data presented as means ± S.E. ($n \geq 114$ cells). n.s.: $p > 0.05$, *$p < 0.05$, **$p < 0.005$, Tukey HSD. Reprinted from (Mubarok et al. 2022a) with permission from MDPI.

Myoblasts showed different morphologies on Gelatin-Ph hydrogels obtained through different H_2O_2 exposure times **(Fig. 3-8 (a))**. The cells cultured on the hydrogel obtained through 30 min of the exposure, which has the highest mechanical property, had a large and elongated morphology, shown from the largest cell area (**Fig. 3-8 (b))** and lowest cell circularity **(Fig. 3-8 (c))**. In contrast, cells cultured on hydrogels obtained through 15 min and 60 min of exposure to air containing H_2O_2 that have lower stiffness, had more circular morphology shown from lower cell area and higher circularity.

These results show that the adhesion of myoblasts depends on the stiffness of the Gelatin-Ph hydrogel. This phenomenon is similar to previous studies that cultured human mesenchymal stem cells, human adipose-derived stem cells and fibroblasts on Gelatin-Ph hydrogel (Wang et al. 2010a; Mubarok et al. 2021). Additionally, smooth muscle cells and myoblasts also showed stiffness-dependent cell spreading on collagen-coated polyacrylamide gels and alginate hydrogel (Engler et al. 2004a; Engler et al. 2004b; Boontheekul et al. 2007). For adherent cells, including myoblasts, the adhesion dynamic depends on actin polymerization and tension. Stiffer substrate allows actin polymerization and assembly to occur and cells to maintain the cytoskeletal tension, which resulted in the cell elongation (Parsons et al. 2010; Iskratsch et al. 2014). In contrast, cells cultured on the soft substrate cannot form F-actin bundles and stress fibres, thus, cells appear in round morphology (Dupont 2016).

Interestingly, it was also found that cells cultured on Gelatin-Ph hydrogel obtained through 30 min of the exposure time have more elongated shape than cells on the plastic surface of the culture well plate, observed from the significantly lower circularity ($p < 0.005$, Tukey HSD) **(Fig. 3-8 (c))**. The stiffness of the culture well plate is much higher (~1 GPa) (Syed et al. 2015), than the Gelatin-Ph hydrogel (0.77 – 3.53 kPa). Therefore, despite having lower stiffness, the cell-adhesive property of Gelatin-Ph could be beneficial to control the elongation of the myoblasts. This phenomenon is possibly mediated by the focal adhesion kinase (FAK), the

regulator of the cell elongation, that is activated by the interaction between RGD of the Gelatin-Ph with integrins (Katoh 2020).

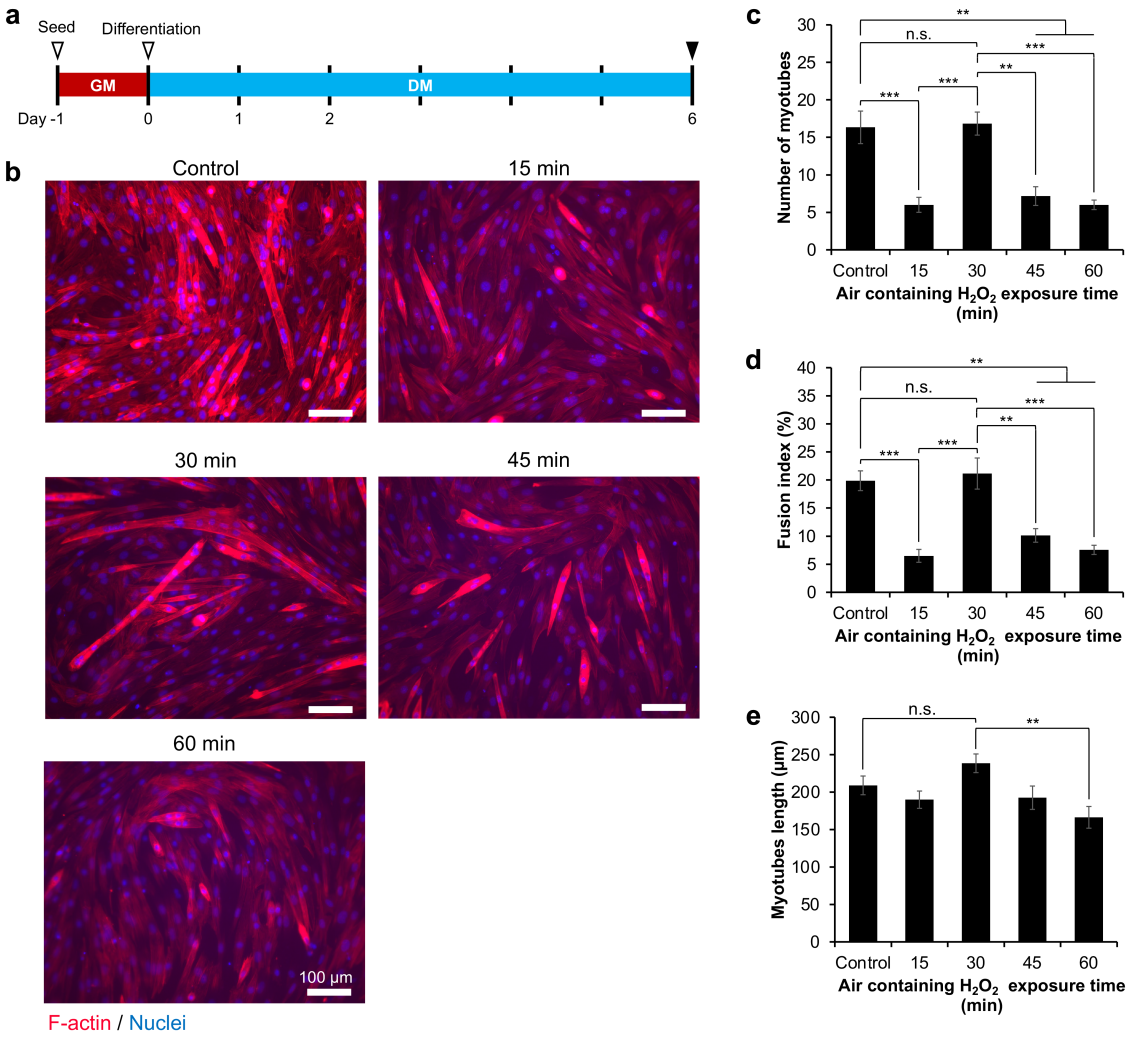

Fig. 3-9 The differentiation of myoblasts to myotubes on the Gelatin-Ph hydrogel fabricated by altering the exposure time to air containing 16 ppm H_2O_2 for 15–60 min. (a) Experimental setup for inducing differentiation. After seeding, cells were cultured in growth medium (GM: DMEM + 10% v/v fetal bovine serum). After 1 day in GM, the medium was changed to differentiation medium (DM: DMEM + 2% v/v horse serum). (b) Fluorescence observation of C2C12 cells after 6 days in differentiation medium stained with phalloidin and DAPI, staining F-actin and nuclei, respectively. (c) Number of myotubes (n = 6), (d) fusion index (n = 6), and (e) myotubes length ($n \geq 24$). Bar: S.E. n.s.: $p > 0.05$, $^{**}p < 0.005$, $^{***}p < 0.0005$, Tukey HSD. Reprinted from (Mubarok et al. 2022a) with permission from MDPI.

3.4 Myoblasts Differentiation

Finally, myoblasts' differentiation into myotubes on the Gelatin-Ph hydrogels obtained from different exposures to H_2O_2 was investigated. First, the cells were seeded on the culture well plate (control) and Gelatin-Ph hydrogels. After 1 day in growth medium (DMEM + 10% v/v FBS), cells density had already reached > 80% confluence. Therefore, the medium was changed to a differentiation medium consisting of DMEM supplied with 2% v/v horse serum **(Fig. 3-9 (a))**. After 6 days, the myotube formation was determined by observing the multinucleated cells, in which the F-actin and nuclei of the cells were stained with Phalloidin and DAPI, respectively.

The fluorescence observations showed different myoblasts differentiation trends based on the exposure time to air containing H_2O_2 to fabricate Gelatin-Ph hydrogel **(Fig. 3-9 (b))**. Cells cultured on the Gelatin-Ph hydrogel obtained through 30 min of H_2O_2 exposure showed the highest myotube formation, similar to control on the culture well plate, shown by the highest number of myotubes **(Fig. 3-9 (c))** and fusion index **(Fig. 3-9 (d))**. In contrast, on the hydrogels fabricated through 15, 45, and 60 min of exposure to air containing H_2O_2, C2C12 showed a significantly lower number of myotubes **(Fig. 3-9 (c))** and fusion index **(Fig. 3-9 (d))**. Furthermore, myotubes cultured on hydrogel obtained through 30 min of the exposure also showed the longest myotubes length **(Fig. 3-9 (e))**. These results showed that the myotube formation is also governed by the stiffness of the Gelatin-Ph hydrogel.

In this study, the myogenesis was studied on hydrogel with stiffness range of 0.77 – 3.53 kPa. This stiffness range is lower than previous studies, in which Tomasch et al. used 5 – 20 kPa fibrin hydrogels (Tomasch et al. 2022), Boonen et al. used Matrigel-coated polyacrylamide gels with stiffness of 3 – 80 kPa (Boonen et al. 2009), while Romanazzo et al. used 0.9 – 133.2 MPa poly-ε-caprolactone film (Romanazzo et al. 2012). However, the stiffness of the Gelatin-Ph hydrogel in this study is within the range of the reported stiffness of an intact (~0.5 kPa)

and damaged skeletal muscle tissue (2 – 5 kPa) (Lacraz et al. 2015; Trensz et al. 2015; Silver et al. 2021). The stiffness-dependent myotube formation observed in this study is in accordance with the previous reports (Boonen et al. 2009; Romanazzo et al. 2012; Tomasch et al. 2022).

The possible explanation for the higher myogenesis in stiffness of 3.53 kPa than 0.77 kPa in this study is that similar with the native skeletal muscle tissue (Lacraz et al. 2015), higher myoblasts proliferation and differentiation is observed in damaged tissue than intact tissue. Similar conclusion was also reported by Trensz et al. that model intact and damaged tissue stiffness using polyacrylamide gels (Trensz et al. 2015). Mechanically, the lower myogenesis on softer substrate also could be explained by the deformation or collapse of the substrate under cell traction or contraction forces, which inhibits the myotubes formation (Levy-Mishali et al. 2009).

From mechanotransduction standpoint, interaction between the RGD sequence of the gelatin and the myoblasts receptor, *e.g.*, integrins, could be the key regulator (Robinson et al. 2003; Wang et al. 2012; Gribova et al. 2013). Integrins could affect the YAP/TAZ pathway, which is reported to play a role in cell adhesion (Dupont 2016; Nardone et al. 2017) and differentiation (van Putten et al. 2016). Additionally, there is a possibility that the mechanical property changes in Gelatin-Ph hydrogel also affect the cell-cell communication that triggers myoblast fusion to form myotubes. During myogenesis, myotubes are formed by the fusion between myoblasts or myoblast-myotube. Hindi et al. reported that the myoblast fusion could be mediated by integrins that increased the expression of β1D integrin and caveolin-3 via focal adhesion kinase (FAK) (Hindi et al. 2013). Alternatively, gelatin-based scaffold could also regulate the Intercellular Adhesion Molecule-1 (ICAM-1) (Nosenko et al. 2017), that plays role in myoblast fusion (Goh et al. 2015; Pizza et al. 2017).

Taken together, this study demonstrates that the contradictory effect of H_2O_2 on inducing cross-linking and degrading polymer of Gelatin-Ph hydrogel could modulate the adhesion and

differentiation of myoblasts. The findings of this study could be useful in the field of biomedical engineering aimed for the regeneration of muscular tissue, which requires the knowledge of cell-substrate interaction (Alarcin et al. 2021). Additionally, this finding could also be applied in the development of scaffolds with tunable mechanical property and biological properties for biomedical applications.

4. Conclusion

The results presented in this chapter demonstrated the modulatory effect of H_2O_2 in HRP-catalysed cross-linking and polymer degradation of Gelatin-Ph hydrogel on controlling the myogenesis. The myoblasts showed high viability on Gelatin-Ph hydrogel. Myoblasts adhesion showed that air containing H_2O_2-mediated changes in hydrogels' stiffness could control the adhesion of the cells, with cells cultured on stiff hydrogel had more prominent elongation. Most importantly, the myotube formation could be tuned by adjusting the stiffness of the hydrogel, in which the soft hydrogel inhibits the myogenesis. Taken together, these results showed that the H_2O_2-mediated changes on the properties of the Gelatin-Ph could govern the myogenesis. The findings of this study could be useful for skeletal muscle tissue engineering to control the cell fate to form new muscle cells. Additionally, this finding could be applied to cell studies and the development of functional tissues and artificial organs.

Chapter IV

Modulation of Cell-Cycle Progression by Hydrogen Peroxide-Mediated Cross-Linking and Degradation of Cell-Adhesive Hydrogels

1. Introduction

Based on the findings in Chapter II-III, in this chapter, the effect of H_2O_2 to control the cross-linking and degradation is investigated to hydrogel composite consisted of two different materials: Gelatin-Ph/hyaluronic acid (HA)-Ph. Using this system, the effect of hydrogel properties to modulate cell-cycle progression is studied.

The cell-cycle is an intricate process for cell growth. Regulation of the cell-cycle is fundamental to successful cell culture technology and tissue engineering. Additionally, dysregulation of the cell-cycle is a hallmark of cancer cells. Thus, cell-cycle modulation of cancer cells has been a target for developing anticancer drugs (Stewart et al. 2003; Jingwen et al. 2017).

In the cellular microenvironment, physical cues including mechanical property of the substrate and biochemical cues in the form of cell-adhesive ligands are known to modulate cellular behaviours including adhesion (Ni and Chiang 2007; Sun et al. 2018) and proliferation (Hadjipanayi et al. 2009; Yeh et al. 2012; Kalli and Stylianopoulos 2018). Gelatin and HA are abundantly found in various tissues of humans and animals (Lebl et al. 2007; Camci-Unal et al. 2013; Lee et al. 2020), and are important biomaterials that facilitate strong biological activities (Fraser et al. 1997; Jiang et al. 2007; Gomez-Guillen et al. 2011). The scaffolds composed of multiple polymers provide the microenvironment with multiple properties, attributed to each polymer. For example, gelatin/HA mixture could combine the cell-adhesive property of the RGD sequence and degradability of the gelatin with the physicochemical properties and regulation of cell behaviour and immune response function of HA. Therefore,

various studies have reported the usefulness of gelatin/HA composite hydrogel scaffolds in tissue-engineering applications for biomimicking of the extracellular matrix (ECM) of the native tissues (Li et al. 2006; Camci-Unal et al. 2013; Rezaeeyazdi et al. 2018; Lam et al. 2019).

The biological activities of HA are related to its molecular weight. HMW-HA is required for wound healing (Nyman et al. 2013), while sHA act as an activator of dendritic cells and macrophages during inflammation (Termeer et al. 2000; Termeer et al. 2002). More importantly, the molecular weight of HA also governs oncogenesis: HMW-HA inhibits the progression of tumour growth, while LMW-HA has an opposing effect (Fuchs et al. 2013; Liu et al. 2019; Ooki et al. 2019).

Hydrogen peroxide (H_2O_2) is widely used for degrading high-molecular-weight HA, gelatin, and various other polymers, through oxidative cleavage of the bonds (Chang et al. 2001; Li et al. 2010; Liu et al. 2014a; Chen et al. 2019). Apart from polymer degradation, H_2O_2 is also used as to induce the cross-linking in horseradish peroxidase (HRP)-mediated reaction resulting in gelation of aqueous solutions of polymers with phenolic hydroxyl groups (Polymer-Ph), including Gelatin-Ph and HA-Ph. As mentioned in Chapter II & III, the contradictory function of H_2O_2 can affects the mechanical property of hydrogels, which leads to changes in adhesion of the human adipose-derived stem cells (hASCs) and rat fibroblast cells as well as myoblasts differentiation. However, the contradictory effect of H_2O_2 on regulating other cell behaviours, such as cell-cycle progression, has not been investigated.

Cell-cycle modulation by the physical microenvironment of the cells has recently garnered great interest (Gérard and Goldbeter 2014; Walker et al. 2018). Although previous studies have reported the cell-cycle modulation by HA in collagen matrix (Greco et al. 1998), methacrylated gelatin (Arya et al. 2016), and chitosan-gelatin complex (Mao et al. 2004), no studies have investigated the cell-cycle modulation by Gelatin-Ph/HA-Ph composite hydrogel. This is particularly important considering that Gelatin and HA are known to be the component of the

cancer microenvironment (Sheu et al. 2003; Walker et al. 2018). Therefore, in this chapter, the effect of H_2O_2 to induce HRP-mediated cross-linking and degradation-inducing oxidant of Gelatin-Ph/HA-Ph composite hydrogels on the cell-cycle progression is investigated (**Fig. 4-1**).

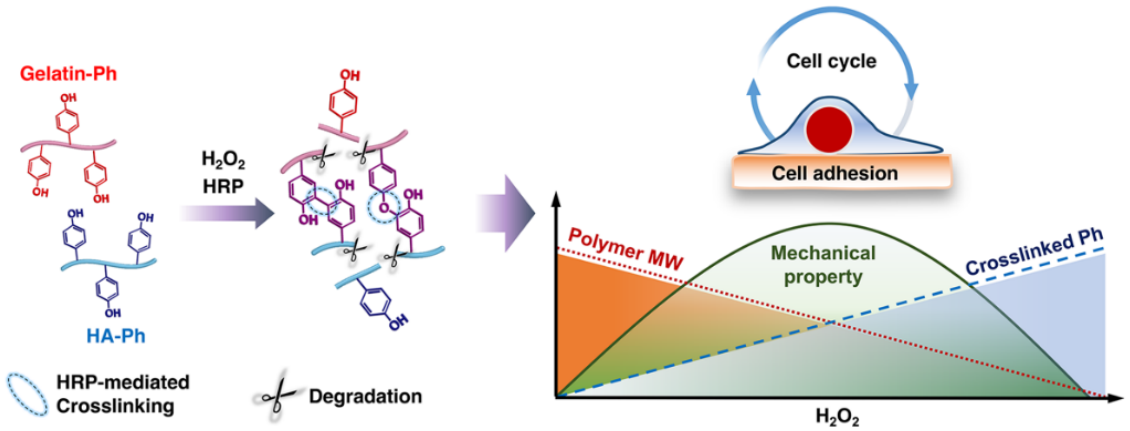

Fig. 4-1 Schematic illustration of H_2O_2-mediated hydrogelation of Gelatin-Ph/hyaluronic acid (HA)-Ph composite through horseradish peroxidase (HRP)–mediated cross-linking of Ph moieties and polymer degradation, and its subsequent effect on cell adhesion and the cell-cycle. Reprinted from (Mubarok et al. 2022b) with permission from MDPI.

This study focuses on the cell-cycle progression of cervical cancer cells, due to its high clinical prevalence worldwide, and being one of the highest causes of death in low-income countries (Vu et al. 2018). Additionally, there is an effort to accelerate the cervical cancer elimination worldwide (Canfell 2019). Hydrogel itself, including hyaluronic acid and gelatin, has been applied to tumour sites following tumour removal surgery to prevent tumour recurrence (Lan et al. 2016; Qian et al. 2021). Herein, the cell-cycle progression of human cervical cancer cells is studied using HeLa cells expressing genetically encoded fluorescent ubiquitylation-based cell-cycle indicator (Fucci2). HeLa cell is selected since it has been extensively used in biomedical study and research on cell-cycle regulation (Ma and Poon 2011), while HeLa/Fucci2 cell has been used to study cell response following drug-induced

cell-cycle arrest (Sakaue-Sawano et al. 2011). Fucci2 is composed of two chimeric fluorescent proteins, mCherry-hCdt1 and mVenus-hGem. Reciprocal accumulation of these two proteins turns cell nuclei red-fluorescent in G1 phase and green-fluorescent in the S/G2/M phases.

Additionally, the cell-cycle progression of non-transformed mouse mammary gland epithelial cell line (NMuMG) expressing Fucci2 was also investigated. NMuMG is widely used to study the epithelial-to-mesenchymal transition (EMT), a physiological change that is necessary for cancer invasion and metastasis (Meyer-Schaller et al. 2019; Shin et al. 2019). In addition, previous study has reported that HeLa/Fucci2 and NMuMG/Fucci2 have different cell-cycle response following chemical treatment (Sakaue-Sawano et al. 2011). Therefore, HeLa/Fucci2 and NMuMG/Fucci2 cell-cycle are studied to investigate whether cell type-specific phenomenon also occurs when cultured on Gelatin-Ph/HA-Ph composite hydrogel with different mechanical property.

2. Materials and Methods

2.1 Materials

Gelatin (Type B; ca. 225 g bloom, bovine skin) and insulin were purchased from Sigma–Aldrich (St. Louis, MO, USA). Sodium hyaluronate (HA, MW ~ 1000 kDa) was purchased from Kewpie (Tokyo, Japan). HRP (140 U mg^{-1}), NHS, DMF, HPPA, H_2O_2 aqueous solution (31% w/w), and catalase from bovine liver were purchased from Wako Pure Chemical Industries (Osaka, Japan). WSCD·HCl was obtained from Peptide Institute (Osaka, Japan). Tyramine hydrochloride was purchased from Chem-Impex Int'l. Inc. (Wood Dale, IL, USA). DMEM was purchased from Nissui Pharmaceutical (Tokyo, Japan). Calcein–AM was purchased from Nacalai Tesque Inc. (Kyoto, Japan) and propidium iodide (PI, Cellstain®) was purchased from Dojindo (Kumamoto, Japan). CytoPainter Phalloidin–iFluor 488 Reagent (ab176753) was purchased from Abcam (Cambridge, UK).

2.2 Polymer-Ph Preparation

Gelatin-Ph (1.9×10^{-4} mol-Ph g-Gelatin-Ph^{-1}) and HA-Ph (1.5×10^{-4} mol-Ph g-HA-Ph^{-1}) were prepared by conjugating HPPA with gelatin and tyramine hydrochloride with HA, respectively, using WSCD / NHS as previously reported (Hu et al. 2009; Sakai et al. 2015).

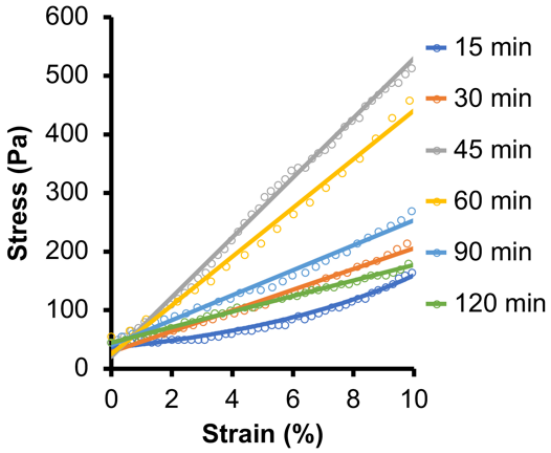

Fig. 4-2 Stress–strain curves of Gelatin-Ph/HA-Ph hydrogel obtained from 3.0% w/v Gelatin-Ph + 0.5% w/v HA-Ph and 1 U mL^{-1} HRP exposed with various air containing H_2O_2 exposure time. Reprinted from (Mubarok et al. 2022b) with permission from MDPI.

2.3 Mechanical Property Measurement

An aqueous solution (600 µL well^{-1}) containing 3.0% w/v Gelatin-Ph, 0.5% w/v HA-Ph, and 1 U mL^{-1} HRP was poured into a well of 12-well plate. The well-plate was then put into a plastic box (13.5 cm × 9.5 cm × 7 cm) and exposed to air containing H_2O_2 for 15, 30, 45, 60, 90, and 120 min. The air containing H_2O_2 was prepared by bubbling air into a solution containing 1 M H_2O_2. Concentration of the air containing H_2O_2 was measured at 16 ppm using gas detector (C-16 PortaSense II, Analytical Technology, Inc., Collegeville, PA, USA). The Young's moduli of the resultant Gelatin-Ph/HA-Ph composite hydrogels were measured using a material tester (EZ-Test, Shimadzu, Kyoto, Japan) by compressing the hydrogels with a probe

(diameter, 8 mm) at a compression rate of 6.0 mm min^{-1}. The Young's modulus was calculated from the data obtained in the range 1 – 10% compression strain **(Fig. 4-2)**.

2.4 Molecular Weight Measurement

A solution containing 3.0% w/v Gelatin-Ph or 0.5% w/v HA-Ph was incubated with 0, 0.003, 0.03, 0.06, and 0.15% w/v H_2O_2 overnight at 60 °C. The molecular weight of the Gelatin-Ph and HA-Ph were then measured using HPLC (LC-20AD, Shimadzu, Kyoto, Japan) equipped with RI detector (RID-20A, Shimadzu, Kyoto, Japan).

2.5 Cell Culture

HeLa/Fucci2 and NMuMG/Fucci2 cell lines were obtained from RIKEN Bio-Resource Center (Ibaraki, Japan). HeLa/Fucci2 was cultured in DMEM containing 10% v/v FBS. NMuMG/Fucci2 was cultured in DMEM supplied with 10% v/v FBS and 10 μg mL^{-1} insulin (Sakaue-Sawano et al. 2011). Cells were cultured at 37 °C in a 5% humidified CO_2 incubator.

2.6 Cell Adhesion and Cell-Cycle Analysis

Hydrogel sheets were fabricated from PBS containing 3.0% w/v Gelatin-Ph, 0.5% w/v HA-Ph, and 1 U mL^{-1} HRP. The solution was added to a 12-well plate at 600 μL $well^{-1}$ and exposed to air containing 16 ppm H_2O_2 for 15, 60, and 120 min. One millilitre culture medium containing 1 mg mL^{-1} catalase was then layered on the fabricated hydrogels overnight to degrade the remaining H_2O_2 into H_2O and O_2. The cell-cycle was synchronised to S-phase by incubating the cells in medium containing 4 mM hydroxyurea for 24 h (Apraiz et al. 2017). After the synchronization, cells were harvested and seeded on the fabricated gel sheet at 1.0×10^4 cells $well^{-1}$ (2.6×10^3 cells cm^{-2}). The cell-cycle was observed at 1 and 2 days after seeding based on the fluorescence expression of the mCherry-hCdt1 (red) and mVenus-hGem (green)

of the Fucci2, using fluorescence microscope (BZ-9000, Keyence, Tokyo, Japan). Red fluorescence indicates G1, yellow indicates G1/S, and green indicates late S/G2/M phase **(Fig. 4-3)**. The number of cells on each phase was counted using ImageJ (2.1.0/1.53c, NIH, Bethesda, MD, USA) from 5 – 10 randomly selected areas.

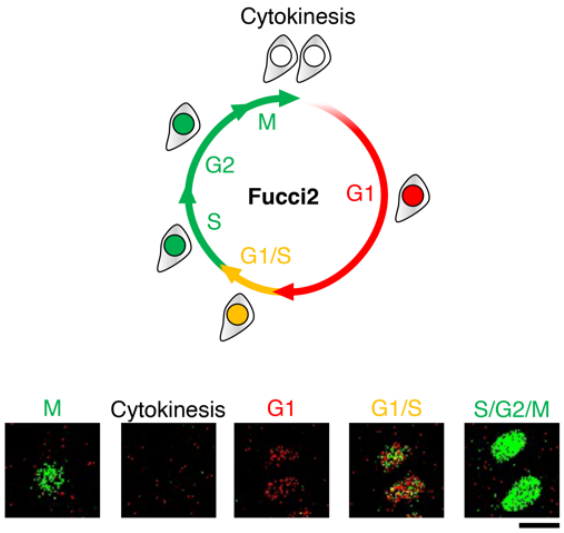

Fig. 4-3 Diagram of the Fucci2 expression and representative confocal laser-scanning microscope observation of the Fucci2 expression. mCherry-hCdt1 is expressed in G1 phase shown as red fluorescence, mVenus-hGem expressed in late S/G2/M phase, and G1/S transition observed as yellow fluorescence (co-expression of red and green). Scale bar: 10 µm. Reprinted from (Mubarok et al. 2022b) with permission from MDPI.

For live imaging, cells were observed using confocal laser-scanning microscope (C2; Nikon, Tokyo, Japan). The 12-well plate containing cells on fabricated hydrogel were placed in a stage-top incubator (STXG-WSKMX; Tokai Hit, Shizuoka, Japan) set at 37 °C supplied with 5% CO_2 + 20% O_2 + N_2. Time-lapses were conducted for 48 h. Cell adhesion analysis was conducted by analysing the morphology of the cells including cell area, perimeter, aspect ratio, and circularity of more than 50 cells for each set of conditions using ImageJ. Aspect ratio was defined as the ratio between major axis / minor axis of the fitted ellipse. Circularity was calculated using the formula: $4\pi \times (\text{area}/\text{perimeter}^2)$. Higher aspect ratio indicates elongated morphology. Higher circularity value (near 1.0) indicates a circular shape.

2.7 Viability Analysis

Viability of the cells was analysed by staining the cells with Calcein–AM and PI. Cells were incubated with PBS containing 3.3 µg mL^{-1} Calcein–AM and PI for 10 min at 37 °C. Live cells stained with Calcein–AM and dead cells stained with PI were observed using fluorescence microscope. Number of viable and dead cells were counted using ImageJ from micrographs taken on 6 randomly selected areas. Viability was calculated as percentage of number of live cells / total number of cells.

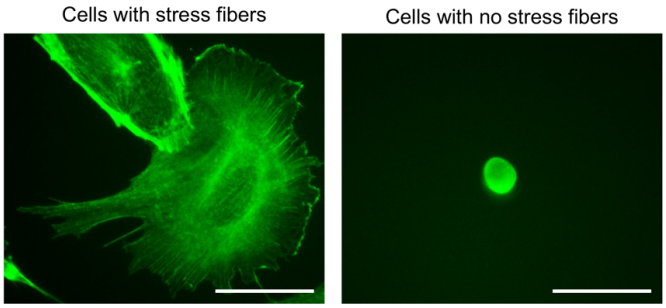

Fig. 4-4 Representative image of cells with stress fibres and no stress fibres. Cells with stress fibres are characterised by the visible fibres in the cell's cytoplasm and nucleus. Cells: NMuMG/Fucci2 cells. Scale bars: 50 µm. Reprinted from (Mubarok et al. 2022b) with permission from MDPI.

2.8 F-actin Analysis

F-actin of the cells was stained with CytoPainter Phalloidin–iFluor 488 Reagent. Briefly, cells were fixed with 4% paraformaldehyde (PFA) in PBS, permeabilised in HEPES (pH 5.5) and stained with CytoPainter Phalloidin–iFluor 488 Reagent (1X) according to the manufacturer's protocol. The number of cells with stress fibres was counted using ImageJ based on the presence/absence of visible stress fibres **(Fig. 4-4)**. F-actin fluorescence intensity was measured using ImageJ by measuring integrated density defined as sums of all the intensity in the pixel of the selected areas.

2.9 Statistical Analysis

Data were statistically analysed using Microsoft® Excel® 2019 (Version 1808, Microsoft Corp., Redmond, WA, USA). Statistical analysis was conducted using one-way analysis of variance (ANOVA) followed by post hoc *t*-test using Tukey HSD. Data were considered significantly different if $p < 0.05$.

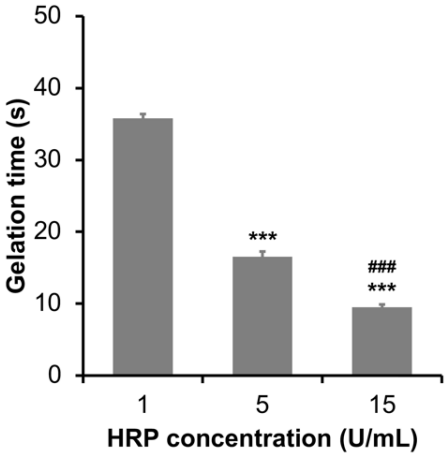

Fig. 4-5 Gelation time of 3.0% w/v Gelatin-Ph / 0.5% w/v HA-Ph solutions containing 1, 5, and 15 U mL^{-1} HRP exposed to air containing H_2O_2. Bar: S.E. ($n = 5$). ***$p < 0.0005$, compared to 1 U mL^{-1}, $^{###}p < 0.0005$ compared to 5 U mL^{-1}, Tukey HSD. Reprinted from (Mubarok et al. 2022b) with permission from MDPI.

3. Results and Discussion

3.1 Mechanical Property

First, the effect of H_2O_2 exposure time (15–120 min) on the stiffness of Gelatin-Ph/HA-Ph composite hydrogels was investigated by measuring the Young's modulus. Using this setup, hydrogel could be fabricated within 40 s **(Fig. 4-5)**. The result obtained from this experiment showed that H_2O_2 exposure time governed the Young's modulus of the composite hydrogels ($p < 0.005$) **(Fig. 4-6)**. The Young's modulus of the hydrogels increased as the exposure time to H_2O_2 was extended to 45 min, from 0.20 ± 0.01 kPa and 0.20 ± 0.03 kPa at 15 and 30 min

of the exposure, respectively, to 0.44 ± 0.02 kPa at 45 min of the exposure. Extending the exposure time to 60 min resulted in the hydrogel with the highest Young's modulus of 1.27 ± 0.30 kPa. Prolonging the exposure time to 90 and 120 min, however, resulted in the decrease of Young's modulus to 0.41 ± 0.05 kPa and 0.40 ± 0.04 kPa, respectively **(Fig. 4-6)**.

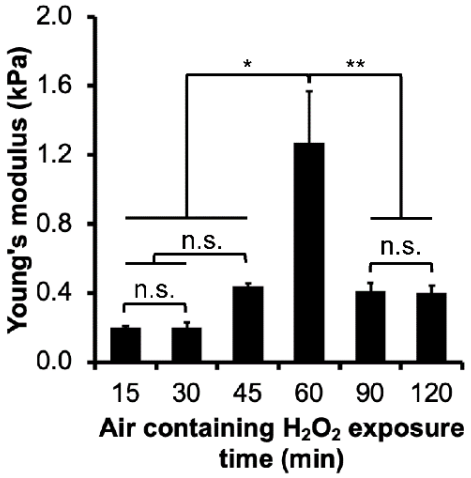

Fig. 4-6 Effect of exposure time to H_2O_2 on the Young's modulus of Gelatin-Ph/HA-Ph composite hydrogels obtained from 3.0% w/v Gelatin-Ph, 0.5% w/v HA-Ph, and 1 U mL^{-1} HRP. Bars: S.E. (n = 3). *p < 0.05, **p < 0.005, n.s.: no significant difference (p > 0.05), Tukey HSD. Reprinted from (Mubarok et al. 2022b) with permission from MDPI.

This result is in accordance with the results observed in Gelatin-Ph hydrogel shown in Chapter II & III (Mubarok et al. 2021; Mubarok et al. 2022a). The mechanism of the exposure time-dependent transition of the stiffness of the hydrogels can be explained by the correlation between the degrees of the progress of cross-linking formation catalysed by HRP, HRP inactivation, and Gelatin-Ph/HA-Ph degradation, which all involve H_2O_2. The inactivation of HRP (Sakai and Nakahata 2017), and degradation of organic molecules including Gelatin and HA by H_2O_2 have been reported (Takahashi et al. 1998; Chang et al. 2001; Li et al. 2010). In this study, H_2O_2 was supplied continuously to the system containing Gelatin-Ph/HA-Ph and HRP. Thus, the content of the cross-linked Ph moieties should increase by extending the exposure time to H_2O_2, unless HRP inactivation and Gelatin-Ph/HA-Ph degradation occurred.

Therefore, the results shown in **(Fig. 4-6)** that demonstrate the decrease of Young's modulus with increasing the exposure time from 60 to 120 min, indicate the occurrences of Gelatin-Ph/HA-Ph degradation. Indeed, degradation of the Gelatin-Ph and HA-Ph polymer by H_2O_2 was confirmed based on the molecular weight measurement **(Fig. 4-7)**. Taken together, a tunable control of Gelatin-Ph/HA-Ph Young's modulus was achieved by simple control of the exposure time to H_2O_2 contained in the air.

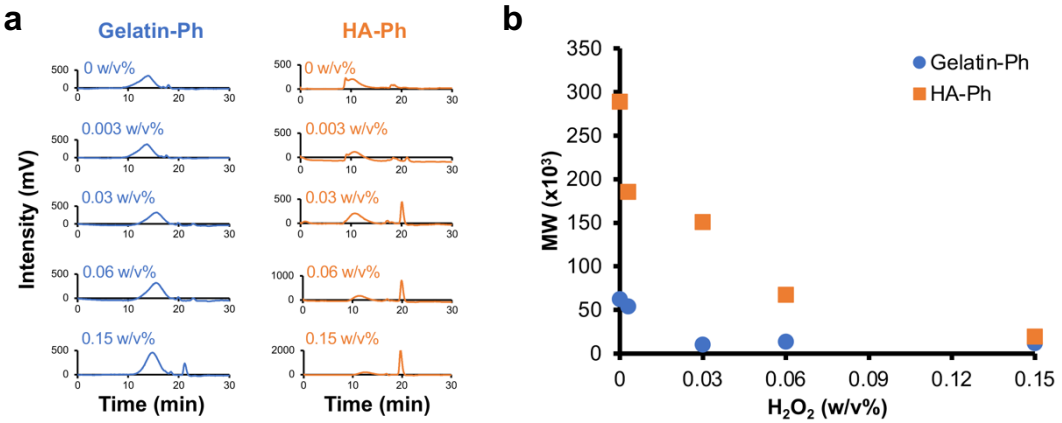

Fig. 4-7 Degradation of Gelatin-Ph and HA-Ph polymer by H_2O_2. (a) Intensity-time curve of 3.0% w/v Gelatin-Ph and 0.5 w/v% HA-Ph treated by 0, 0.003, 0.03, 0.06 and 0.15% (w/v) H_2O_2 solution. (b) Molecular weight of 3.0% w/v Gelatin-Ph and 0.5% w/v HA-Ph after overnight incubation with H_2O_2. Reprinted from (Mubarok et al. 2022b) with permission from MDPI.

3.2 HeLa/Fucci2 Cell Adhesion and Cell-Cycle Progression

Next, the adhesion and cell-cycle progression of cervical cancer cells was investigated by using HeLa/Fucci2 cells. In the initial experiment, the viability of the cells was investigated. HeLa/Fucci2 cells showed high viability regardless of the exposure time to air containing H_2O_2 **(Fig. 4-8 (a))**. This result could be attributed to the well-known biocompatibility of both Gelatin-Ph and HA-Ph (Le Thi et al. 2017; Sakai et al. 2019).

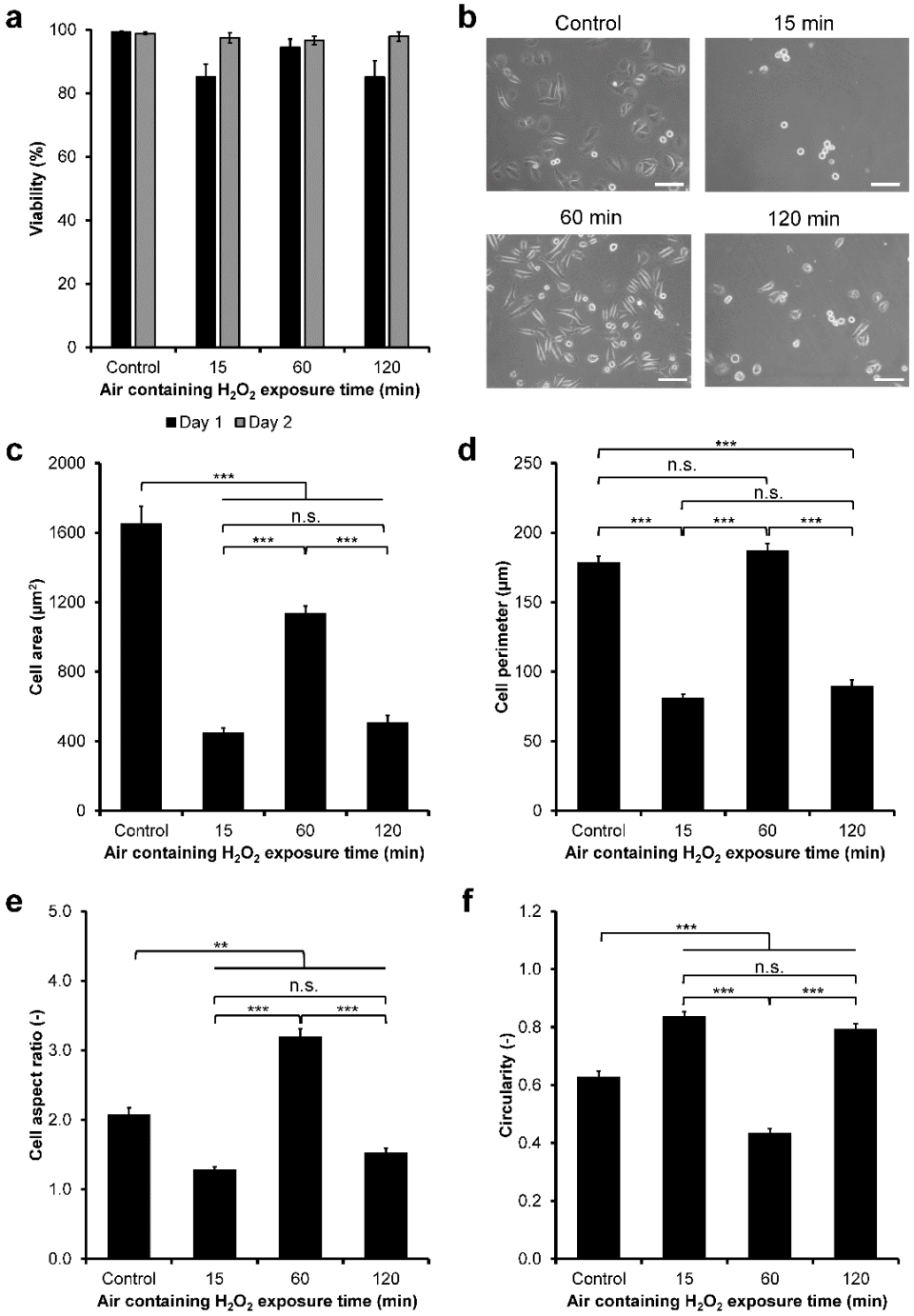

Fig. 4-8 Viability and morphology of HeLa/Fucci2 cell on Gelatin-Ph/HA-Ph composite hydrogels obtained through different exposure time to H_2O_2. (a) Viability of HeLa/Fucci2 cells calculated based on Calcein–AM/PI staining. Bar: S.E. (n = 6). (b) Micrograph of HeLa/Fucci2 cells on the composite hydrogels after 1 day cultured on well-plate (control) and the hydrogels obtained through 15, 60, and 120 min exposure to H_2O_2. Scale bars: 100 μm. (c) Area, (d) perimeter, (e) aspect ratio, and (f) circularity of HeLa/Fucci2 cells. Bar: S.E. (n > 100 cells). **p < 0.005, ***p < 0.0005, n.s.: no significant difference (p > 0.05) based on Tukey HSD. Reprinted from (Mubarok et al. 2022b) with permission from MDPI.

Next, HeLa/Fucci2 cell adhesion was investigated by analysing the morphology of the cells. HeLa/Fucci2 cells had different morphology on the hydrogels **(Fig. 4-8 (b))**. The cells cultured on the hydrogels obtained through 15 min and 120 min exposure to H_2O_2 showed no significant difference ($p > 0.05$) in the cell area **(Fig. 4-8 (c))**, perimeter **(Fig. 4-8 (d))**, aspect ratio **(Fig. 4-8 (e))**, and circularity **(Fig. 4-8 (f))**. These cells appeared to be small and circular indicated by the smallest area and perimeter, lowest aspect ratio, as well as the highest circularity. Meanwhile, the cells cultured on the hydrogel obtained through 60 min of exposure to H_2O_2 showed a larger area and perimeter, highest aspect ratio, and the lowest circularity, indicating large and elongated morphology, relatively similar to those control cell cultured on cell culture dish.

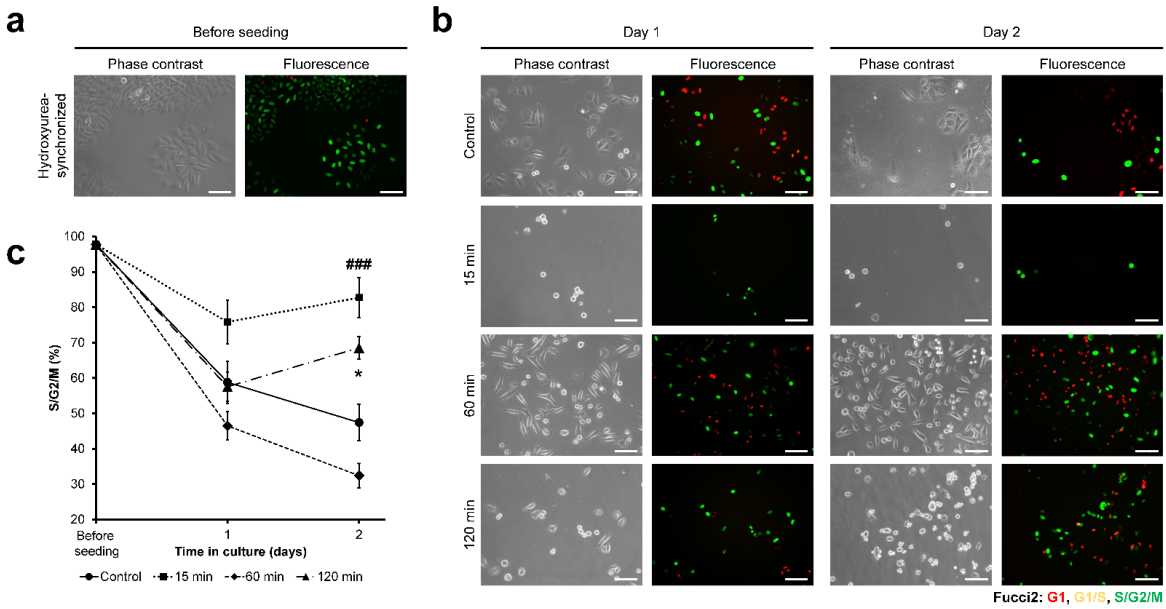

Fig. 4-9 Exposure time to H_2O_2-dependent changes in Gelatin-Ph/HA-Ph composite hydrogel stiffness could modulate the cancer cell-cycle progression. (a) Phase-contrast and fluorescence observation of the HeLa/Fucci2 before seeding, showing cell synchronised in S-phase, and (b) cells at day 1 to day 2 after seeding on the hydrogels. Cells cultured on well-plate were used as control. Fluorescence expression of Fucci2: red indicates G1, yellow indicates G1/S, and green indicates late S/G2/M phase. Scale bar: 100 µm. (c) Percentage of HeLa/Fucci2 cells in S/G2/M phase. Bar: S.E. ($n = 10$). $^{###}p < 0.0005$, 15 min compared to control; $^{*}p < 0.05$, 120 min compared to control, using Tukey HSD. Reprinted from (Mubarok et al. 2022b) with permission from MDPI.

Next, the cell-cycle progression of HeLa/Fucci2 cells was investigated. Fucci2 allows observation of the expression of mCherry-hCdt1 (red) and mVenus-hGem (green), observed at G1 and S/G2/M, respectively. G1/S transition could be observed as yellow fluorescence. Before seeding, the cell-cycle was synchronised with hydroxyurea. After 24 h of 4 mM hydroxyurea exposure, HeLa/Fucci2 predominantly found in S-phase, shown as green fluorescence **(Fig. 4-9 (a))**. The cells were then seeded on the composite hydrogels obtained through the different time of exposure to H_2O_2, and the cell-cycle was observed for two days after seeding **(Fig. 4-9 (b))**.

Cell-cycle analysis shows that the cells on cell culture well-plate (control) showed progression of the cell-cycle marked by a continuous decrease in the percentage of cells at S/G2/M phase, from 97.8% before seeding to 58.8% at day 1 and 47.4% at day 2 **(Fig. 4-9 (c))**. The cells cultured on the hydrogel obtained through 60 min of exposure to H_2O_2 showed a similar trend as those on cell well-plate (control, $p > 0.05$), with a decreasing percentage of cells at S/G2/M phase, to 32.4% at day 2 after seeding. In contrast, the cells cultured on the hydrogels obtained through 15 and 120 min of the exposure remained at S/G2/M phase, with 82.7% and 68.5% of the cells were found in S/G2/M phase at day 2, respectively **(Fig. 4-9 (c))**.

To further confirm this observation, a live-imaging experiment was conducted by observing the HeLa/Fucci2 cells from 8 – 48 h post-seeding. Live-imaging observation showed higher mitosis frequency in HeLa/Fucci2 cells cultured on 60 min composite hydrogel and control. Additionally, cell growth was analysed by calculating the cell density on day 1 and day 2 post-seeding. Cells cultured on hydrogel obtained from 15 and 120 min of the exposure showed no significant growth in cells density from day 1 to day 2 ($p > 0.05$). On the other hand, cells cultured on hydrogel obtained from 60 min exposure time to H_2O_2 and control cultured on well-plate showed a significant increase in cell density ($p < 0.05$) **(Fig. 4-10)**.

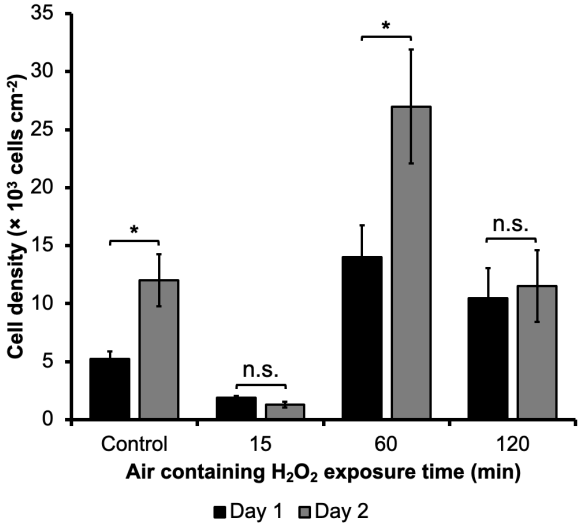

Fig. 4-10 Density of HeLa/Fucci2 cells on Gelatin-Ph/HA-Ph composite hydrogel obtained from different H_2O_2 exposure time. Bar: S.E. (n = 5). *p < 0.05, n.s.: no significant difference (p > 0.05), Tukey HSD.

Based on these results, HeLa/Fucci2 cells had a mechanical property-dependent changes in cell adhesion **(Fig. 4-8)** and cell-cycle progression **(Fig. 4-9)**. The stiffness-dependent change in cell morphology is consistent with the results of previous studies using human adipose-derived stem cells cultured in Gelatin-Ph/HA-Ph hydrogel (Sakai et al. 2019) and fibroblast cells on DNA-cross-linked hydrogel (Previtera et al. 2012), which showed a spherical shape on soft substrates and an elongated shape on stiff substrates. Based on these results, H_2O_2 exposure time-mediated changes to Gelatin-Ph/HA-Ph stiffness could govern the adhesion of HeLa/Fucci2 cells.

As for the cell-cycle progression, the result of this study showed that a stiffer hydrogel is required for HeLa/Fucci2 cell-cycle progression. This result is consistent with the result by Paszek et al which reported that cancer cells cultured on soft collagen gel have lower growth and adhesion (Paszek et al. 2005). Wall et al. reported that melanoma cells cultured on fibrillar collagen have a cell-cycle arrest in G2 (Wall et al. 2007). The progression of cell-cycle on stiffer substrates observed in this study is consistent with the results reported by Klein et al.

about the cell-cycle progression on stiff polyacrylamide hydrogels, but not on soft hydrogels, after nocodazole-mediated G2/M arrest (Klein et al. 2009).

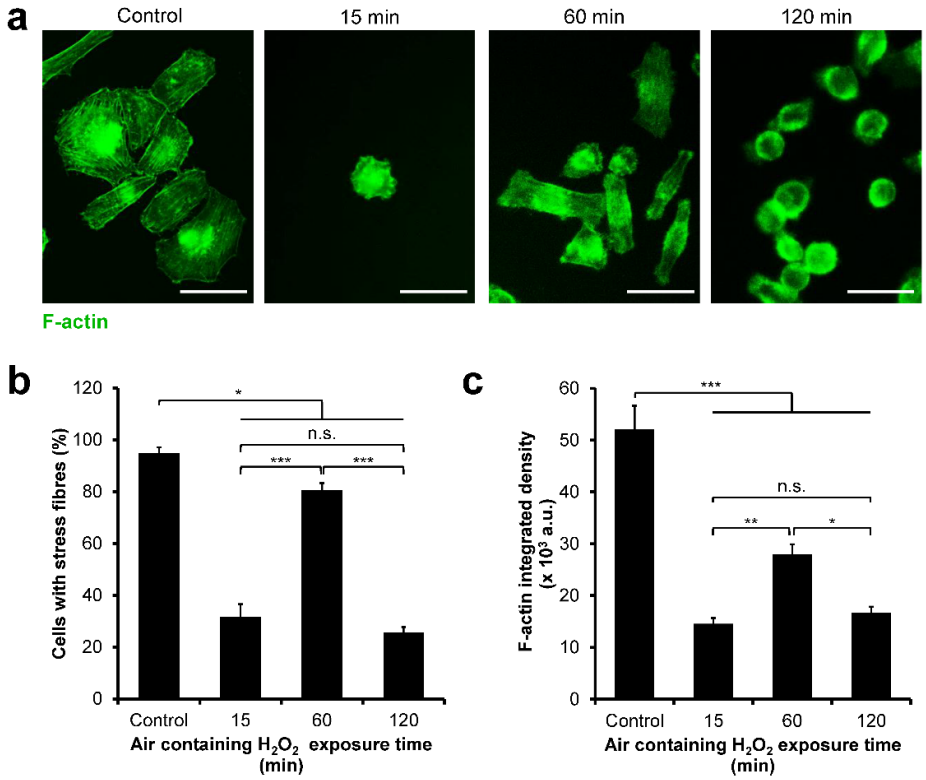

Fig. 4-11 F-actin reorganization in HeLa/Fucci2 cells cultured on Gelatin-Ph/HA-Ph composite hydrogels obtained through 15, 60, and 120 min of exposure to H_2O_2. (a) Fluorescence observation of the F-actin of HeLa/Fucci2 cells cultured on well-plate (control) and the hydrogels. Scale bar: 100 µm. (b) Percentage of cells with stress fibres. Bar: S.E. (n = 6). (c) F-actin integrated density. Bar: S.E. (n = 45 cells). *$p < 0.05$, **$p < 0.005$, ***$p < 0.0005$, n.s.: no significant difference, Tukey HSD. Reprinted from (Mubarok et al. 2022b) with permission from MDPI.

The difference in cell-cycle progression of the cells cultured on each hydrogel might be mediated by the cytoskeleton reorganization. Therefore, the F-actin of the cells was stained, and the formation of stress fibres was investigated **(Fig. 4-11 (a))**. Most of the cells cultured on cell culture well-plate (control) and those on the hydrogel obtained through 60 min of exposure to H_2O_2 had stress fibres. However, cells cultured on the hydrogel obtained through

15 and 120 min of the exposure had a significantly lower percentage of cells with stress fibres ($p < 0.0005$) **(Fig. 4-11 (b))**. A similar trend was observed in F-actin integrated density with cells cultured on the hydrogel obtained through the 60 min of exposure to H_2O_2: the cells had significantly higher integrated density ($p < 0.05$) compared to those on the hydrogel obtained through 15 and 120 min of the exposure to H_2O_2 **(Fig. 4-11 (c))**.

Previous studies have reported that actin plays a key role in mitosis (Reshetnikova et al. 2000; Kunda and Baum 2009). More importantly, actin disruption is reported to induce G2/M arrest in transformed cancer cell line IMR-90 and MCF-7 cells (Shin et al. 2011; Shrestha et al. 2018). Accordingly, cells cultured on composite hydrogel obtained through 15 min and 120 min of H_2O_2-exposure that showed a reduction in stress fibres assembly **(Fig. 4-11)** also showed G2/M arrest **(Fig. 4-9)**. This indicates that one of the possible causes of cell-cycle arrest at G2/M phase observed in the HeLa/Fucci2 cells cultured on soft hydrogel obtained through 15 min and 120 min of exposure to H_2O_2 is due to the reduction in stress fibres assembly.

3.3 NMuMG/Fucci2 Cell Adhesion and Cell-Cycle Progression

Next, the adhesion and cell-cycle progression of NMuMG/Fucci2 cells was investigated. Similar with the result in HeLa/Fucci2 cells, NMuMG/Fucci2 cells showed high viability from day 1 to day 2 on the Gelatin-Ph/HA-Ph composite hydrogel, independent of the H_2O_2 exposure time **(Fig. 4-12 (a))**. The morphology of the NMuMG/Fucci2 cells on the composite hydrogel was then investigated. The cells on the surface of the well-plate (control) and those on the hydrogels obtained through 60 and 120 min of exposure to H_2O_2 elongated similarly **(Fig. 4-12 (b))**. The cells on the hydrogel obtained through 15 min of the exposure showed a small and round morphology attributed to the smallest area **(Fig. 4-12 (c))** and perimeter **(Fig. 4-12 (d))**, aspect ratio near 1.0 **(Fig. 4-12 (e))**, and highest circularity **(Fig. 4-12 (f))**.

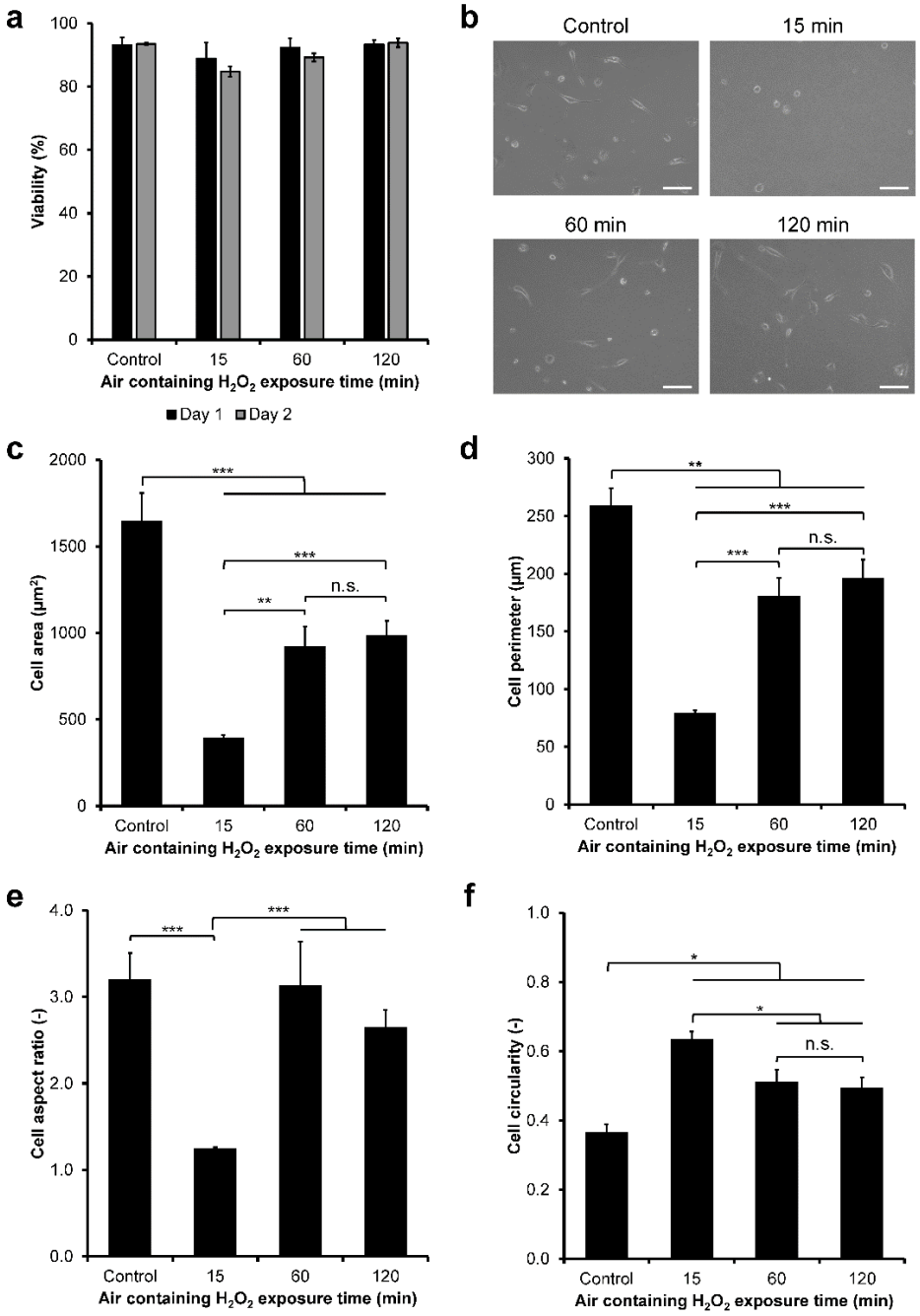

Fig. 4-12 Viability and morphology of NMuMG/Fucci2 cells on Gelatin-Ph/HA-Ph hydrogel obtained through different exposure time to H_2O_2 in the air. (a) Viability of NMuMG/Fucci2 cells on day 1 and day 2 of culture. Bar: S.E. (n = 6). (b) Representative phase-contrast image of NMuMG/Fucci2 cells on the hydrogels obtained through 15, 60, and 120 min of the exposure. As a control, cells were cultured on plastic surface of the well-plate. Scale bars: 100 μm. (c) Area, (d) perimeter, (e) aspect ratio, and (f) circularity of NMuMG/Fucci2 cells. Bar: S.E. (n > 50 cells). *p < 0.05, **p < 0.005, ***p < 0.0005, n.s.: no significant difference, Tukey HSD. Reprinted from (Mubarok et al. 2022b) with permission from MDPI.

The cells on the hydrogel obtained through 60 min of the exposure showed significantly larger and elongated shapes attributed to a larger area and perimeter **(Fig. 4-12 (c-d))**, higher aspect ratio **(Fig. 4-12 (e))**, and lower circularity **(Fig. 4-12 (f))**, compared to cells on hydrogel obtained through 15 min of the exposure. Interestingly, the cells on the hydrogel obtained through 120 min of the exposure had no significant differences ($p > 0.05$) in their morphological characteristics as to those cultured on the hydrogel obtained through 60 min of the exposure **(Fig. 4-12 (b-f))**. This result is different with the cell adhesion of HeLa/Fucci2 cells. This phenomenon is similar to the result in Chapter II in which human adipose-derived stem cells (hASCs) and rat fibroblast (3Y1) cells cultured on Gelatin-Ph hydrogel showed elongated morphology on the hydrogel obtained through 60 min of exposure to H_2O_2 despite having similar stiffness with hydrogel obtained through 15 min of the exposure (Mubarok et al. 2021).

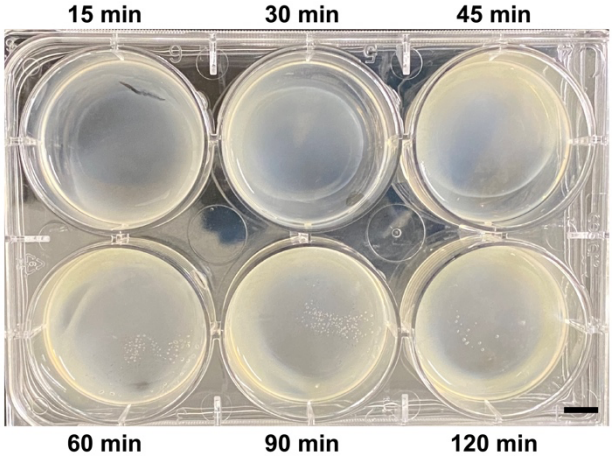

Fig. 4-13 Phase separation in Gelatin-Ph/HA-Ph composite hydrogel fabricated after exposure to H_2O_2 for 15 to 120 min. Notice the cloudy appearance of the hydrogel in extended exposure time, indicating phase-separation occurrence. Scale bar: 5 mm. Reprinted from (Mubarok et al. 2022b) with permission from MDPI.

This phenomenon could be attributed to other factors such as mesoscale topographical changes and mesh size (Scott et al. 2020). In the prolonged exposure time to H_2O_2, the phase-

separation phenomenon might occur, resulting in the formation of a domain. Phase-separation could be observed from the cloudy appearance of the fabricated hydrogel **(Fig. 4-13)**. This phase-separation could induce clustering of cell surface receptors (see (Case et al. 2019) for review), which could induce alteration of cell shape.

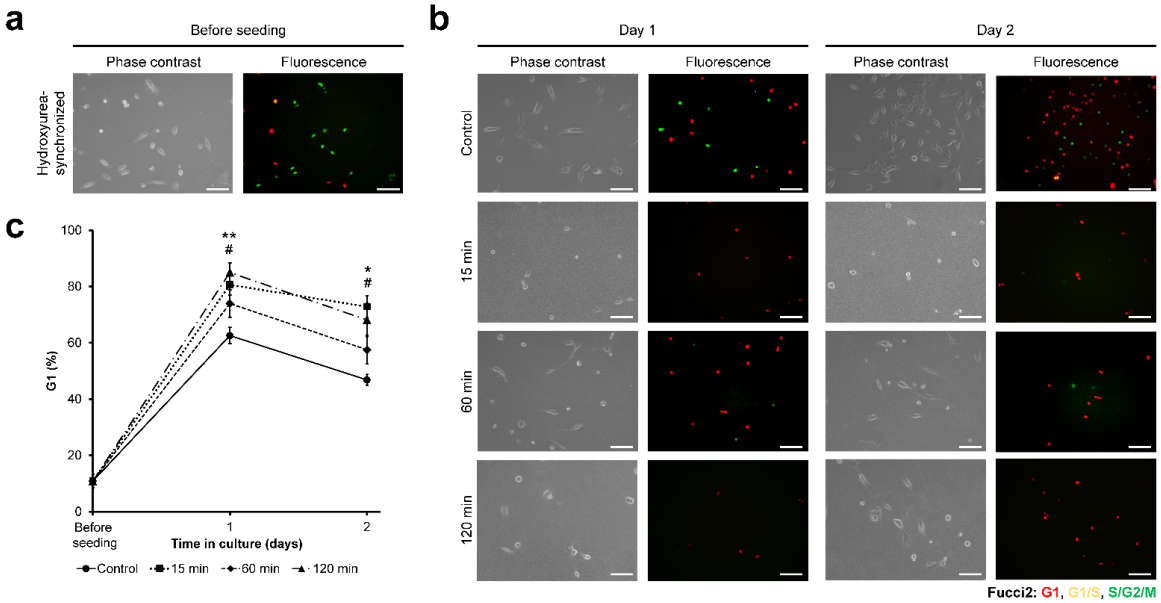

Fig. 4-14 NMuMG/Fucci2 cell-cycle progression on Gelatin-Ph/HA-Ph composite hydrogels obtained through different exposure time to H_2O_2. (a) Representative micrograph of NMuMG/Fucci2 cells before seeding, synchronised by hydroxyurea to S-phase, and (b) NMuMG/Fucci2 cells on Gelatin-Ph/HA-Ph hydrogel and well-plate (control) for 2 days. Scale bars: 100 µm. (c) Percentage of NMuMG/Fucci2 cells in G1 phase. Bar: S.E. ($n \geq 5$). $^{\#}p < 0.05$, 15 min compared to control; $^{*}p < 0.05$, $^{**}p < 0.005$, 120 min compared to control, using Tukey HSD. Reprinted from (Mubarok et al. 2022b) with permission from MDPI.

Another factor that could induce better adhesion in the cells cultured on the hydrogel obtained through 120 min of the exposure is the low molecular weight fragments out of the polymer. As shown in **Fig. 4-7**, H_2O_2 could degrade both Gelatin-Ph and HA-Ph. HA is well-known to have different modulatory effects based on their molecular weight (Termeer et al. 2000; Termeer et al. 2002; Nyman et al. 2013). LMW-HA is reported to induce better adhesion

in human epithelial cells HT1080, mediated by receptor for hyaluronic acid-mediated motility (RHAMM) (Kouvidi et al. 2011). LMW-HA also induces EGF-induced branching of mammary epithelial cells EpH4 and NMuMG cells, while the HMW-HA inhibits the morphological changes, a process that is mediated by HA receptors CD44 and RHAMM (Tolg et al. 2017).

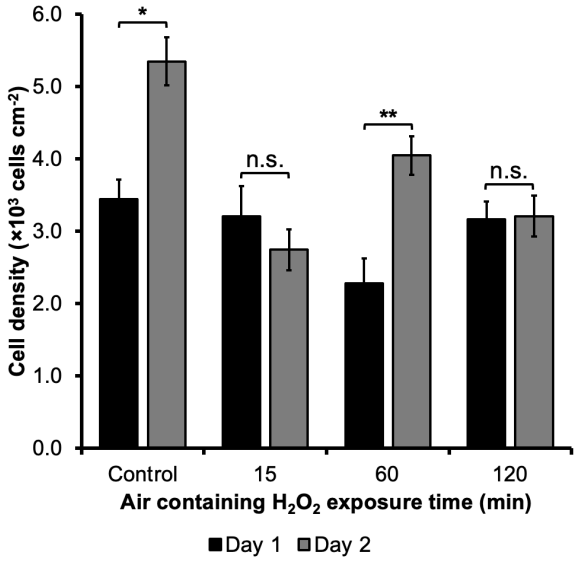

Fig. 4-15 NMuMG/Fucci2 cell density cultured on Gelatin-Ph/HA-Ph hydrogel obtained from varying H_2O_2 exposure time. Bar: S.E. (n = 5). *p < 0.05, **p < 0.005, n.s.: no significant difference, Tukey HSD.

Next, the cell-cycle progression of NMuMG/Fucci2 cells on the composite hydrogels was investigated. Hydroxyurea synchronization before seeding resulted in 84.0% S-phase cells **(Fig. 4-14 (a))**. Cell-cycle observation based on the Fucci2 expression **(Fig. 4-14 (b))** showed that the cells on the hydrogels obtained through 15 and 120 min of exposure to H_2O_2 had a significantly higher (p < 0.05) percentage of cells at G1 phase from day 1 to day 2 on the hydrogels compared to those on cell well-plate (control) **(Fig. 4-14 (c))**. In contrast, the percentage of G1-phase cells on the hydrogel obtained through 60 min of the exposure was not significantly different from that of control (p > 0.05) **(Fig. 4-14 (c))**. Time-lapse observation

also showed higher mitotic cells in control and those cultured on composite hydrogel obtained from 60 min H_2O_2 exposure time, compared to cells on 15 min and 120 min hydrogel. Cell growth analysis also showed significant cell density increase only in cells cultured on well-plate (control) and 60 min hydrogel **(Fig. 4-15)**.

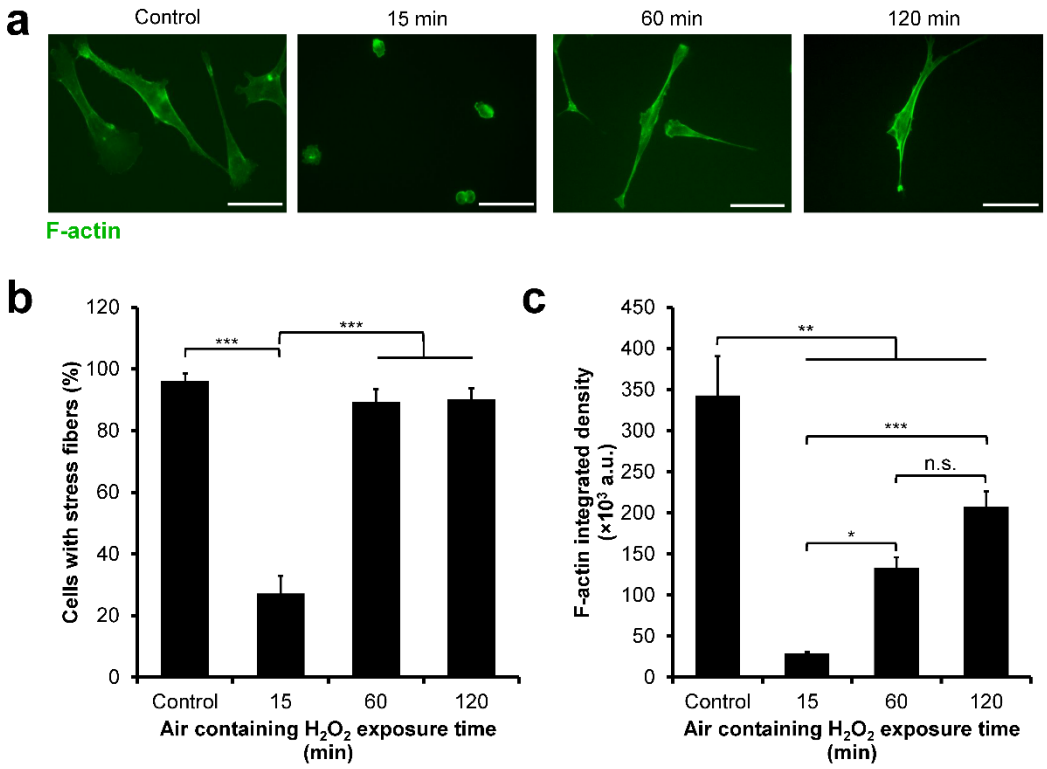

Fig. 4-16 F-actin reorganization of NMuMG/Fucci2 cells cultured on Gelatin-Ph/HA-Ph composite hydrogel obtained through different exposure time to H_2O_2 in the air. (a) Representative fluorescence micrograph of the F-actin of NMuMG/Fucci2 cells cultured on Gelatin-Ph/HA-Ph hydrogel obtained through 15–120 min of exposure to H_2O_2. Cells cultured on well-plate were used as control. Scale bars: 50 µm. (b) Comparison of percentage of cells with stress fibres. Bar: S.E. ($n \geq 5$). (c) F-actin integrated density of NMuMG/Fucci2 cells. Bar: S.E. ($n = 50$ cells). *$p < 0.05$, *$p < 0.005$, ***$p < 0.0005$, n.s.: no significant difference based on Tukey HSD. Reprinted from (Mubarok et al. 2022b) with permission from MDPI.

Next, the F-actin organization of the NMuMG/Fucci2 cells was investigated by staining the actin stress fibres of the cells **(Fig. 4-16 (a))**. Analysis of the presence of stress fibres showed

that the cells cultured on the composite hydrogels obtained through 15 min of exposure to H_2O_2 had the lowest percentage of cells with stress fibres **(Fig. 4-16 (b))**. Similarly, these cells had the lowest F-actin integrated density **(Fig. 4-16 (c))**. In contrast, 89.4% of the cells on the hydrogel obtained through 60 min of the exposure had stress fibres, relatively similar to those on cell culture well-plate (control, 96.1%) **(Fig. 4-16 (b))** and significantly higher F-actin integrated density ($p < 0.05$) than those on the hydrogel obtained through 15 min of the exposure **(Fig. 4-16 (c))**. Interestingly, the cells cultured on the hydrogel obtained through 120 min of the exposure had no significant difference ($p > 0.05$) in the presence of actin stress fibres **(Fig. 4-16 (b))** and F-actin integrated density **(Fig. 4-16 (c))** compared to the cells cultured on the hydrogel obtained through 60 min of exposure to H_2O_2.

Based on these results, NMuMG/Fucci2 had a different cell-cycle progression with HeLa/Fucci2 cells. While HeLa/Fucci2 cells showed cell-cycle arrest at G2/M **(Fig. 4-9)** in soft hydrogel obtained 15 min (0.20 kPa) and 120 min (0.40 kPa) of H_2O_2-exposure, NMuMG/Fucci2 cells showed an arrested cell-cycle at G1 phase **(Fig. 4-14)**. This difference was also reported in the previous report by Sakaue-Sawano et al. (2011), in which the cell type-dependent response is observed following exposure to Cdk4 inhibitor drugs, with HeLa/Fucci2 cells arrested at G2/M phase while NMuMG/Fucci2 cells are arrested at G1 phase (Sakaue-Sawano et al. 2011). At the moment, the intricate mechanism on how the H_2O_2 exposure time to Gelatin-Ph/HA-Ph hydrogel induced cell-cycle arrest at a different phase in HeLa/Fucci2 and NMuMG/Fucci2 is unknown. However, there is a possibility that NMuMG/Fucci2 cultured on Gelatin-Ph/HA-Ph hydrogel obtained through 120 min of the exposure had an epithelial-to-mesenchymal transition (EMT).

EMT is a physiological transition or reprogramming of epithelial cells to mesenchymal cells, marked by a morphological change into spindle-like mesenchymal cells, which plays an important role in the malignancy and invasiveness of cancer (Meyer-Schaller et al. 2019; Shin

et al. 2019). Recent study by Fan et al. (2021) shows that soft substrate (0.5 kPa) promotes the EMT in SKOV-3 ovarian cancer cells (Fan et al. 2021). This stiffness is close with the Young's modulus of the Gelatin-Ph/HA-Ph hydrogel obtained through 120 min of H_2O_2-exposure at 0.40 kPa. Moreover, LMW-HA is also known to induce the EMT in MCF-7 and MDA-MB-231 cells (Jariyal et al. 2020). This might explain why despite both Gelatin-Ph/HA-Ph composite hydrogel obtained through 15 min (0.20 kPa) and 120 min (0.40 kPa) of H_2O_2-exposure had low Young's modulus, but, the NMuMG/Fucci2 cells adhesion **(Fig. 4-12)** and F-actin organization **(Fig. 4-16)** were different: the molecular weight of HA-Ph exposed to H_2O_2 for 120 min was probably lower due to H_2O_2 degradation, which promotes the EMT due to interaction with HA receptors such as CD44 or RHAMM.

As for the cell-cycle arrest in G1 observed in NMuMG/Fucci2 cells cultured on the hydrogel obtained through 120 min of H_2O_2-exposure **(Fig. 4-14)**, despite having similar F-actin organization with cells cultured on the hydrogel obtained through 60 min of H_2O_2-exposure **(Fig. 4-16)**, this could also be explained by the EMT process. EMT is known to induce cell-cycle arrest (Vega et al. 2004; Lovisa et al. 2015; Prakash et al. 2019). Additionally, *Snai1* and *Snai2* which belong to the SNAIL family transcription factors that regulate the EMT process are also known to regulate G1 phase transition (Assani and Zhou 2019).

Taken together, the contradictory effect of H_2O_2 to induce HRP-mediated cross-linking and degrade the Gelatin-Ph and HA-Ph polymers could affect the adhesion and cell-cycle progression of HeLa/Fucci2 and NMuMG/Fucci2 cells in cell type-dependent manner. These findings can be useful in biomedical field especially for creating tissues by combining cells and hydrogels obtained through HRP-mediated cross-linking. Development of various artificial tissues have been attempted by combining cells and the hydrogels for surgical transplantation and *in vitro* model for drug screening (Gantumur et al. 2019; Pierantoni et al. 2021). The control and understanding of the cell-cycle in these engineered tissues are important

for creating functional tissues and for accurately interpreting cellular responses to drug candidates, including anticancer drugs. Additionally, phenomenon reported in this study could be used to study the cancer cell behaviour affected by the mechanical property of their surrounding ECM.

4. Conclusion

The results presented in this chapter demonstrated the H_2O_2 effect to induce HRP-mediated cross-linking and degrade polymer in Gelatin-Ph/HA-Ph composite hydrogel and its subsequent effect on cell adhesion and cell-cycle progression. Young's moduli of the Gelatin-Ph/HA-Ph composite hydrogels could be controlled by simple adjustment of the exposure time to H_2O_2 contained in the air, in which the stiffness increased after extending the exposure time from 15 to 60 min, followed by a decrease in extended exposure time to 120 min. The exposure time-dependent changes to the hydrogel stiffness governed the adhesion and cell-cycle progression of HeLa/Fucci2 cells and NMuMG/Fucci2 cells, in a cell-type-dependent manner. Although soft hydrogel leads to cell-cycle arrest at G2/M phase for HeLa/Fucci2, NMuMG/Fucci2 cells were arrested at G1 phase. Apart from hydrogel stiffness, the NMuMG/Fucci2 cell-cycle progression was also modulated by the H_2O_2-mediated degradation of HA in the composite, which produced low-molecular-weight HA. From these results, the contradictory effects of H_2O_2 to Gelatin-Ph/HA-Ph composite hydrogel could be used to control the cell adhesion and cell-cycle progression, which could be used in cancer studies and tissue-engineering purposes.

General Conclusions

This dissertation described the influence of H_2O_2 on the mechanical property of the hydrogel obtained from HRP-catalysed cross-linking and its application to modulate the cell behaviour. Chapter II of the dissertation described the influence of H_2O_2 to the mechanical property of Gelatin-Ph and its effect on cell adhesion. Chapter III described the application of the H_2O_2-mediated changes on Gelatin-Ph hydrogels' mechanical property to regulate myogenesis. Chapter IV described the effect of H_2O_2 on the mechanical property of Gelatin-Ph/HA-Ph composite hydrogel and its effect on cell-cycle progression. The following results were obtained.

In Chapter II, the contradictory effect of H_2O_2 that simultaneously induces cross-linking while degrading the polymer was demonstrated in Gelatin-Ph. The gelation time and mechanical property of the Gelatin-Ph hydrogel could be controlled by tuning the HRP concentration and the exposure time to air containing H_2O_2. The changes in the Young's modulus of the hydrogels with initial stiffening followed by decreasing stiffness in extended exposure time to air containing H_2O_2 could be mediated by the balance of H_2O_2 activity to induces the cross-linking and degrades the Gelatin-Ph. The mechanical property of the Gelatin-Ph hydrogel modulated by H_2O_2 could alter the adhesion of hASCs and fibroblast cells. The mechanical property and molecular weight of the hydrogel that were influenced by H_2O_2 could be promising for tuning the cells' behaviour for cell study and biomedical applications.

In Chapter III, the H_2O_2-mediated changes in the properties of Gelatin-Ph hydrogel was applied to control the formation of new muscle cells (myogenesis). Tuning the exposure time to air containing H_2O_2 resulted in the Gelatin-Ph hydrogels with a physiologically relevant stiffness mimicking the native skeletal muscle tissue. The cytocompatibility of the system was demonstrated by the high viability of the cells regardless of the exposure time to air containing

H_2O_2. In addition, myoblasts' adhesion and differentiation also could be controlled by the exposure time to air containing H_2O_2, in which higher stiffness was preferable for the cell elongation and myotube formation. This finding could be useful in the biomedical engineering field aimed at regenerating muscular tissue.

In Chapter IV, the versatility of the system to control the mechanical property was demonstrated to Gelatin-Ph/HA-Ph composite hydrogel. This system was applied to study the cell-cycle progression of the cancer cells. In addition to the mechanical property, the degradation of HA-Ph in the composite hydrogel by H_2O_2 could affect the adhesion and cell-cycle progression of HeLa/Fucci2 and NMuMG/Fucci2 cells on the hydrogels in a cell-type dependent manner. The possible mechanism via F-actin assembly was also reported. These findings could be useful in cancer studies and tissue engineering purposes.

The objective of this study was thus achieved based on these investigations that the influence of H_2O_2 on the mechanical property of gelatin-based hydrogels obtained from HRP-catalysed cross-linking could control various cell behaviours. These findings are expected to contribute to the biomedical applications of hydrogels obtained through HRP-mediated cross-linking.

Suggestions for Future Works

Based on the findings of this study, the H_2O_2 influence on hydrogel properties can be applied to the following studies in the future.

(1) Fabrication of Substrates with Complex Stiffness Gradient

Artificial tissue is important as *in vitro* model to study developmental processes and disease progression. Artificial tissue can also be applied to directly regenerate damaged tissues or organs. Therefore, it is essential to recreate a cell microenvironment similar to the native tissue and organs to successfully study physiological processes *in vitro*. Although bulk hydrogels can provide a platform for different cell types and applications, they often lack the ability to replicate the optimal cell conditions. Natural tissues and organs exhibit a varying stiffness gradient, such as osteochondral (cartilage-to-bone) interaction in the articulating joints and the neural tube during embryonic development. Therefore, there is a need to develop a method to fabricate hydrogel with a complex stiffness gradient.

Previous studies that reported the gradient stiffness normally yield a linear stiffness gradient (Hadden et al. 2017; Chin et al. 2021). Based on the findings in Chapter II-IV, a non-linear trend of the hydrogel stiffness is observed following extending the exposure time to air containing H_2O_2. Therefore, this system can be applied to fabricate a structure with non-linear stiffness gradient. One proposed method is to temporally slide the mask covering the solution containing Polymer-Ph & HRP **(Fig. S-1)**. Using this method, a non-linear gradient stiffness can be fabricated, with the middle point being the stiffest. Adjusting the position of the mask also can be used to control the position of the stiffest point of the hydrogel. This system, thus, can be used to study the cellular behaviour and mechanotransduction in response to gradient stiffness, *e.g.*, cell adhesion, durotaxis, and differentiation of the stem cells or progenitor cells.

This technique is advantageous on several points. In addition to simple control of the hydrogelation, this technique is versatile as it can be applied to fabricate hydrogel from a wide variety of materials, such as Gelatin-Ph (Chapter II-III), composite Gelatin-Ph/HA-Ph hydrogel (Chapter IV), and other Polymer-Ph. More importantly, the cytocompatibility of this method demonstrated in Chapter III and IV also solves the limitations of previous techniques that require toxic monomers and cross-linkers (Hadden et al. 2017).

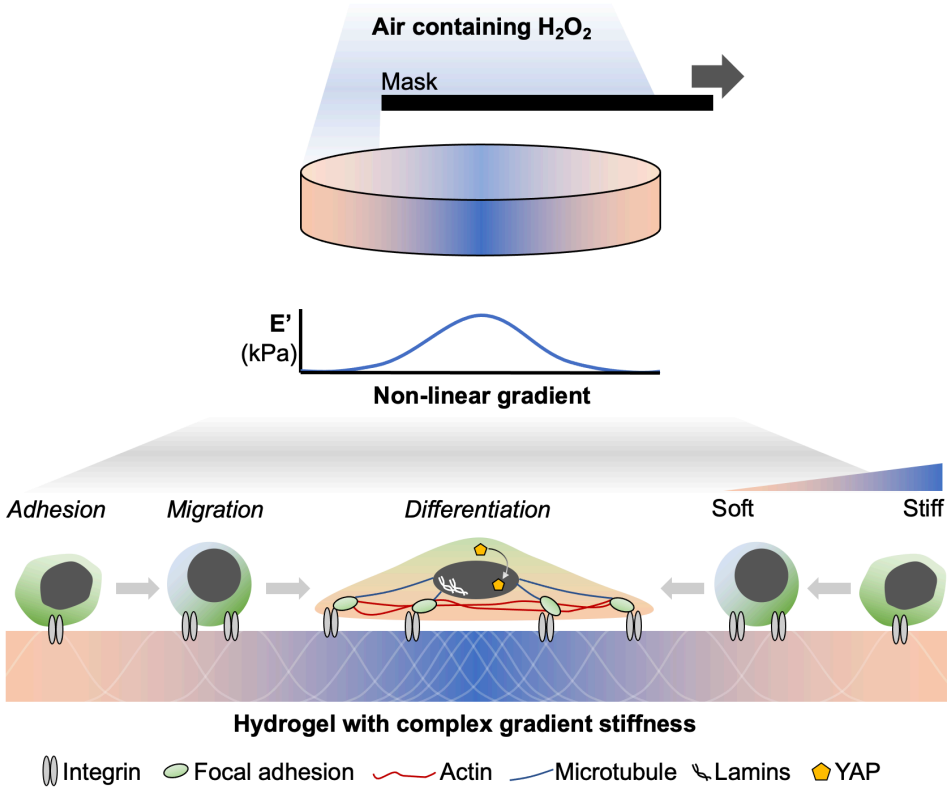

Fig. S-1 Schematic illustration of fabrication of hydrogel with non-linear gradient stiffness utilising air containing H_2O_2 exposure time-mediated stiffening and softening of the substrate.

(2) Fabrication of Cartilage-to-Bone (Osteochondral) Model Fabricated by Extrusion Printing

Osteochondral is an area around the articulating joint comprised of complex gradient stiffness from soft cartilage to stiff bone. Utilising the system developed in this study, a large-

scale osteochondral model with complex hydrogel stiffness can be developed **(Fig. S-2).** Stiffness gradient can be fabricated using two different inks containing HRP and different polymer solutions: Gelatin-Ph only and Gelatin-Ph/HA-Ph mixture exposed with air containing H_2O_2. Gelatin-Ph/HA-Ph mixture has higher stiffness and more functional effect on cells compared to only Gelatin-Ph. Thus, this structure will have both stiffness and functional gradient. To fabricate a functional artificial osteochondral tissue, induced pluripotent stem cells (iPSC) can be used. The combination of chemical cues by the biomaterials and physical properties of the substrate can be used to control the iPSC adhesion, migration, and, most importantly, spontaneous differentiation to bone and cartilage cells.

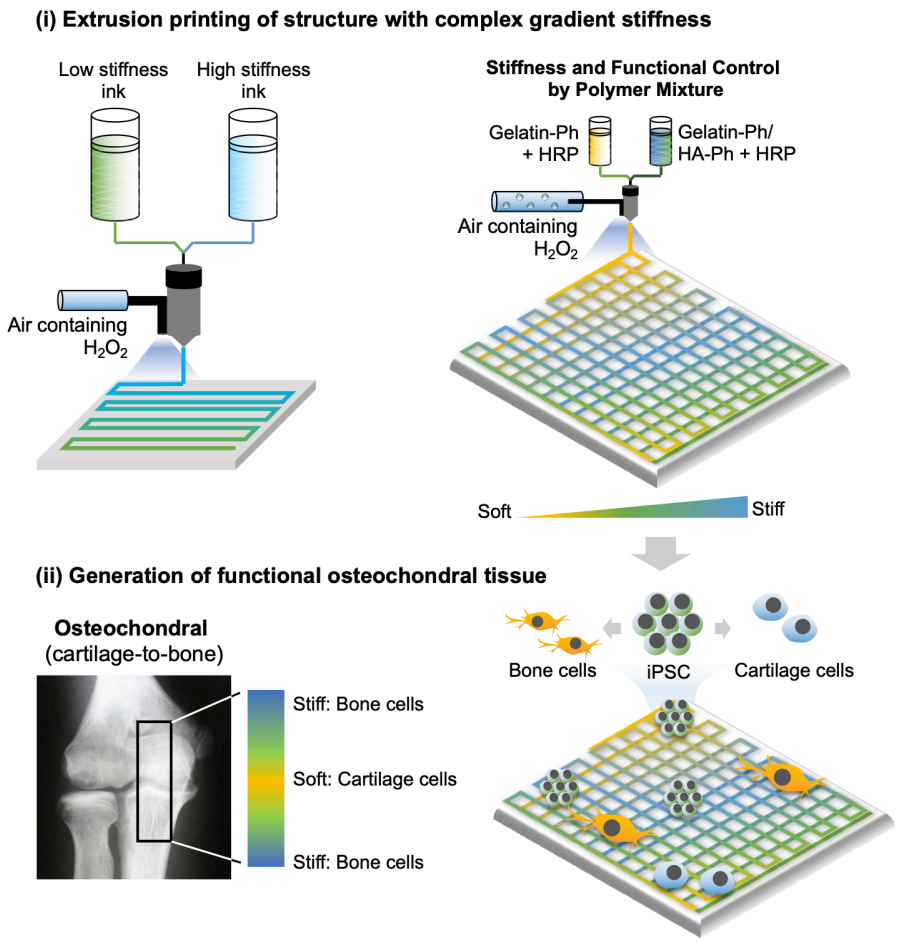

Fig. S-2 Schematic illustration of the fabrication of osteochondral tissue with complex gradient stiffness by extrusion printing of gelatin-based ink exposed with air containing H_2O_2.

References

Abalymov, A., Parakhonskiy, B. and Skirtach, A.G. 2020. Polymer-and hybrid-based biomaterials for interstitial, connective, vascular, nerve, visceral and musculoskeletal tissue engineering. *Polymers* 12(3), p. 620. doi: 10.3390/polym12030620.

Abreu-Rejón, A.D., Herrera-Kao, W., May-Pat, A., Ávila-Ortega, A., Rodríguez-Fuentes, N., Uribe-Calderón, J.A. and Cervantes-Uc, J.M. 2022. Effect of PEG grafting density on surface properties of polyurethane substrata and the viability of osteoblast and fibroblast cells. *Journal of Materials Science: Materials in Medicine* 33(6), p. 45. doi: 10.1007/s10856-022-06668-1.

Agarwal, V. et al. 2014. Evaluating the effects of nacre on human skin and scar cells in culture. *Toxicology Research* 3(4), pp. 223–227. doi: 10.1039/c4tx00004h.

Agheb, M., Dinari, M., Rafienia, M. and Salehi, H. 2017. Novel electrospun nanofibers of modified gelatin-tyrosine in cartilage tissue engineering. *Materials Science and Engineering C* 71, pp. 240–251. doi: 10.1016/j.msec.2016.10.003.

Ahmed, E.M. 2015. Hydrogel: Preparation, characterization, and applications: A review. *Journal of Advanced Research* 6(2), pp. 105–121. doi: 10.1016/j.jare.2013.07.006.

Alarcin, E. et al. 2021. Current strategies for the regeneration of skeletal muscle tissue. *International Journal of Molecular Sciences* 22(11), p. 5929. doi: 10.3390/ijms22115929.

Alexander, S., Koehl, G.E., Hirschberg, M., Geissler, E.K. and Friedl, P. 2008. Dynamic imaging of cancer growth and invasion: A modified skin-fold chamber model. *Histochemistry and Cell Biology* 130(6), pp. 1147–1154. doi: 10.1007/s00418-008-0529-1.

Alsberg, E., Kong, H.J., Hirano, Y., Smith, M.K., Albeiruti, A. and Mooney, D.J. 2003. Regulating bone formation via controlled scaffold degradation. *Journal of Dental Research* 82(11), pp. 903–908. doi: 10.1177/154405910308201111.

Apraiz, A., Mitxelena, J. and Zubiaga, A. 2017. Studying cell cycle-regulated gene expression by two complementary cell synchronization protocols. *Journal of Visualized Experiments* 124, p. e55745. doi: 10.3791/55745.

Arimori, T. et al. 2021. Structural mechanism of laminin recognition by integrin. *Nature Communications* 12(1), p. 4012. doi: 10.1038/s41467-021-24184-8.

Arnao, M.B., Acosta, M., del Rio, J.A., Varón, R. and García-Cánovas, F. 1990. A kinetic study on the suicide inactivation of peroxidase by hydrogen peroxide. *Biochimica et Biophysica Acta* 1041(1), pp. 43–47. doi: 10.1016/0167-4838(90)90120-5.

Arya, A.D. et al. 2016. Gelatin Methacrylate Hydrogels as Biomimetic Three-Dimensional Matrixes for Modeling Breast Cancer Invasion and Chemoresponse in Vitro. *ACS Applied Materials and Interfaces* 8(34), pp. 22005–22017. doi: 10.1021/acsami.6b06309.

Asano, S., Ito, S., Takahashi, K., Furuya, K., Kondo, M., Sokabe, M. and Hasegawa, Y. 2017. Matrix stiffness regulates migration of human lung fibroblasts. *Physiological Reports* 5(9), p. e13281. doi: 10.14814/phy2.13281.

Asano, T., Ishizua, T. and Yawo, H. 2012. Optically controlled contraction of photosensitive skeletal muscle cells. *Biotechnology and Bioengineering* 109(1), pp. 199–204. doi: 10.1002/bit.23285.

Asano, T., Ishizuka, T., Morishima, K. and Yawo, H. 2015. Optogenetic induction of contractile ability in immature C2C12 myotubes. *Scientific Reports* 5, p. 8317. doi: 10.1038/srep08317.

Assani, G. and Zhou, Y. 2019. Effect of modulation of epithelial-mesenchymal transition regulators Snail1 and Snail2 on cancer cell radiosensitivity by targeting of the cell cycle, cell apoptosis and cell migration/invasion (Review). *Oncology Letters* 17(1), pp. 23–30. doi: 10.3892/ol.2018.9636.

Avigdor, A. et al. 2004. CD44 and hyaluronic acid cooperate with SDF-1 in the trafficking of

human CD34+ stem/progenitor cells to bone marrow. *Blood* 103(8), pp. 2981–2989. doi: 10.1182/blood-2003-10-3611.

Bae, J.W., Choi, J.H., Lee, Y. and Park, K.D. 2015. Horseradish peroxidase-catalysed in situ-forming hydrogels for tissue-engineering applications. *Journal of Tissue Engineering and Regenerative Medicine* 9, pp. 1225–1232. doi: 10.1016/j.trsl.2010.06.007.

Baynton, K.J., Bewtra, J.K., Biswas, N. and Taylor, K.E. 1994. Inactivation of horseradish peroxidase by phenol and hydrogen peroxide: a kinetic investigation. *Biochimica et Biophysica Acta* 1206(2), pp. 272–278. doi: 10.1016/0167-4838(94)90218-6.

Bertero, T. et al. 2016. Vascular stiffness mechanoactivates YAP/TAZ-dependent glutaminolysis to drive pulmonary hypertension. *Journal of Clinical Investigation* 126(9), pp. 3313–3335. doi: 10.1172/JCI86387.

Bessho, M., Kojima, T., Okuda, S. and Hara, M. 2007. Radiation-induced cross-linking of gelatin by using γ-rays: Insoluble gelatin hydrogel formation. *Bulletin of the Chemical Society of Japan* 80(5), pp. 979–985. doi: 10.1246/bcsj.80.979.

Bettadapur, A. et al. 2016. Prolonged Culture of Aligned Skeletal Myotubes on Micromolded Gelatin Hydrogels. *Scientific Reports* 6, p. 28855. doi: 10.1038/srep28855.

Blobel, C.P. 2005. ADAMs: Key components in egfr signalling and development. *Nature Reviews Molecular Cell Biology* 6(1), pp. 32–43. doi: 10.1038/nrm1548.

Boonen, K.J.M., Rosaria-Chak, K.Y., Baaijens, F.P.T., Van Der Schaft, D.W.J. and Post, M.J. 2009. Essential environmental cues from the satellite cell niche: Optimizing proliferation and differentiation. *American Journal of Physiology - Cell Physiology* 296(6), pp. 1338–1345. doi: 10.1152/ajpcell.00015.2009.

Boontheekul, T., Hill, E.E., Kong, H.J. and Mooney, D.J. 2007. Regulating myoblast phenotype through controlled gel stiffness and degradation. *Tissue Engineering* 13(7), pp. 1431–1442. doi: 10.1089/ten.2006.0356.

Brooks, P.C., Montgomery, A.M.P., Rosenfeld, M., Reisfeld, R.A., Hu, T., Klier, G. and Cheresh, D.A. 1994. Integrin αvβ3 antagonists promote tumor regression by inducing apoptosis of angiogenic blood vessels. *Cell* 79(7), pp. 1157–1164. doi: 10.1016/0092-8674(94)90007-8.

Bryja, V., Bonilla, S. and Arenas, E. 2006. Derivation of mouse embryonic stem cells. *Nature Protocols* 1(4), pp. 2082–2087. doi: 10.1038/nprot.2006.355.

Burattini, S., Ferri, R., Battistelli, M., Curci, R., Luchetti, F. and Falcieri, E. 2004. C2C12 murine myoblasts as a model of skeletal muscle development: Morpho-functional characterization. *European Journal of Histochemistry* 48(3), pp. 223–233.

Calvo, F. et al. 2013. Mechanotransduction and YAP-dependent matrix remodelling is required for the generation and maintenance of cancer-associated fibroblasts. *Nature Cell Biology* 15(6), pp. 637–646. doi: 10.1038/ncb2756.

Camci-Unal, G., Cuttica, D., Annabi, N., Demarchi, D. and Khademhosseini, A. 2013. Synthesis and characterization of hybrid hyaluronic acid-gelatin hydrogels. *Biomacromolecules* 14(4), pp. 1085–1092. doi: 10.1021/bm3019856.

Canfell, K. 2019. Towards the global elimination of cervical cancer. *Papillomavirus Research* 8, p. 100170. Available at: https://doi.org/10.1016/j.pvr.2019.100170.

Cao, H., Duan, L., Zhang, Y., Cao, J. and Zhang, K. 2021. Current hydrogel advances in physicochemical and biological response-driven biomedical application diversity. *Signal Transduction and Targeted Therapy* 6, p. 426. doi: 10.1038/s41392-021-00830-x.

Carvalho, R.H., Lemos, F., Lemos, M.A.N.D.A., Vojinović, V., Fonseca, L.P. and Cabral, J.M.S. 2006. Kinetic modelling of phenol co-oxidation using horseradish peroxidase. *Bioprocess and Biosystems Engineering* 29(2), pp. 99–108. doi: 10.1007/s00449-006-0057-0.

Case, L.B., Ditlev, J.A. and Rosen, M.K. 2019. Regulation of Transmembrane Signaling by

Phase Separation. *Annual Review of Biophysics* 48, pp. 465–494. doi: 10.1146/annurev-biophys-052118-115534.

Cataldo, F., Ursini, O., Lilla, E. and Angelini, G. 2008. Radiation-induced crosslinking of collagen gelatin into a stable hydrogel. *Journal of Radioanalytical and Nuclear Chemistry* 275(1), pp. 125–131. doi: 10.1007/s10967-007-7003-8.

Catelas, I., Sese, N., Wu, B.M., Dunn, J.C.Y., Helgerson, S. and Tawil, B. 2006. Human mesenchymal stem cell proliferation and osteogenic differentiation in fibrin gels in vitro. *Tissue Engineering* 12(8), pp. 2385–2396. doi: 10.1089/ten.2006.12.2385.

Chang, K.L.B., Tai, M.C. and Cheng, F.H. 2001. Kinetics and products of the degradation of chitosan by hydrogen peroxide. *Journal of Agricultural and Food Chemistry* 49(10), pp. 4845–4851. doi: 10.1021/jf001469g.

Chen, B.H., Tzen, J.T.C., Bresnick, A.R. and Chen, H. 2002. Roles of Rho-associated kinase and myosin light chain kinase in morphological and migratory defects of focal adhesion kinase-null cells. *Journal of Biological Chemistry* 277(37), pp. 33857–33863. doi: 10.1074/jbc.M204429200.

Chen, H., Qin, J. and Hu, Y. 2019. Efficient degradation of high-molecular-weight hyaluronic acid by a combination of ultrasound, hydrogen peroxide, and copper ion. *Molecules* 24(3), p. 617. doi: 10.3390/molecules24030617.

Chen, T., Small, D.A., McDermott, M.K., Bentley, W.E. and Payne, G.F. 2003. Enzymatic methods for in situ cell entrapment and cell release. *Biomacromolecules* 4(6), pp. 1558–1563. doi: 10.1021/bm034145k.

Chin, I.L., Hool, L. and Choi, Y.S. 2021. Interrogating cardiac muscle cell mechanobiology on stiffness gradient hydrogels. *Biomaterials Science* 9(20), pp. 6795–6806. doi: 10.1039/d1bm01061a.

Chiu, W.-T., Wang, Y.-H., Tang, M.-J. and Shen, M.-R. 2007. Soft Substrate Induces

Apoptosis by the Disturbance of Ca2+ Homeostasis in Renal Epithelial LLC-PK1 Cells. *Journal Cellular Physiology* 212, pp. 401–410. doi: 10.1002/jcp.21037.

Clark, R.A.F., Tonnesen, M.G., Gailit, J. and Cheresh, D.A. 1996. Transient functional expression of αvβ3 on vascular cells during wound repair. *American Journal of Pathology* 148(5), pp. 1407–1421.

Csapo, R., Gumpenberger, M. and Wessner, B. 2020. Skeletal Muscle Extracellular Matrix – What Do We Know About Its Composition, Regulation, and Physiological Roles? A Narrative Review. *Frontiers in Physiology* 11, p. 253. doi: 10.3389/fphys.2020.00253.

De Becker, A., Van Hummelen, P., Bakkus, M., Broek, I. Vande, De Wever, J., De Waele, M. and Van Riet, I. 2007. Migration of culture-expanded human mesenchymal stem cells through bone marrow endothelium is regulated by matrix metalloproteinase-2 and tissue inhibitor of metalloproteinase-3. *Haematologica* 92(4), pp. 440–449. doi: 10.3324/haematol.10475.

Denes, L.T., Riley, L.A., Mijares, J.R., Arboleda, J.D., McKee, K., Esser, K.A. and Wang, E.T. 2019. Culturing C2C12 myotubes on micromolded gelatin hydrogels accelerates myotube maturation. *Skeletal Muscle* 9(1), p. 17. doi: 10.1186/s13395-019-0203-4.

Dinda, S., Sarkar, S. and Das, P.K. 2018. Glucose oxidase mediated targeted cancer-starving therapy by biotinylated self-assembled vesicles. *Chemical Communications* 54(71), pp. 9929–9932. doi: 10.1039/c8cc03599g.

Doolin, M.T., Moriarty, R.A. and Stroka, K.M. 2020. Mechanosensing of Mechanical Confinement by Mesenchymal-Like Cells. *Frontiers in Physiology* 11, p. 365. doi: 10.3389/fphys.2020.00365.

Du, J. et al. 2016. Extracellular matrix stiffness dictates Wnt expression through integrin pathway. *Scientific Reports* 6(1), p. 20395. doi: 10.1038/srep20395.

Du, W., Hong, S., Scapin, G., Goulard, M. and Shah, D.I. 2019. Directed Collective Cell

Migration Using Three-Dimensional Bioprinted Micropatterns on Thermoresponsive Surfaces for Myotube Formation. *ACS Biomaterials Science and Engineering* 5(8), pp. 3935–3943. doi: 10.1021/acsbiomaterials.8b01359.

Dupont, S. 2016. Role of YAP/TAZ in cell-matrix adhesion-mediated signalling and mechanotransduction. *Experimental Cell Research* 343(1), pp. 42–53. doi: 10.1016/j.yexcr.2015.10.034.

Engler, A., Bacakova, L., Newman, C., Hategan, A., Griffin, M. and Discher, D. 2004a. Substrate Compliance versus Ligand Density in Cell on Gel Responses. *Biophysical Journal* 86(1), pp. 617–628. doi: 10.1016/S0006-3495(04)74140-5.

Engler, A.J., Griffin, M.A., Sen, S., Bönnemann, C.G., Sweeney, H.L. and Discher, D.E. 2004b. Myotubes differentiate optimally on substrates with tissue-like stiffness: Pathological implications for soft or stiff microenvironments. *Journal of Cell Biology* 166(6), pp. 877–887. doi: 10.1083/jcb.200405004.

Engler, A.J., Sen, S., Sweeney, H.L. and Discher, D.E. 2006. Matrix Elasticity Directs Stem Cell Lineage Specification. *Cell* 126(4), pp. 677–689. doi: 10.1016/j.cell.2006.06.044.

Fan, Y., Sun, Q., Li, X., Feng, J., Ao, Z., Li, X. and Wang, J. 2021. Substrate Stiffness Modulates the Growth, Phenotype, and Chemoresistance of Ovarian Cancer Cells. *Frontiers in Cell and Developmental Biology* 9, p. 718834. doi: 10.3389/fcell.2021.718834.

Farris, S., Song, J. and Huang, Q. 2010. Alternative reaction mechanism for the cross-linking of gelatin with glutaraldehyde. *Journal of Agricultural and Food Chemistry* 58(2), pp. 998–1003. doi: 10.1021/jf9031603.

Felgueiras, H.P., Antunes, J.C., Martins, M.C.L. and Barbosa, M.A. 2017. Fundamentals of protein and cell interactions in biomaterials. In: *Biomedicine & Pharmacotherapy*. Elsevier Ltd., pp. 956–970. Available at: https://doi.org/10.1016/B978-0-08-100803-4.00001-2.

Flanagan, L.A., Ju, Y. El, Marg, B., Osterfield, M. and Janmey, P.A. 2002. Neurite branching

on deformable substrates. *NeuroReport* 13(18), pp. 2411–2415. doi: 10.1097/00001756-200212200-00007.

Frantz, C., Stewart, K.M. and Weaver, V.M. 2010. The extracellular matrix at a glance. *Journal of Cell Science* 123(24), pp. 4195–4200. doi: 10.1242/jcs.023820.

Fraser, J.R.E., Laurent, T.C. and Laurent, U.B.G. 1997. Hyaluronan: Its nature, distribution, functions and turnover. *Journal of Internal Medicine* 242(1), pp. 27–33. doi: 10.1046/j.1365-2796.1997.00170.x.

Friedl, P. and Alexander, S. 2011. Cancer invasion and the microenvironment: Plasticity and reciprocity. *Cell* 147(5), pp. 992–1009. doi: 10.1016/j.cell.2011.11.016.

Fuchs, K., Hippe, A., Schmaus, A., Homey, B., Sleeman, J.P. and Orian-Rousseau, V. 2013. Opposing effects of high-and low-molecular weight hyaluronan on CXCL12-induced CXCR4 signaling depend on CD44. *Cell Death and Disease* 4(10), p. e819. doi: 10.1038/cddis.2013.364.

Ganesan, M., Dagur, R.S., Makarov, E., Poluektova, L.I., Kidambi, S. and Osna, N.A. 2018. Matrix stiffness regulate apoptotic cell death in HIV-HCV co-infected hepatocytes: Importance for liver fibrosis progression. *Biochemical and Biophysical Research Communications* 500(3), pp. 717–722. Available at: https://doi.org/10.1016/j.bbrc.2018.04.142.

Gantumur, E., Kimura, M., Taya, M., Horie, M., Nakamura, M. and Sakai, S. 2019. Inkjet micropatterning through horseradish peroxidase-mediated hydrogelation for controlled cell immobilization and microtissue fabrication. *Biofabrication* 12(1), p. 011001. doi: 10.1088/1758-5090/ab3b3c.

Gantumur, E., Nakahata, M., Kojima, M. and Sakai, S. 2020. Extrusion-based bioprinting through glucose-mediated enzymatic hydrogelation. *International Journal of Bioprinting* 6(1), pp. 43–52. doi: 10.18063/ijb.v6i1.250.

Gérard, C. and Goldbeter, A. 2014. The balance between cell cycle arrest and cell proliferation: Control by the extracellular matrix and by contact inhibition. *Interface Focus* 4(3). doi: 10.1098/rsfs.2013.0075.

Ghandforoushan, P., Hanaee, J., Aghazadeh, Z., Samiei, M., Navali, A.M., Khatibi, A. and Davaran, S. 2022. Enhancing the function of PLGA-collagen scaffold by incorporating TGF-β1-loaded PLGA-PEG-PLGA nanoparticles for cartilage tissue engineering using human dental pulp stem cells. *Drug Delivery and Translational Research* . Available at: https://doi.org/10.1007/s13346-022-01161-2.

Ghatak, S., Misra, S. and Toole, B.P. 2002. Hyaluronan oligosaccharides inhibit anchorage-independent growth of tumor cells by suppressing the phosphoinositide 3-kinase/Akt cell survival pathway. *Journal of Biological Chemistry* 277(41), pp. 38013–38020. doi: 10.1074/jbc.M202404200.

Gillmor, J.R., Connelly, R.W., Colby, R.H. and Tan, J.S. 1999. Effect of sodium poly(styrene sulfonate) on thermoreversible gelation of gelatin. *Journal of Polymer Science, Part B: Polymer Physics* 37(16), pp. 2287–2295. doi: 10.1002/(SICI)1099-0488(19990815)37:16<2287::AID-POLB31>3.0.CO;2-N.

Glorieux, F.H. 2008. Osteogenesis imperfecta. *Best Practice and Research: Clinical Rheumatology* 22(1), pp. 85–100. doi: 10.1016/j.berh.2007.12.012.

Goh, Q., Dearth, C.L., Corbett, J.T., Pierre, P., Chadee, D.N. and Pizza, F.X. 2015. Intercellular adhesion molecule-1 expression by skeletal muscle cells augments myogenesis. *Experimental Cell Research* 331(2), pp. 292–308. doi: 10.1016/j.yexcr.2014.09.032.

Gomez-Guillen, M.C., Gimenez, B., Lopez-Caballero, M.E. and Montero, M.P. 2011. Functional and bioactive properties of collagen and gelatin from alternative sources: A review. *Food Hydrocolloids* 25(8), pp. 1813–1827. doi: 10.1016/j.foodhyd.2011.02.007.

Greco, R.M., Iocono, J.A. and Ehrlich, H.P. 1998. Hyaluronic acid stimulates human fibroblast

proliferation within a collagen matrix. *Journal of Cellular Physiology* 177(3), pp. 465–473. doi: 10.1002/(SICI)1097-4652(199812)177:3<465::AID-JCP9>3.0.CO;2-5.

Gribova, V., Gauthier-Rouvière, C., Albigès-Rizo, C., Auzely-Velty, R. and Picart, C. 2013. Effect of RGD functionalization and stiffness modulation of polyelectrolyte multilayer films on muscle cell differentiation. *Acta Biomaterialia* 9(5), pp. 6468–6480. doi: 10.1016/j.actbio.2012.12.015.

Gupta, D., Santoso, J.W. and McCain, M.L. 2021. Characterization of gelatin hydrogels cross-linked with microbial transglutaminase as engineered skeletal muscle substrates. *Bioengineering* 8(1), p. 6. doi: 10.3390/bioengineering8010006.

Guvendiren, M. and Burdick, J.A. 2012. Stiffening hydrogels to probe short- and long-term cellular responses to dynamic mechanics. *Nature Communications* 3(1), p. 792. doi: 10.1038/ncomms1792.

Hadden, W.J. et al. 2017. Stem cell migration and mechanotransduction on linear stiffness gradient hydrogels. *Proceedings of the National Academy of Sciences of the United States of America* 114(22), pp. 5647–5652. doi: 10.1073/pnas.1618239114.

Hadjipanayi, E., Mudera, V. and Brown, R.A. 2009. Close dependence of fibroblast proliferation on collagen scaffold matrix stiffness. *Journal of Tissue Engineering and Regenerative Medicine* 3, pp. 77–84. doi: 10.1016/j.trsl.2010.06.007.

Harada, T. et al. 2014. Nuclear lamin stiffness is a barrier to 3D migration, but softness can limit survival. *Journal of Cell Biology* 204(5), pp. 669–682. doi: 10.1083/jcb.201308029.

Hayashi, K. et al. 2022. One-Step Synthesis of Gelatin-Conjugated Supramolecular Hydrogels for Dynamic Regulation of Adhesion Contact and Morphology of Myoblasts. *ACS Applied Polymer Materials* 4(4), pp. 2595–2603. doi: 10.1021/acsapm.1c01902.

Hindi, S.M., Tajrishi, M.M. and Kumar, A. 2013. Signaling mechanisms in mammalian myoblast fusion. *Science Signaling* 6(272), p. re2. doi: 10.1126/scisignal.2003832.

Hoshiba, T., Yoshihiro, A. and Tanaka, M. 2017. Evaluation of initial cell adhesion on poly (2-methoxyethyl acrylate) (PMEA) analogous polymers. *Journal of Biomaterials Science, Polymer Edition* 28(10–12), pp. 986–999. doi: 10.1080/09205063.2017.1312738.

Hosseini, V. et al. 2012. Engineered contractile skeletal muscle tissue on a microgrooved methacrylated gelatin substrate. *Tissue Engineering - Part A* 18(23–24), pp. 2453–2465. doi: 10.1089/ten.tea.2012.0181.

Hou, J., Li, C., Guan, Y., Zhang, Y. and Zhu, X.X. 2015. Enzymatically crosslinked alginate hydrogels with improved adhesion properties. *Polymer Chemistry* 6(12), pp. 2204–2213. doi: 10.1039/c4py01757a.

Hu, M. et al. 2009. Cell immobilization in gelatin-hydroxyphenylpropionic acid hydrogel fibers. *Biomaterials* 30(21), pp. 3523–3531. doi: 10.1016/j.biomaterials.2009.03.004.

Huang, D. et al. 2019. Viscoelasticity in natural tissues and engineered scaffolds for tissue reconstruction. *Acta Biomaterialia* 97, pp. 74–92. Available at: https://doi.org/10.1016/j.actbio.2019.08.013.

Huang, Q., Huang, Q., Pinto, R.A., Griebenow, K., Schweitzer-Stenner, R. and Weber, W.J. 2005. Inactivation of horseradish peroxidase by phenoxyl radical attack. *Journal of the American Chemical Society* 127(5), pp. 1431–1437. doi: 10.1021/ja045986h.

Ikeda, K., Ito, A., Imada, R., Sato, M., Kawabe, Y. and Kamihira, M. 2017. In vitro drug testing based on contractile activity of C2C12 cells in an epigenetic drug model. *Scientific Reports* 7, p. 44570. doi: 10.1038/srep44570.

Iskratsch, T., Wolfenson, H. and Sheetz, M.P. 2014. Appreciating force and shape-the rise of mechanotransduction in cell biology. *Nature Reviews Molecular Cell Biology* 15(12), pp. 825–833. doi: 10.1038/nrm3903.

Ito, A. et al. 2003. Transglutaminase-mediated gelatin matrices incorporating cell adhesion factors as a biomaterial for tissue engineering. *Journal of Bioscience and Bioengineering*

95(2), pp. 196–199. doi: 10.1263/jbb.95.196.

Jabłońska-Trypuć, A., Matejczyk, M. and Rosochacki, S. 2016. Matrix metalloproteinases (MMPs), the main extracellular matrix (ECM) enzymes in collagen degradation, as a target for anticancer drugs. *Journal of Enzyme Inhibition and Medicinal Chemistry* 31, pp. 177–183. doi: 10.3109/14756366.2016.1161620.

Jaipan, P., Nguyen, A. and Narayan, R.J. 2017. Gelatin-based hydrogels for biomedical applications. *MRS Communications* 7(3), pp. 416–426. doi: 10.1557/mrc.2017.92.

Janmey, P.A., Fletcher, D.A. and Reinhart-King, C.A. 2020. Stiffness sensing by cells. *Physiological Reviews* 100(2), pp. 695–724. doi: 10.1152/physrev.00013.2019.

Jariyal, H., Gupta, C. and Srivastava, A. 2020. Hyaluronic acid induction on breast cancer stem cells unfolds subtype specific variations in stemness and epithelial-to-mesenchymal transition. *International Journal of Biological Macromolecules* 160, pp. 1078–1089. doi: 10.1016/j.ijbiomac.2020.05.236.

Järveläinen, H., Sainio, A., Koulu, M., Wight, T.N. and Penttinen, R. 2009. Extracellular matrix molecules: Potential targets in pharmacotherapy. *Pharmacological Reviews* 61(2), pp. 198–223. doi: 10.1124/pr.109.001289.

Jiang, D., Liang, J. and Noble, P.W. 2007. Hyaluronan in tissue injury and repair. *Annual Review of Cell and Developmental Biology* 23, pp. 435–461. doi: 10.1146/annurev.cellbio.23.090506.123337.

Jingwen, B., Yaochen, L. and Guojun, Z. 2017. Cell cycle regulation and anticancer drug discovery. *Cancer Biology & Medicine* 14(4), p. 348. doi: 10.20892/j.issn.2095-3941.2017.0033.

Johnson, L.A., Rodansky, E.S., Sauder, K.L., Horowitz, J.C., Mih, J.D., Tschumperlin, D.J. and Higgins, P.D. 2013. Matrix stiffness corresponding to strictured bowel induces a fibrogenic response in human colonic fibroblasts. *Inflammatory Bowel Diseases* 19(5), pp.

891–903. doi: 10.1097/MIB.0b013e3182813297.

Judge, D.P. and Dietz, H.C. 2005. Marfan's syndrome. *Lancet* 366, pp. 1965–1976. doi: 10.1016/S0140-6736(05)67789-6.

Kaijzel, E.L., Koolwijk, P., Van Erck, M.G.M., Van Hinsbergh, V.W.M. and De Maat, M.P.M. 2006. Molecular weight fibrinogen variants determine angiogenesis rate in a fibrin matrix in vitro and in vivo. *Journal of Thrombosis and Haemostasis* 4(9), pp. 1975–1981. doi: 10.1111/j.1538-7836.2006.02081.x.

Kalli, M. and Stylianopoulos, T. 2018. Defining the role of solid stress and matrix stiffness in cancer cell proliferation and metastasis. *Frontiers in Oncology* 8, p. 55. doi: 10.3389/fonc.2018.00055.

Katoh, K. 2020. FAK-Dependent Cell Motility and Cell Elongation. *Cells* 9(1), p. 192. doi: 10.3390/cells9010192.

Kessenbrock, K., Plaks, V. and Werb, Z. 2010. Matrix Metalloproteinases: Regulators of the Tumor Microenvironment. *Cell* 141(1), pp. 52–67. doi: 10.1016/j.cell.2010.03.015.

Khanmohammadi, M., Dastjerdi, M.B., Ai, A., Ahmadi, A., Godarzi, A., Rahimi, A. and Ai, J. 2018. Horseradish peroxidase-catalyzed hydrogelation for biomedical applications. *Biomaterials Science* 6(6), pp. 1286–1298. doi: 10.1039/c8bm00056e.

Kim, B.Y., Park, K.M., Joung, Y.K. and Park, K.D. 2012. Preparation and characterizations of in situ shell cross-linked 4-arm-poly(propylene oxide)-poly(ethylene oxide) micelles via enzyme-mediated reaction for controlled drug delivery. *Journal of Bioactive and Compatible Polymers* 27(3), pp. 185–197. doi: 10.1177/0883911512441098.

Kim, J., Wang, Z.M., Heymsfield, S.B., Baumgartner, R.N. and Gallagher, D. 2002. Total-body skeletal muscle mass: Estimation by a new dual-energy X-ray absorptiometry method. *American Journal of Clinical Nutrition* 76(2), pp. 378–383. doi: 10.1093/ajcn/76.2.378.

Kirchmajer, D.M., Watson, C.A., Ranson, M. and Panhuis, M. In Het 2013. Gelapin, a

degradable genipin cross-linked gelatin hydrogel. *RSC Advances* 3(4), pp. 1073–1081. doi: 10.1039/c2ra22859a.

Klein, E.A. et al. 2009. Cell-Cycle Control by Physiological Matrix Elasticity and In Vivo Tissue Stiffening. *Current Biology* 19(18), pp. 1511–1518. doi: 10.1016/j.cub.2009.07.069.

Kojima, T., Bessho, M., Furuta, M., Okuda, S. and Hara, M. 2004. Characterization of biopolymer hydrogels produced by γ-ray irradiation. *Radiation Physics and Chemistry* 71(1–2), pp. 235–238. doi: 10.1016/j.radphyschem.2004.04.069.

Kondo, D., Ogino, Y., Ayukawa, Y., Sakai, S., Kawakami, K. and Koyano, K. 2013. Bone Regeneration of Tibial Defects in Rats with Enzymatic Hydrogelation of Gelatin Derivative and Recombinant Human Platelet-Derived Growth Factor-BB Complex. *The International Journal of Oral & Maxillofacial Implants* 28(5), pp. 1377–1385. doi: 10.11607/jomi.2861.

Kouvidi, K. et al. 2011. Role of Receptor for Hyaluronic Acid-mediated Motility (RHAMM) in Low Molecular Weight Hyaluronan (LMWHA)- mediated fibrosarcoma cell adhesion. *Journal of Biological Chemistry* 286(44), pp. 38509–38520. doi: 10.1074/jbc.M111.275875.

Kumar, S. and Parekh, S.H. 2020. Linking graphene-based material physicochemical properties with molecular adsorption, structure and cell fate. *Communications Chemistry* 3(1), p. 8. doi: 10.1038/s42004-019-0254-9.

Kunda, P. and Baum, B. 2009. The actin cytoskeleton in spindle assembly and positioning. *Trends in Cell Biology* 19(4), pp. 174–179. doi: 10.1016/j.tcb.2009.01.006.

Lacraz, G. et al. 2015. Increased stiffness in aged skeletal muscle impairs muscle progenitor cell proliferative activity. *PLoS ONE* 10(8), p. e0136217. doi: 10.1371/journal.pone.0136217.

Lai, J.Y., Lu, P.L., Chen, K.H., Tabata, Y. and Hsiue, G.H. 2006. Effect of charge and molecular weight on the functionality of gelatin carriers for corneal endothelial cell therapy.

Biomacromolecules 7(6), pp. 1836–1844. doi: 10.1021/bm0601575.

Lam, T. et al. 2019. Photopolymerizable gelatin and hyaluronic acid for stereolithographic 3D bioprinting of tissue-engineered cartilage. *Journal of Biomedical Materials Research - Part B Applied Biomaterials* 107(8), pp. 2649–2657. doi: 10.1002/jbm.b.34354.

Lan, T. et al. 2016. Cross-linked hyaluronic acid gel inhibits metastasis and growth of gastric and hepatic cancer cells: In vitro and in vivo studies. *Oncotarget* 7(40), pp. 65418–65428. doi: 10.18632/oncotarget.11739.

Le Thi, P., Lee, Y., Nguyen, D.H. and Park, K.D. 2017. In situ forming gelatin hydrogels by dual-enzymatic cross-linking for enhanced tissue adhesiveness. *Journal of Materials Chemistry B* 5(4), pp. 757–764. doi: 10.1039/c6tb02179d.

Lebl, M.D.A., Martins, J.R.M., Nader, H.B., Simões, M.D.J. and De Biase, N. 2007. Concentration and distribution of hyaluronic acid in human vocal folds. *Laryngoscope* 117(4), pp. 595–599. doi: 10.1097/MLG.0b013e31802ffe17.

Lee, F., Chung, J.E. and Kurisawa, M. 2008. An injectable enzymatically crosslinked hyaluronic acid-tyramine hydrogel system with independent tuning of mechanical strength and gelation rate. *Soft Matter* 4(4), pp. 880–887. doi: 10.1039/b719557e.

Lee, K.Y. and Mooney, D.J. 2001. Hydrogels for tissue engineering. *Chemical Reviews* 101(7), pp. 1869–1879. doi: 10.1021/cr000108x.

Lee, S., Kim, J., Do, M., Namkoong, E., Lee, H., Ryu, J.H. and Park, K. 2020. Developmental role of hyaluronic acid and its application in salivary gland tissue engineering. *Acta Biomaterialia* 115, pp. 275–287. Available at: https://doi.org/10.1016/j.actbio.2020.08.030.

Levy-Mishali, M., Zoldan, J. and Levenberg, S. 2009. Effect of scaffold stiffness on myoblast differentiation. *Tissue Engineering - Part A* 15(4), pp. 935–944. doi: 10.1089/ten.tea.2008.0111.

Li, H., Wijekoon, A. and Leipzig, N.D. 2012. 3D Differentiation of Neural Stem Cells in

Macroporous Photopolymerizable Hydrogel Scaffolds. *PLoS ONE* 7(11), p. e48824. doi: 10.1371/journal.pone.0048824.

Li, J., He, A., Zheng, J. and Han, C.C. 2006. Gelatin and gelatin - Hyaluronic acid nanofibrous membranes produced by electrospinning of their aqueous solutions. *Biomacromolecules* 7(7), pp. 2243–2247. doi: 10.1021/bm0603342.

Li, X., Xu, A., Xie, H., Yu, W., Xie, W. and Ma, X. 2010. Preparation of low molecular weight alginate by hydrogen peroxide depolymerization for tissue engineering. *Carbohydrate Polymers* 79(3), pp. 660–664. doi: 10.1016/j.carbpol.2009.09.020.

Lim, C.T., Bershadsky, A. and Sheetz, M.P. 2010. Mechanobiology. *Journal of the Royal Society Interface* 7(3), pp. S291–S293. doi: 10.1098/rsif.2010.0150.focus.

Lim, K.S. et al. 2019. Visible Light Cross-Linking of Gelatin Hydrogels Offers an Enhanced Cell Microenvironment with Improved Light Penetration Depth. *Macromolecular Bioscience* 19(6), pp. 1–14. doi: 10.1002/mabi.201900098.

Liu, J., Si, S., Qin, Y., Zhang, B., Song, S. and Guo, Y. 2015. The effect of different molecular weight collagen peptides on MC3T3-E1 cells differentiation. *Bio-Medical Materials and Engineering* 26, pp. S2041–S2047. doi: 10.3233/BME-151509.

Liu, L., Eckert, M.A., Riazifar, H., Kang, D.K., Agalliu, D. and Zhao, W. 2013. From blood to the brain: Can systemically transplanted mesenchymal stem cells cross the blood-brain barrier? *Stem Cells International* 2013, p. 43509. doi: 10.1155/2013/435093.

Liu, M., Tolg, C. and Turley, E. 2019. Dissecting the dual nature of hyaluronan in the tumor microenvironment. *Frontiers in Immunology* 10, p. 947. doi: 10.3389/fimmu.2019.00947.

Liu, X., Jiang, Y., He, H. and Ping, W. 2014a. Hydrogen peroxide-induced degradation of type I collagen fibers of tilapia skin. *Food Structure* 2(1–2), pp. 41–48. doi: 10.1016/j.foostr.2014.08.001.

Liu, Y., Sakai, S., Kawa, S. and Taya, M. 2014b. Identification of hydrogen peroxide-secreting

cells by cytocompatible coating with a hydrogel membrane. *Analytical Chemistry* 86(23), pp. 11592–11598. doi: 10.1021/ac503342k.

Lovisa, S. et al. 2015. Epithelial-to-mesenchymal transition induces cell cycle arrest and parenchymal damage in renal fibrosis. *Nature Medicine* 21(9), pp. 998–1009. doi: 10.1038/nm.3902.

Ma, H.T. and Poon, R.Y.C. 2011. Synchronization of HeLa Cells. In: Banfalvi, G. ed. *Methods in Molecular Biology (Methods and Protocols)*. New York, NY, USA: Humana Press, pp. 151–161. doi: 10.1007/978-1-61779-182-6_10.

Ma, Z., Liu, Z., Myers, D.P. and Terada, L.S. 2008. Mechanotransduction and anoikis: Death and the homeless cell. *Cell Cycle* 7(16), pp. 2462–2465. doi: 10.4161/cc.7.16.6463.

Maccabi, A. et al. 2018. Quantitative characterization of viscoelastic behavior in tissue-mimicking phantoms and ex vivo animal tissues. *PLoS ONE* 13(1), p. e0191919. doi: 10.1371/journal.pone.0191919.

Mad-Ali, S., Benjakul, S., Prodpran, T. and Maqsood, S. 2016. Characteristics and gel properties of gelatin from goat skin as affected by pretreatments using sodium sulfate and hydrogen peroxide. *Journal of the Science of Food and Agriculture* 96(6), pp. 2193–2203. doi: 10.1002/jsfa.7336.

Madduma-Bandarage, U.S.K. and Madihally, S. V. 2021. Synthetic hydrogels: Synthesis, novel trends, and applications. *Journal of Applied Polymer Science* 138(19), pp. 1–23. doi: 10.1002/app.50376.

Madl, C.M. et al. 2017. Maintenance of neural progenitor cell stemness in 3D hydrogels requires matrix remodelling. *Nature Materials* 16(12), pp. 1233–1242. doi: 10.1038/nmat5020.

Makita, R., Akasaka, T., Tamagawa, S., Yoshida, Y., Miyata, S., Miyaji, H. and Sugaya, T. 2018. Preparation of micro/nanopatterned gelatins crosslinked with genipin for

biocompatible dental implants. *Beilstein Journal of Nanotechnology* 9(1), pp. 1735–1754. doi: 10.3762/bjnano.9.165.

Maleiner, B., Tomasch, J., Heher, P., Spadiut, O., Rünzler, D. and Fuchs, C. 2018. The importance of biophysical and biochemical stimuli in dynamic skeletal muscle models. *Frontiers in Physiology* 9, p. 1130. doi: 10.3389/fphys.2018.01130.

Mannarino, M.M., Bassett, M., Donahue, D.T. and Biggins, J.F. 2020. Novel high-strength thromboresistant poly(vinyl alcohol)-based hydrogel for vascular access applications. *Journal of Biomaterials Science, Polymer Edition* 31(5), pp. 601–621. Available at: https://doi.org/10.1080/09205063.2019.1706148.

Mao, J.S., Cui, Y.L., Wang, X.H., Sun, Y., Yin, Y.J., Zhao, H.M. and Yao, K. De 2004. A preliminary study on chitosan and gelatin polyelectrolyte complex cytocompatibility by cell cycle and apoptosis analysis. *Biomaterials* 25(18), pp. 3973–3981. doi: 10.1016/j.biomaterials.2003.10.080.

Marastoni, S., Ligresti, G., Lorenzon, E., Colombatti, A. and Mongiat, M. 2008. Extracellular matrix: A matter of life and death. *Connective Tissue Research* 49(3–4), pp. 203–206. doi: 10.1080/03008200802143190.

Martino, F., Perestrelo, A.R., Vinarský, V., Pagliari, S. and Forte, G. 2018. Cellular mechanotransduction: From tension to function. *Frontiers in Physiology* 9, p. 824. doi: 10.3389/fphys.2018.00824.

Mascarenhas, M.M. et al. 2004. Low Molecular Weight Hyaluronan from Stretched Lung Enhances Interleukin-8 Expression. *American Journal of Respiratory Cell and Molecular Biology* 30(1), pp. 51–60. doi: 10.1165/rcmb.2002-0167OC.

Matsiko, A., Gleeson, J.P. and O'Brien, F.J. 2015. Scaffold mean pore size influences mesenchymal stem cell chondrogenic differentiation and matrix deposition. *Tissue Engineering - Part A* 21(3–4), pp. 486–497. doi: 10.1089/ten.tea.2013.0545.

McMahon, D.K. et al. 1994. C2C12 cells: biophysical, biochemical and immunocytochemical properties. *American Journal of Physiology - Cell Physiology* 266(6), pp. C1795–C1802. doi: 10.1152/ajpcell.1994.266.6.c1795.

Meng, Y., Cao, J., Chen, Y., Yu, Y. and Ye, L. 2020. 3D printing of a poly(vinyl alcohol)-based nano-composite hydrogel as an artificial cartilage replacement and the improvement mechanism of printing accuracy. *Journal of Materials Chemistry B* 8(4), pp. 677–690. doi: 10.1039/c9tb02278c.

Meyer-Schaller, N. et al. 2019. A Hierarchical Regulatory Landscape during the Multiple Stages of EMT. *Developmental Cell* 48(4), pp. 539–553. doi: 10.1016/j.devcel.2018.12.023.

Milewicz, D.M.G., Pyeritz, R.E., Stanley Crawford, E. and Byers, P.H. 1992. Marfan syndrome: Defective synthesis, secretion, and extracellular matrix formation of fibrillin by cultured dermal fibroblasts. *Journal of Clinical Investigation* 89(1), pp. 79–86. doi: 10.1172/JCI115589.

Morello, R. 2018. Osteogenesis imperfecta and therapeutics. *Matrix Biology* 71–72, pp. 294–312. Available at: https://doi.org/10.1016/j.matbio.2018.03.010.

Moriarty, R.A. and Stroka, K.M. 2018. Physical confinement alters sarcoma cell cycle progression and division. *Cell Cycle* 17(19–20), pp. 2360–2373. Available at: https://doi.org/10.1080/15384101.2018.1533776.

Mubarok, W., Elvitigala, K.C.M.L. and Sakai, S. 2022a. Tuning Myogenesis by Controlling Gelatin Hydrogel Properties. *Gels* 8(6), p. 387. doi: 10.3390/gels8060387.

Mubarok, W., Elvitigala, K.C.M.L., Nakahata, M., Kojima, M. and Sakai, S. 2022b. Modulation of Cell-Cycle Progression by Hydrogen Peroxide-Mediated Cross-Linking and Degradation of Cell-Adhesive Hydrogels. *Cells* 11(5), p. 881. doi: 10.3390/cells11050881.

Mubarok, W., Qu, Y. and Sakai, S. 2021. Influence of Hydrogen Peroxide-Mediated Cross-Linking and Degradation on Cell-Adhesive Gelatin Hydrogels. *ACS Applied Bio Materials*

4(5), pp. 4184–4190. doi: 10.1021/acsabm.0c01675.

Murakami, Y., Yokoyama, M., Okano, T., Nishida, H., Tomizawa, Y., Endo, M. and Kurosawa, H. 2007. A novel synthetic tissue-adhesive hydrogel using a crosslinkable polymeric micelle. *Journal of Biomedical Materials Research Part A* 80, pp. 421–427.

Nakahata, M., Gantumur, E., Furuno, K., Sakai, S. and Taya, M. 2018. Versatility of hydrogelation by dual-enzymatic reactions with oxidases and peroxidase. *Biochemical Engineering Journal* 131, pp. 1–8. doi: 10.1016/j.bej.2017.12.003.

Nam, S. and Chaudhuri, O. 2018. Mitotic cells generate protrusive extracellular forces to divide in three-dimensional microenvironments. *Nature Physics* 14(6), pp. 621–628. doi: 10.1038/s41567-018-0092-1.

Narasimhan, B.N., Horrocks, M.S. and Malmström, J. 2021. Hydrogels with Tunable Physical Cues and Their Emerging Roles in Studies of Cellular Mechanotransduction. *Advanced NanoBiomed Research* 1(10), p. 2100059. doi: 10.1002/anbr.202100059.

Nardone, G. et al. 2017. YAP regulates cell mechanics by controlling focal adhesion assembly. *Nature Communications* 8(1), p. 15321. doi: 10.1038/ncomms15321.

Nguyen, A.K., Goering, P.L., Elespuru, R.K., Das, S.S. and Narayan, R.J. 2020. The photoinitiator lithium phenyl (2,4,6-Trimethylbenzoyl) phosphinate with exposure to 405 nm light is cytotoxic to mammalian cells but not mutagenic in bacterial reverse mutation assays. *Polymers* 12(7), p. 1489. doi: 10.3390/polym12071489.

Ni, Y. and Chiang, M.Y.M. 2007. Cell morphology and migration linked to substrate rigidity. *Soft Matter* 3(10), pp. 1285–1292. doi: 10.1039/b703376a.

Nickerson, M.T., Patel, J., Heyd, D. V., Rousseau, D. and Paulson, A.T. 2006. Kinetic and mechanistic considerations in the gelation of genipin-crosslinked gelatin. *International Journal of Biological Macromolecules* 39(4–5), pp. 298–302. doi: 10.1016/j.ijbiomac.2006.04.010.

Ninan, N., Grohens, Y., Elain, A., Kalarikkal, N. and Thomas, S. 2013. Synthesis and characterisation of gelatin/zeolite porous scaffold. *European Polymer Journal* 49(9), pp. 2433–2445. doi: 10.1016/j.eurpolymj.2013.02.014.

Nosenko, M.A., Maluchenko, N. V., Drutskaya, M.S., Arkhipova, A.Y., Agapov, I.I., Nedospasov, S.A. and Moisenovich, M.M. 2017. Induction of ICAM-1 expression in mouse embryonic fibroblasts cultured on fibroin-gelatin scaffolds. *Acta Naturae* 9(3), pp. 89–93. doi: 10.32607/20758251-2017-9-3-89-93.

Nuytinck, L., Freund, M., Lagae, L., Pierard, G.E., Hermanns-Le, T. and De Paepe, A. 2000. Classical Ehlers-Danlos syndrome caused by a mutation in type I collagen. *American Journal of Human Genetics* 66(4), pp. 1398–1402. doi: 10.1086/302859.

Nyman, E., Huss, F., Nyman, T., Junker, J. and Kratz, G. 2013. Hyaluronic acid, an important factor in the wound healing properties of amniotic fluid: In vitro studies of re-epithelialisation in human skin wounds. *Journal of Plastic Surgery and Hand Surgery* 47(2), pp. 89–92. doi: 10.3109/2000656X.2012.733169.

Ogushi, Y., Sakai, S. and Kawakami, K. 2009. Phenolic hydroxy groups incorporated for the peroxidase-catalyzed gelation of a carboxymethylcehulose support: Cellular adhesion and proliferation. *Macromolecular Bioscience* 9(3), pp. 262–267. doi: 10.1002/mabi.200800263.

Ohkawara, Y., Tamura, G., Iwasaki, T., Tanaka, A., Kikuchi, T. and Shirato, K. 2000. Activation and transforming growth factor-β production in eosinophils by hyaluronan. *American Journal of Respiratory Cell and Molecular Biology* 23(4), pp. 444–451. doi: 10.1165/ajrcmb.23.4.3875.

Ondeck, M.G. et al. 2019. Dynamically stiffened matrix promotes malignant transformation of mammary epithelial cells via collective mechanical signaling. *Proceedings of the National Academy of Sciences of the United States of America* 116(9), pp. 3502–3507. doi:

10.1073/pnas.1814204116.

Ondeck, M.G. and Engler, A.J. 2016. Mechanical characterization of a dynamic and tunable methacrylated hyaluronic acid hydrogel. *Journal of Biomechanical Engineering* 138(2), pp. 1–6. doi: 10.1115/1.4032429.

Ooki, T., Murata-Kamiya, N., Takahashi-Kanemitsu, A., Wu, W. and Hatakeyama, M. 2019. High-Molecular-Weight Hyaluronan Is a Hippo Pathway Ligand Directing Cell Density-Dependent Growth Inhibition via PAR1b. *Developmental Cell* 49(4), pp. 590–604. doi: 10.1016/j.devcel.2019.04.018.

Park, J. et al. 2019. In Situ Cross-linking Hydrogel as a Vehicle for Retinal Progenitor Cell Transplantation. *Cell Transplantation* 28(5), pp. 596–606. doi: 10.1177/0963689719825614.

Parsons, J.T., Horwitz, A.R. and Schwartz, M.A. 2010. Cell adhesion: Integrating cytoskeletal dynamics and cellular tension. *Nature Reviews Molecular Cell Biology* 11(9), pp. 633–643. doi: 10.1038/nrm2957.

Paszek, M.J. et al. 2005. Tensional homeostasis and the malignant phenotype. *Cancer Cell* 8(3), pp. 241–254. doi: 10.1016/j.ccr.2005.08.010.

Peláez, R. et al. 2017. β3 integrin expression is required for invadopodia-mediated ECM degradation in lung carcinoma cells. *PLoS ONE* 12(8), p. e0181579. doi: 10.1371/journal.pone.0181579.

Peng, H.T., Blostein, M.D. and Shek, P.N. 2009. Experimental optimization of an in situ forming hydrogel for hemorrhage control. *Journal of Biomedical Materials Research - Part B Applied Biomaterials* 89(1), pp. 199–209. doi: 10.1002/jbm.b.31206.

Piccolo, S., Dupont, S. and Cordenonsi, M. 2014. The biology of YAP/TAZ: Hippo signaling and beyond. *Physiological Reviews* 94(4), pp. 1287–1312. doi: 10.1152/physrev.00005.2014.

Pierantoni, L. et al. 2021. Horseradish Peroxidase-Crosslinked Calcium-Containing Silk Fibroin Hydrogels as Artificial Matrices for Bone Cancer Research. *Macromolecular Bioscience* 21(4), p. 2000425. doi: 10.1002/mabi.202000425.

Pizza, F.X., Martin, R.A., Springer, E.M., Leffler, M.S., Woelmer, B.R., Recker, I.J. and Leaman, D.W. 2017. Intercellular adhesion molecule-1 augments myoblast adhesion and fusion through homophilic trans-interactions. *Scientific Reports* 7, p. 5094. doi: 10.1038/s41598-017-05283-3.

Poursamar, S.A., Lehner, A.N., Azami, M., Ebrahimi-Barough, S., Samadikuchaksaraei, A. and Antunes, A.P.M. 2016. The effects of crosslinkers on physical, mechanical, and cytotoxic properties of gelatin sponge prepared via in-situ gas foaming method as a tissue engineering scaffold. *Materials Science and Engineering C* 63, pp. 1–9. doi: 10.1016/j.msec.2016.02.034.

Prakash, V. et al. 2019. Ribosome biogenesis during cell cycle arrest fuels EMT in development and disease. *Nature Communications* 10(1), p. 2110. doi: 10.1038/s41467-019-10100-8.

Prasertsung, I., Damrongsakkul, S. and Saito, N. 2013. Crosslinking of a gelatin solutions induced by pulsed electrical discharges in solutions. *Plasma Processes and Polymers* 10(9), pp. 792–797. doi: 10.1002/ppap.201200148.

Previtera, M.L., Trout, K.L., Verma, D., Chippada, U., Schloss, R.S. and Langrana, N.A. 2012. Fibroblast morphology on dynamic softening of hydrogels. *Annals of Biomedical Engineering* 40(5), pp. 1061–1072. doi: 10.1007/s10439-011-0483-2.

Qian, Q. et al. 2021. A pure molecular drug hydrogel for post-surgical cancer treatment. *Biomaterials* 265, p. 120403. doi: 10.1016/j.biomaterials.2020.120403.

Rainer, A., Forte, G. and Gargioli, C. 2019. Editorial: Physico-chemical control of cell function. *Frontiers in Physiology* 10, p. 355. doi: 10.3389/fphys.2019.00355.

Ratanavaraporn, J., Rangkupan, R., Jeeratawatchai, H., Kanokpanont, S. and Damrongsakkul, S. 2010. Influences of physical and chemical crosslinking techniques on electrospun type A and B gelatin fiber mats. *International Journal of Biological Macromolecules* 47(4), pp. 431–438. doi: 10.1016/j.ijbiomac.2010.06.008.

Reihmann, M. and Ritter, H. 2006. Synthesis of phenol polymers using peroxidases. *Advances in Polymer Science* 194(1), pp. 1–49. doi: 10.1007/12_034.

Ren, K., He, C., Xiao, C., Li, G. and Chen, X. 2015. Injectable glycopolypeptide hydrogels as biomimetic scaffolds forcartilage tissue engineering. *Biomaterials* 51, pp. 238–249. doi: 10.1016/j.biomaterials.2015.02.026.

Ren, K., Li, B., Xu, Q., Xiao, C., He, C., Li, G. and Chen, X. 2017. Enzymatically crosslinked hydrogels based on linear poly(ethylene glycol) polymer: Performance and mechanism. *Polymer Chemistry* 8(45), pp. 7017–7024. doi: 10.1039/c7py01597f.

Reshetnikova, G., Barkan, R., Popov, B., Nikolsky, N. and Chang, L.S. 2000. Disruption of the actin cytoskeleton leads to inhibition of mitogen-induced cyclin E expression, Cdk2 phosphorylation, and nuclear accumulation of the retinoblastoma protein-related p107 protein. *Experimental Cell Research* 259(1), pp. 35–53. doi: 10.1006/excr.2000.4966.

Rezaeeyazdi, M., Colombani, T., Memic, A. and Bencherif, S.A. 2018. Injectable hyaluronic acid-co-gelatin cryogels for tissue-engineering applications. *Materials* 11(8), pp. 23–25. doi: 10.3390/ma11081374.

Robinson, P.A., Brown, S., McGrath, M.J., Coghill, I.D., Gurung, R. and Mitchell, C.A. 2003. Skeletal muscle LIM protein 1 regulates integrin-mediated myoblast adhesion, spreading, and migration. *American Journal of Physiology - Cell Physiology* 284(3), pp. C681–C695. doi: 10.1152/ajpcell.00370.2002.

Romanazzo, S. et al. 2012. Substrate stiffness affects skeletal myoblast differentiation in vitro. *Science and Technology of Advanced Materials* 13(6), p. 064211. doi: 10.1088/1468-

6996/13/6/064211.

Rose, J.B., Pacelli, S., El Haj, A.J., Dua, H.S., Hopkinson, A., White, L.J. and Rose, F.R.A.J. 2014. Gelatin-based materials in ocular tissue engineering. *Materials* 7(4), pp. 3106–3135. doi: 10.3390/ma7043106.

Rossi, C.A., Pozzobon, M. and De Coppi, P. 2010. Advances in musculoskeletal tissue engineering: Moving towards therapy. *Organogenesis* 6(3), pp. 167–172. doi: 10.4161/org.6.3.12419.

Rowlands, A.S., George, P.A. and Cooper-White, J.J. 2008. Directing osteogenic and myogenic differentiation of MSCs: Interplay of stiffness and adhesive ligand presentation. *American Journal of Physiology - Cell Physiology* 295(4), pp. 1037–1044. doi: 10.1152/ajpcell.67.2008.

Sabeh, F. et al. 2004. Tumor cell traffic through the extracellular matrix is controlled by the membrane-anchored collagenase MT1-MMP. *Journal of Cell Biology* 167(4), pp. 769–781. doi: 10.1083/jcb.200408028.

Sakai, S., Hirose, K., Moriyama, K. and Kawakami, K. 2010. Control of cellular adhesiveness in an alginate-based hydrogel by varying peroxidase and H_2O_2 concentrations during gelation. *Acta Biomaterialia* 6(4), pp. 1446–1452. doi: 10.1016/j.actbio.2009.10.004.

Sakai, S., Hirose, K., Taguchi, K., Ogushi, Y. and Kawakami, K. 2009a. An injectable, in situ enzymatically gellable, gelatin derivative for drug delivery and tissue engineering. *Biomaterials* 30(20), pp. 3371–3377. doi: 10.1016/j.biomaterials.2009.03.030.

Sakai, S. and Kawakami, K. 2007. Synthesis and characterization of both ionically and enzymatically cross-linkable alginate. *Acta Biomaterialia* 3(4), pp. 495–501. doi: 10.1016/j.actbio.2006.12.002.

Sakai, S., Komatani, K. and Taya, M. 2012. Glucose-triggered co-enzymatic hydrogelation of aqueous polymer solutions. *RSC Advances* 2(4), pp. 1502–1507. doi: 10.1039/c1ra01060c.

Sakai, S., Mochizuki, K., Qu, Y., Mail, M., Nakahata, M. and Taya, M. 2018. Peroxidase-catalyzed microextrusion bioprinting of cell-laden hydrogel constructs in vaporized ppm-level hydrogen peroxide. *Biofabrication* 10(4), p. 045007. doi: 10.1088/1758-5090/aadc9e.

Sakai, S. and Nakahata, M. 2017. Horseradish Peroxidase Catalyzed Hydrogelation for Biomedical, Biopharmaceutical, and Biofabrication Applications. *Chemistry - An Asian Journal* 12(24), pp. 3098–3109. doi: 10.1002/asia.201701364.

Sakai, S., Ohi, H. and Taya, M. 2019. Gelatin / Hyaluronic Acid Content in Hydrogels Obtained through Blue Light-Induced Gelation A ffects Hydrogel Properties and Adipose Stem. *Biomolecules* 9, p. 342. doi: 10.3390/biom9080342.

Sakai, S., Tsumura, M., Inoue, M., Koga, Y., Fukano, K. and Taya, M. 2013. Polyvinyl alcohol-based hydrogel dressing gellable on-wound via a co-enzymatic reaction triggered by glucose in the wound exudate. *Journal of Materials Chemistry B* 1(38), pp. 5067–5075. doi: 10.1039/c3tb20780c.

Sakai, S., Ueda, K. and Taya, M. 2015. Peritoneal adhesion prevention by a biodegradable hyaluronic acid-based hydrogel formed in situ through a cascade enzyme reaction initiated by contact with body fluid on tissue surfaces. *Acta Biomaterialia* 24, pp. 152–158. doi: 10.1016/j.actbio.2015.06.023.

Sakai, S., Yamada, Y., Zenke, T. and Kawakami, K. 2009b. Novel chitosan derivative soluble at neutral pH and in-situ gellable via peroxidase-catalyzed enzymatic reaction. *Journal of Materials Chemistry* 19(2), pp. 230–235. doi: 10.1039/b812086b.

Sakai, S., Yamamoto, Y., Enkhtuul, G., Ueda, K., Arai, K., Taya, M. and Nakamura, M. 2017. Inkjetting Plus Peroxidase-Mediated Hydrogelation Produces Cell-Laden, Cell-Sized Particles with Suitable Characters for Individual Applications. *Macromolecular Bioscience* 17(5), p. 1600416. doi: 10.1002/mabi.201600416.

Sakaue-Sawano, A., Kobayashi, T., Ohtawa, K. and Miyawaki, A. 2011. Drug-induced cell

cycle modulation leading to cell-cycle arrest, nuclear mis-segregation, or endoreplication. *BMC Cell Biology* 12(1), p. 2. doi: 10.1186/1471-2121-12-2.

Schäfer, M., Myers, C., Brown, R.D., Frid, M.G., Tan, W., Hunter, K. and Stenmark, K.R. 2016. Pulmonary Arterial Stiffness: Toward a New Paradigm in Pulmonary Arterial Hypertension Pathophysiology and Assessment. *Current Hypertension Reports* 18(1), p. 4. doi: 10.1007/s11906-015-0609-2.

Scott, R.A., Robinson, K.G., Kiick, K.L. and Akins, R.E. 2020. Human Adventitial Fibroblast Phenotype Depends on the Progression of Changes in Substrate Stiffness. *Advanced Healthcare Materials* 9, p. 1901593. doi: 10.1002/adhm.201901593.

Sheu, B.C., Lien, H.C., Ho, H.N., Lin, H.H., Chow, S.N., Huang, S.C. and Hsu, S.M. 2003. Increased expression and activation of gelatinolytic matrix metalloproteinases is associated with the progression and recurrence of human cervical cancer. *Cancer Research* 63(19), pp. 6537–6542.

Shin, I.J., Ahn, Y.T., Kim, Y., Kim, J.M. and An, W.G. 2011. Actin disruption agents induce phosphorylation of histone H2AX in human breast adenocarcinoma MCF-7 cells. *Oncology Reports* 25(5), pp. 1313–1319. doi: 10.3892/or.2011.1214.

Shin, S., Buel, G.R., Nagiec, M.J., Han, M.J., Roux, P.P., Blenis, J. and Yoon, S.O. 2019. ERK2 regulates epithelial-to-mesenchymal plasticity through DOCK10-dependent Rac1/FoxO1 activation. *Proceedings of the National Academy of Sciences of the United States of America* 116(8), pp. 2967–2976. doi: 10.1073/pnas.1811923116.

Shin, Y.C. et al. 2015a. Cell-adhesive matrices composed of RGD peptide-displaying M13 bacteriophage/poly(lactic-co-glycolic acid) nanofibers beneficial to myoblast differentiation. *Journal of Nanoscience and Nanotechnology* 15(10), pp. 7907–7912. doi: 10.1166/jnn.2015.11214.

Shin, Y.C. et al. 2015b. Stimulated myoblast differentiation on graphene oxide-impregnated

PLGA-collagen hybrid fibre matrices matrices. *Journal of Nanobiotechnology* 13(1), p. 21. doi: 10.1186/s12951-015-0081-9.

Shrestha, D., Choi, D. and Song, K. 2018. Actin dysfunction induces cell cycle delay at G2/M with sustained ERK and RSK activation in IMR-90 normal human fibroblasts. *Molecules and Cells* 41(5), pp. 436–443. doi: 10.14348/molcells.2018.2266.

Sicard, D., Fredenburgh, L.E. and Tschumperlin, D.J. 2017. Measured pulmonary arterial tissue stiffness is highly sensitive to AFM indenter dimensions. *Journal of the Mechanical Behavior of Biomedical Materials* 74(May), pp. 118–127. doi: 10.1016/j.jmbbm.2017.05.039.

Silver, J.S. et al. 2021. Injury-mediated stiffening persistently activates muscle stem cells through YAP and TAZ mechanotransduction. *Science Advances* 7(11), p. eabe4501. doi: 10.1126/SCIADV.ABE4501.

Steingen, C., Brenig, F., Baumgartner, L., Schmidt, J., Schmidt, A. and Bloch, W. 2008. Characterization of key mechanisms in transmigration and invasion of mesenchymal stem cells. *Journal of Molecular and Cellular Cardiology* 44(6), pp. 1072–1084. doi: 10.1016/j.yjmcc.2008.03.010.

Stewart, Z.A., Westfall, M.D. and Pietenpol, J.A. 2003. Cell-cycle dysregulation and anticancer therapy. *Trends in Pharmacological Sciences* 24(3), pp. 139–145. doi: 10.1016/S0165-6147(03)00026-9.

Suga, T., Osada, S., Narita, T., Oishi, Y. and Kodama, H. 2015. Promotion of cell adhesion by low-molecular-weight hydrogel by Lys based amphiphile. *Materials Science and Engineering C* 47, pp. 345–350. doi: 10.1016/j.msec.2014.11.032.

Sun, M. et al. 2018. Effects of matrix stiffness on the morphology, adhesion, proliferation and osteogenic differentiation of mesenchymal stem cells. *International Journal of Medical Sciences* 15(3), pp. 257–268. doi: 10.7150/ijms.21620.

Sun, Y., Deng, R., Ren, X., Zhang, K. and Li, J. 2019. 2D Gelatin Methacrylate Hydrogels with Tunable Stiffness for Investigating Cell Behaviors. *ACS Applied Bio Materials* 2(1), pp. 570–576. doi: dw.

Sun, Z., Guo, S.S. and Fässler, R. 2016. Integrin-mediated mechanotransduction. *Journal of Cell Biology* 215(4), pp. 445–456. doi: 10.1083/jcb.201609037 JCB.

Syed, S., Karadaghy, A. and Zustiak, S. 2015. Simple polyacrylamide-based multiwell stiffness assay for the study of stiffness-dependent cell responses. *Journal of Visualized Experiments* 97, p. e52643. doi: 10.3791/52643.

Takahashi, S., Itoh, N., Kawamura, Y. and Hayashi, R. 1998. Physical and Chemical Changes of Gelatins by Oxidation Treatment. *Bulletin of The Society of Scientific Photography of Japan* 51(1), pp. 22-28 (in Japanese). doi: https://doi.org/10.11454/photogrst1964.51.22.

Tang, Y. et al. 2013. MT1-MMP-Dependent Control of Skeletal Stem Cell Commitment via a β1-Integrin/YAP/TAZ Signaling Axis. *Developmental Cell* 25(4), pp. 402–416. doi: 10.1016/j.devcel.2013.04.011.

Tavianatou, A.G., Caon, I., Franchi, M., Piperigkou, Z., Galesso, D. and Karamanos, N.K. 2019. Hyaluronan: molecular size-dependent signaling and biological functions in inflammation and cancer. *FEBS Journal* 286(15), pp. 2883–2908. doi: 10.1111/febs.14777.

Termeer, C. et al. 2002. Oligosaccharides of hyaluronan activate dendritic cells via Toll-like receptor 4. *Journal of Experimental Medicine* 195(1), pp. 99–111. doi: 10.1084/jem.20001858.

Termeer, C.C., Hennies, J., Voith, U., Ahrens, T., M. Weiss, J., Prehm, P. and Simon, J.C. 2000. Oligosaccharides of Hyaluronan Are Potent Activators of Dendritic Cells. *The Journal of Immunology* 165(4), pp. 1863–1870. doi: 10.4049/jimmunol.165.4.1863.

Thangprasert, A., Tansakul, C., Thuaksubun, N. and Meesane, J. 2019. Mimicked hybrid hydrogel based on gelatin/PVA for tissue engineering in subchondral bone interface for

osteoarthritis surgery. *Materials and Design* 183, p. 108113. Available at: https://doi.org/10.1016/j.matdes.2019.108113.

Tolg, C. et al. 2017. Hyaluronan modulates growth factor induced mammary gland branching in a size dependent manner. *Matrix Biology* 63, pp. 117–132. doi: 10.1016/j.matbio.2017.02.003.

Tomasch, J. et al. 2022. Changes in Elastic Moduli of Fibrin Hydrogels Within the Myogenic Range Alter Behavior of Murine C2C12 and Human C25 Myoblasts Differently. *Frontiers in Bioengineering and Biotechnology* 10, p. 836520. doi: 10.3389/fbioe.2022.836520.

Trensz, F. et al. 2015. Increased microenvironment stiffness in damaged myofibers promotes myogenic progenitor cell proliferation. *Skeletal Muscle* 5(1), p. 5. doi: 10.1186/s13395-015-0030-1.

Tse, J.R. and Engler, A.J. 2011. Stiffness gradients mimicking in vivo tissue variation regulate mesenchymal stem cell fate. *PLoS ONE* 6(1), p. e15978. doi: 10.1371/journal.pone.0015978.

van Putten, S., Shafieyan, Y. and Hinz, B. 2016. Mechanical control of cardiac myofibroblasts. *Journal of Molecular and Cellular Cardiology* 93, pp. 133–142. doi: 10.1016/j.yjmcc.2015.11.025.

Vasudevan, J., Lim, C.T. and Fernandez, J.G. 2020. Cell Migration and Breast Cancer Metastasis in Biomimetic Extracellular Matrices with Independently Tunable Stiffness. *Advanced Functional Materials* 30(49), p. 2005383. doi: 10.1002/adfm.202005383.

Vazquez, K., Saraswathibhatla, A. and Notbohm, J. 2022. Effect of substrate stiffness on friction in collective cell migration. *Scientific Reports* 12(1), p. 2474. Available at: https://doi.org/10.1038/s41598-022-06504-0.

Vega, S., Morales, A. V., Ocaña, O.H., Valdés, F., Fabregat, I. and Nieto, M.A. 2004. Snail blocks the cell cycle and confers resistance to cell death. *Genes and Development* 18(10),

pp. 1131–1143. doi: 10.1101/gad.294104.

Vincent, L.G., Choi, Y.S., Alonso-Latorre, B., Del Álamo, J.C. and Engler, A.J. 2013. Mesenchymal stem cell durotaxis depends on substrate stiffness gradient strength. *Biotechnology Journal* 8(4), pp. 472–484. doi: 10.1002/biot.201200205.

Vu, M., Do, J.Y., Awolude, O.A. and Chuang, L. 2018. Cervical cancer worldwide. *Current Problems in Cancer* 42(5), pp. 457–465. doi: 10.1016/j.currproblcancer.2018.06.003.

Walker, C., Mojares, E. and Del Río Hernández, A. 2018. Role of extracellular matrix in development and cancer progression. *International Journal of Molecular Sciences* 19, p. 3028. doi: 10.3390/ijms19103028.

Wall, S.J., Zhong, Z.D. and DeClerck, Y.A. 2007. The cyclin-dependent kinase inhibitors p15INK4B and p21 CIP1 are critical regulators of fibrillar collagen-induced tumor cell cycle arrest. *Journal of Biological Chemistry* 282(33), pp. 24471–24476. doi: 10.1074/jbc.M702697200.

Wallace, K., Burt, A.D. and Wright, M.C. 2008. Liver fibrosis. *Biochemical Journal* 411(1), pp. 1–18. doi: 10.1042/BJ20071570.

Wang, L.S., Boulaire, J., Chan, P.P.Y., Chung, J.E. and Kurisawa, M. 2010a. The role of stiffness of gelatin-hydroxyphenylpropionic acid hydrogels formed by enzyme-mediated crosslinking on the differentiation of human mesenchymal stem cell. *Biomaterials* 31(33), pp. 8608–8616. doi: 10.1016/j.biomaterials.2010.07.075.

Wang, L.S., Chung, J.E., Pui-Yik Chan, P. and Kurisawa, M. 2010b. Injectable biodegradable hydrogels with tunable mechanical properties for the stimulation of neurogenesic differentiation of human mesenchymal stem cells in 3D culture. *Biomaterials* 31(6), pp. 1148–1157. doi: 10.1016/j.biomaterials.2009.10.042.

Wang, P.Y., Thissen, H. and Tsai, W.B. 2012. The roles of RGD and grooved topography in the adhesion, morphology, and differentiation of C2C12 skeletal myoblasts. *Biotechnology*

and Bioengineering 109(8), pp. 2104–2115. doi: 10.1002/bit.24452.

Wirth, F., Lubosch, A., Hamelmann, S. and Nakchbandi, I.A. 2020. Fibronectin and Its Receptors in Hematopoiesis. *Cells* 9(12), p. 2717. doi: 10.3390/cells9122717.

Wisdom, K.M. et al. 2018. Matrix mechanical plasticity regulates cancer cell migration through confining microenvironments. *Nature Communications* 9, p. 4144. doi: 10.1038/s41467-018-06641-z.

Wisotzki, E.I. et al. 2014. Tailoring the material properties of gelatin hydrogels by high energy electron irradiation. *Journal of Materials Chemistry B* 2(27), pp. 4297–4309. doi: 10.1039/c4tb00429a.

Wolf, K. et al. 2007. Multi-step pericellular proteolysis controls the transition from individual to collective cancer cell invasion. *Nature Cell Biology* 9(8), pp. 893–904. doi: 10.1038/ncb1616.

Wolf, K. et al. 2013. Physical limits of cell migration: Control by ECM space and nuclear deformation and tuning by proteolysis and traction force. *Journal of Cell Biology* 201(7), pp. 1069–1084. doi: 10.1083/jcb.201210152.

Xue, M. and Jackson, C.J. 2015. Extracellular Matrix Reorganization During Wound Healing and Its Impact on Abnormal Scarring. *Advances in Wound Care* 4(3), pp. 119–136. doi: 10.1089/wound.2013.0485.

Yang, G., Xiao, Z., Long, H., Ma, K., Zhang, J., Ren, X. and Zhang, J. 2018. Assessment of the characteristics and biocompatibility of gelatin sponge scaffolds prepared by various crosslinking methods. *Scientific Reports* 8, p. 1616. doi: 10.1038/s41598-018-20006-y.

Yao, M. et al. 2019. New BMSC-Laden Gelatin Hydrogel Formed in Situ by Dual-Enzymatic Cross-Linking Accelerates Dermal Wound Healing. *ACS Omega* 4(5), pp. 8334–8340. doi: 10.1021/acsomega.9b00878.

Yeh, Y.T., Hur, S.S., Chang, J., Wang, K.C., Chiu, J.J., Li, Y.S. and Chien, S. 2012. Matrix

Stiffness Regulates Endothelial Cell Proliferation through Septin 9. *PLoS ONE* 7(10), p. e46889. doi: 10.1371/journal.pone.0046889.

Yeung, T. et al. 2005. Effects of substrate stiffness on cell morphology, cytoskeletal structure, and adhesion. *Cell Motility and the Cytoskeleton* 60(1), pp. 24–34. doi: 10.1002/cm.20041.

Yokoyama, K., Nio, N. and Kikuchi, Y. 2004. Properties and applications of microbial transglutaminase. *Applied Microbiology and Biotechnology* 64(4), pp. 447–454. doi: 10.1007/s00253-003-1539-5.

Yung, C.W., Wu, L.Q., Tullman, J.A., Payne, G.F., Bentley, W.E. and Barbari, T.A. 2007. Transglutaminase crosslinked gelatin as a tissue engineering scaffold. *Journal of Biomedical Materials Research Part A* 83A(4), pp. 1039–1046. Available at: http://www.ncbi.nlm.nih.gov/pubmed/16948146.

Zahari, N.K., Idrus, R.B.H. and Chowdhury, S.R. 2017. Laminin-coated poly(Methyl methacrylate) (PMMA) nanofiber scaffold facilitates the enrichment of skeletal muscle myoblast population. *International Journal of Molecular Sciences* 18(11), p. 2242. doi: 10.3390/ijms18112242.

Zemła, J. et al. 2018. AFM-based nanomechanical characterization of bronchoscopic samples in asthma patients. *Journal of Molecular Recognition* 31(12), p. e2752. doi: 10.1002/jmr.2752.

Zhan, X. 2020. Effect of matrix stiffness and adhesion ligand density on chondrogenic differentiation of mesenchymal stem cells. *Journal of Biomedical Materials Research - Part A* 108(3), pp. 675–683. doi: 10.1002/jbm.a.36847.

Zhao, L. et al. 2019. LOX inhibition downregulates MMP-2 and MMP-9 in gastric cancer tissues and cells. *Journal of Cancer* 10(26), pp. 6481–6490. doi: 10.7150/jca.33223.

Zhao, X. et al. 2016. Photocrosslinkable Gelatin Hydrogel for Epidermal Tissue Engineering. *Advanced Healthcare Materials* 5(1), pp. 108–118. doi: 10.1002/adhm.201500005.

Zhao, X. and Guan, J.L. 2011. Focal adhesion kinase and its signaling pathways in cell migration and angiogenesis. *Advanced Drug Delivery Reviews* 63(8), pp. 610–615. doi: 10.1016/j.addr.2010.11.001.

Zhao, Y. and Sun, Z. 2018. Effects of gelatin-polyphenol and gelatin–genipin cross-linking on the structure of gelatin hydrogels. *International Journal of Food Properties* 20(S3), pp. S2822–S2832. Available at: https://doi.org/10.1080/10942912.2017.1381111.

Zheng, J., Song, W., Huang, H. and Chen, H. 2010. Protein adsorption and cell adhesion on polyurethane/Pluronic® surface with lotus leaf-like topography. *Colloids and Surfaces B: Biointerfaces* 77(2), pp. 234–239. doi: 10.1016/j.colsurfb.2010.01.032.

List of Publications

Papers:

1. Mubarok, W., Qu, Y., & Sakai, S. (2021). Influence of Hydrogen Peroxide-Mediated Cross-Linking and Degradation on Cell-Adhesive Gelatin Hydrogels. *ACS Appl Bio Mater, 4*(5), 4184-4190.

2. Mubarok, W., Elvitigala, K. C. M. L., & Sakai, S. (2022). Tuning Myogenesis by Controlling Gelatin Hydrogel Properties through Hydrogen Peroxide-Mediated Cross-Linking and Degradation. *Gels, 8*(6), 387.

3. Mubarok, W., Elvitigala, K. C. M. L., & Sakai, S. (2022). Modulation of Cell-Cycle Progression by Hydrogen Peroxide-Mediated Cross-Linking and Degradation of Cell-Adhesive Hydrogels. *Cells, 11*(5), 881.

Related Papers:

1. Mubarok, W., Nakahata, M., Kojima, M., & Sakai, S. (2022). Nematode Surface Functionalization with Hydrogel Sheaths Tailored In Situ. *Mater Today Bio,* 100328.

International Conference/Symposium:

1. Wildan Mubarok, Yanfei Qu, Masaki Nakahata, Masaru Kojima, Shinji Sakai, Influence of Hydrogen Peroxide-Mediated Cross-Linking and Degradation on Cell-Adhesive Gelatin Hydrogels, *Society of Chemical Engineering Japan (SCEJ) 86th Annual Meeting*, M319, Tokyo, Japan, March (2021).

2. Wildan Mubarok, Masaki Nakahata, Masaru Kojima, Shinji Sakai, Modulation of Cells Adherence by Hydrogen Peroxide-Mediated Crosslinking and Polymer Degradation, *The 26th Symposium of Young Asian Biological Engineers' Community*, NGA-14, Kobe, Japan, November (2021).

3. Wildan Mubarok, Masaki Nakahata, Masaru Kojima, Shinji Sakai, Influence of Hydrogen Peroxide-Mediated Crosslinking and Polymer Degradation to Cells Adhesion, *The 43rd Annual Meeting of the Japanese Society for Biomaterials & The 8th Asian Biomaterials Congress*, A0-1 H02, Nagoya, Japan, November (2021).

4. Wildan Mubarok, Masaki Nakahata, Masaru Kojima, Shinji Sakai, Interfacing surface of nematodes with alginate-based hydrogels obtained via dual-crosslinking mechanism, *Materials Research Meeting MRM2021*, G1-02-12, Yokohama, Japan, December (2021).

Acknowledgements

The author is deeply grateful to Professor Shinji Sakai (Graduate School of Engineering Science, Osaka University) for his constant guidance, helpful advice, and encouragement throughout this study. The author would like to offer one's special thanks to Associate Professor Masaru Kojima (Graduate School of Engineering Science, Osaka University), Assistant Professor Masaki Nakahata (Graduate School of Science, Osaka University) and Assistant Professor Ikki Horiguchi (Graduate School of Engineering Science, Osaka University) for their valuable guidance and support during this work.

The author is also grateful to Professor Norikazu Nishiyama (Graduate School of Engineering Science, Osaka University) and Professor Shinji Deguchi (Graduate School of Engineering Science, Osaka University) as advisors for their valuable advice and comments to this dissertation.

The author is thankful to Ms. Hanako Nakajima (Graduate Students Section), Ms. Emiko Tasaka and Ms. Hiromi Ishikawa (Σ Advisement Room for International Students) and Ms. Masako Karita for their support in her daily life in Japan. The author would like to thank all the members of Sakai Laboratory for their experimental collaboration and friendship.

The author would like to express the deepest appreciation to his family, Ms. Dian Anggraini, Mr. Mohammad Muslih, Ms. Zulfa Habibah, for their understanding and continuous encouragement throughout his student life in Japan for the past 3 years.

The author gratefully acknowledges the financial support of this study from Japanese Government (MEXT) Scholarship.